The Chemical Reactivity of 1,1-Diamino-2,2-dinitroethene (FOX-7)

A Dissertation

Presented in Partial Fulfillment of the Requirements for the

Degree of Doctorate of Philosophy

with a

Major in Chemistry

in the

College of Graduate Studies

University of Idaho

by

Thao Thanh Vo

May 2014

Major Professor: Jean'ne M. Shreeve, Ph.D.

Authorization to Submit Dissertation

This dissertation of Thao Thanh Vo, submitted for the degree of Doctor of Philosophy with a Major in Chemistry and titled "The Chemical Reactivity of 1,1-Diamino-2,2-dinitroethene (FOX-7)," has been reviewed in final form. Permission as indicated by the signatures and dates below, is now granted to submit final copies to the College of Graduate Studies for approval.

Major Professor: _____ Date: _____
Jean'ne M. Shreeve, Ph.D.

Committee Members: _____ Date: _____
Chien Wai, Ph.D.

_____ Date: _____
Richard Williams, Ph.D.

_____ Date: _____
Daniel Bukvich, M. M.

Department Administrator: _____ Date: _____
Ray von Wandruszka, Ph.D.

Discipline's College Dean: _____ Date: _____
Paul Joyce, Ph.D.

Final Approval and Acceptance

Dean of the College of Graduate Studies: _____ Date: _____
Jie Chen, Ph.D.

Abstract

1,1-Diamino-2,2-dinitroethene (FOX-7), is an insensitive energetic material developed by the Swedish Defense Agency (FOA) in 1998. FOX-7, a "push-pull" nitroenamine, possesses a unique structure with interesting chemical properties that have yet to be fully explored. Its chemical unpredictability and poor solubility in common organic solvents have made the study of its chemical reactivity challenging. In our efforts to expand the chemistry of FOX-7 and to develop derivatives with superior energetic performance, we initiated work to develop the following areas: (1) Metal chemistry, (2) Azo-bridged derivatives of FOX-7, (3) Salt chemistry containing cationic derivatives of FOX-7 and (4) FOX-7 based oxidizers.

Prior to our work, the only known metal chemistry of FOX-7 involved its potassium salt, KFOX, and no literature precedent had been found for the azo derivatives of FOX-7. We have been able to synthesize various silver and copper metal complexes of FOX-7 from simple amines via metathesis reactions. The completion of this work gave rise to the first metal complexes of FOX-7 and insight into the behavior of FOX-7 as a coordinating ligand and an anion. En route to synthesizing desired azo-bridge substrates, we uncovered a new family of halogenated FOX-7 and halogenated azo-bridged FOX-7 derivatives. One of the most interesting features of this work was the discovery that these halogenated FOX-7 and halogenated azo-FOX-7 compounds behaved as hypergolic oxidizers - a new property of FOX-7 derivatives that had yet to be reported. En route to energetic salts of FOX-7, we realized that the reactivity of FOX-7 with bases to give the corresponding anionic species have been developed, we were surprised that the cationic derivatives synthesized from acids have been limited. Upon reacting FOX-7 with a variety of strong acids, we were able to isolate the first salts containing the cationic form of FOX-7. In the process of synthesizing the nitrate salt from nitic acid, we discovered a new oxygen rich oxidizer (TNAA), which has properties that are promising as an ammonium perchlorate replacement. Our contributions to the metal and azo and salt chemistry of FOX-7 have markedly expanded its chemical world.

Acknowledgments

This has been one incredible and life changing experience. I've accomplished more things beyond what I had imagined and this was all possible because one spectacular woman, Dr. Jean'ne Shreeve, took a chance on me. Professor Shreeve has really helped me grow and find my own path during graduate school. I can't express how much I appreciate the freedom she gave me to explore and grow as a chemist. Not only has she given me the tools necessary to be a successful chemist, but she gave me an opportunity to meet many wonderful people such as Dr. Malcom M. Renfrew. I am very grateful for all her unconditional support and guidance over the years and will always cherish our time together.

To my parents, Monica Vo Dang and Tam Vo:

There are no words that can truly describe how amazing my parents have always been. My parents have always and continue to make sacrifices so my brother and I may have a better future. I am especially thankful to my mother as she has been and will always be my my rock throughout life. She is the key reason for all and any success I have. I am very grateful to my parents for all their love and support. Without them, none of this would have been possible.

To my "baby" brother, Brian Vo:

Thank you for staying up with me and picking me up in the late hours of the night from the lab. Thank you for always making me laugh when my days were tough in the lab. Thank you for being the best brother I could have ever asked for.

To my best friend, Jared Rigoli:

What can I say. This has been one heck of a ride and I'm so glad that we had each other to get through all this. Thank you for all your help over the years and always putting a smile on my face.

To my labmates:

I thank them for all their help and encouragement throughout my graduate work. I would like to thank Dr. Young-Hyuk Joo, Dr. Philip Guo, Dr. Haixiang Gao, Dr. John Macijewski for taking the time out to mentor me. I would also like to thank Dr. Chunlin He for being such a great friend to me. He has always being there for me and helped me survive grad school.

To the faculty and staff of the Chemistry Department at U of I:

I can't express how thankful I am to have met such a wonderful group of people that make up this department. I appreciate each and every person that I have had the opportunity to interact with. I would like to especially thank the office staff (Terry, Cindy, and Deb) for all their help and keeping me on track! I am also grateful to Dr. Daniel Stelk, Dr. Patrick Hrdlicka, and Dr. Alaina Nye for all their support and guidance. I'd also like to thank Dr. Tom Bitterwolf for introducing me to the University of Idaho, where I was able to meet so many amazing people.

To Mrs. Melinda Deyasi:

THANK YOU SO MUCH for all your patience and help. I am grateful for your time and conversations throughout this whole process. This dissertation wouldn't have been as "smooth" without you. Thank you for keeping me on track!

To the ladies of the College of Graduate Studies (Cheri Cole, Sue Branting and Kathy Duke):

You all are so amazing! Thank you for making things less stressful and being so helpful. You do so much for everyone and always with a smile on your face. I can't tell you how much I've enjoyed working with all of you. Thank you again!!!

Dedication

I would like to dedicate this to my beloved grandma, Dang Thi Ti. It hasn't been the same without you and I miss you every day. I know you are always with me – looking over from above. I hope I have made you proud and will continue to do so. You taught me the most important life lesson of all – cherish those you love and take advantage of your time with your loved ones.

Table of Contents

List of Figures

List of Tables

List of Schemes

Chapter 1

1.1 Introduction

The development of energetic materials (compounds having the ability to store and release large amounts of chemical energy) can be dated back as far as approximately 220 BC with the discovery of black powder in China.[1] These materials continue to be studied extensively by researchers all around the world, having military and civilian applications in the areas of propellants (e.g., rocket fuels, seat ejectors, airbags), pyrotechnics (e.g., fireworks, signal flares), and explosives (e.g., demolition).[2,3] The design and synthesis of new energetic materials for explosives applications continues to be highly sought to improve the performances of currently used explosives, fulfill the strict safety requirements enforced for handling and transportation purposes (i.e. thermally stable; insensitive to external stimuli), and avoid environmentally toxic byproducts after detonation.[1-3]

In the late 1990s, 1,1-diamino-2,2-dinitroethene (FOX-7), developed by the Swedish defense agency, FOI, emerged as a promising insensitive energetic material.[4] Due to the high thermal stability of this structure, it gained considerable interest as a potential replacement for RDX, a currently used secondary explosive with sensitivity concerns which has been found to be environmentally toxic. The physical properties of FOX-7 are comparable to RDX, but its energetic properties are slightly less than RDX.[5] Since then, researchers have focused on developing new derivatives and theoretical studies to understand and enhance the performance of FOX-7.

In spite of only having a simple enamine structure in the molecule, the FOX-7 displays excellent properties and performance towards the energetic applications, *e.g.*, high density, high thermal stability, high detonation velocity and pressure, and the low sensitivity to impact and friction, *etc.*5 These promising energetic properties are the result of two sides, 1) the existence of extensive strong hydrogen-bond interactions within the molecule, and 2) four energy-containing functional groups (*i.e.* two nitro groups and two amino groups) in its structure. The chemistry of FOX-7 has been intensively studied over the past several years, and great efforts have been made to explore the various aspects of this compound and its derivatives involving the synthesis, properties (*e.g.* structural, spectroscopic, thermal, and explosive properties, *etc.*), and other associated applications in the field of energetic materials.

Many reviews regarding this topic have been available.[1-3, 5]

From the viewpoint of molecular structure, the FOX-7 has a highly polarized C=C bond with positive and negative charges stabilized by two amino groups and two nitro groups, respectively. This unique "push-pull" alkene structure makes FOX-7 chemically relatively stable. The reactivity of FOX-7 can give rise to a fundamental chemistry of considerable interest. Although the chemistry of FOX-7 may be challenging and in some cases unpredictable, a number of reactions involving the FOX-7, *e.g.* alkylation, acylation, acetylation, halogenation, and nitration reactions, *etc.* have been reported, which can also proceed readily under suitable conditions.[6,7] Among the synthesized substrates of FOX-7, the hydrazine derivative, 1-amino-1-hydrazino-2,2-dinitroethene (HFOX), discovered in 2002,[8] has been shown to be a highly energetic material with comparable performances to FOX-7. However, this molecule suffers from drawbacks of high sensitivity towards external stimuli and extremely poor stability (spontaneously combusts).[9] Energetic salt derivatives of HFOX were developed by a strategy of using the HFOX as the anion in combination with some high-nitrogen cations, with the aim of overcoming the drawbacks.[10] By virtue of this strategy, various energetic FOX-derived salts with different structures can be designed, and theoretically, their properties can also be fine-tuned by varying the counter ion to match the requirement of stability and energetic performance.

In continuing our efforts to expand the chemistry of FOX-7 and synthesizing derivatives with enhanced energetic properties, we initiated work to study the chemical reactivity of FOX-7 with 1) metals,[11] 2) the formation of azo derivatives,[12] and 3) the reactivity with strong acids with the goal of gaining a broader knowledge to the chemistry of FOX-7[13-14].

This dissertation is comprised of our recent contributions to the chemistry of FOX-7. The first chapter explores the chemical reactivity of FOX-7 with metals, an unexplored area prior to our work. Azo compounds are known to enhance the energetic performance of energetic compounds due to the additional N=N bond, increasing properties such as the heat of formation (HOF) and nitrogen content, which help increase detonation performance. En route to synthesizing azo-bridged FOX-7 derivatives, the halogenated azo-bridged FOX-7 substrates were discovered. The synthesis and properites of these new halogenated azo-bridged compounds are detailed in the second chapter. It is interesting that while the

chemistry of anionic FOX-7 has been explored extensively, the cation chemistry of FOX-7 was not investigated prior to our work. Chapter 3 discusses our investigation of FOX-7 with strong acids with pKas equal or more negative than -7 to generate salts consisting of the cation of FOX-7. When FOX-7 was reacted with nitric acid (HNO_3), the nitrate salt was not observed, but rather an interesting chemical transformation to form tetranitroacetimidic acid had taken place. Chapter 4 describes the synthesis, characterization of TNAA and its potential role as a perchlorate-free oxidizer to replace ammonium perchlorate.

1.1 References

(1) Klapötke, T. M. *Chemistry of High-Energy Materials*; Walter de Gruyter GmbH & Co. KG:Berlin/New York, **2011**; pp 179–184.

(2) Agrawal, J. P.; Hodgson, R. D. *Organic Chemistry of Explosives*; John Wiley & Sons, Ltd.: Chichester, **2007**; p 243.

(3) Krause, H. H. In *Energetic Materials*; Teipel, U., Ed.; VCH: Weinheim, **2005**; pp 1–25.

(4) Latypov, N. V.; Bergman, J.; Langlet, A.; Wellmar, U.; Bemm, U. Tetrahedron 1998, 54, 11525−11536.

(5) Bellamy, A. J. FOX-7 (1,1-Diamino-2,2-dinitroethene). In High Energy Density Materials; Klapötke, T. M., Ed.; Springer-Verlag:Berlin, Heidelberg, 2007; Struct. Bond. 125, 1−33 and references cited therein.

(6) Hervé, G.; Jacob, G.; Latypov, N. *Tetrahedron* **2005**, *61*, 6743–6748.

(7) Hervé, G.; Jacob, G. *Tetrahedron*, **2007**, *63*, 953–959.

(8) Bellamy, A. J.; Goede, P.; Sandberg, C.; Latypov, N. V. *33rd Int. Annual Conference of ICT,* Karlsruhe, Germany, June 25–28, **2002**, p 3/1.

(9) Bellamy, A. J.; Contini, A. E.; Latypov, N. V. *Propellants Explos. Pyrotech.* **2008**, *33*, 87-88.

(10) Gao, H.; Joo, Y.-H.; Parrish, D. A.; Vo, T.; Shreeve, J. M. *Chem. Eur. J.* **2011**, *17*, 4613–4618.

(11) (a) Garg, S.; Gao, H.; Joo, Y.-H.; Parrish, D. A.; Shreeve, J. M. *J. Am. Chem. Soc.* **2010**, *132*, 8888–8890 and references cited therein. (b) Garg, S.; Gao, H.; Parrish, D. A.; Shreeve, J. M. *Inorg. Chem.* **2011**, *50*, 390–395 and references cited therein. (c) Vo, T. T.; Shreeve, J. M. FOX-7 as a Coordinating Ligand or Anion in Metal Salts. Abstracts from the 66th Northwest Regional Meeting of the American Chemical Society, Portland, OR, June 26–29, **2011**; NORM 188. (d) Vo, T. T.; Parrish, D. A.; Shreeve, J. M. *Inorg. Chem.* **2012**, 51, 1963–1968 and references cited therein.

(12) Vo, T. T.; Zhang, J.; Parrish, D. A.; Twamley, B.; Shreeve, J. M. *J. Am. Chem. Soc.* **2013**, *135*, 11787–11790.
(13) Vo, T. T.; Parrish, D. A.; Shreeve, J. M. *J. Am. Chem. Soc. pending.*
(14) Vo, T. T.; Parrish, D. A.; Shreeve, J. M. *J. Am. Chem. Soc. pending.*

Chapter 2

1,1-Diamino-2,2-dintroethene (FOX-7) in Copper and Nickel Diamine Complexes and Copper FOX-7

by

Thao T. Vo, Damon A. Parrish, and Jean'ne M. Shreeve

Published in

Inorganic Chemistry

(Vo, T. T.; Parrish, D. A. Shreeve, J. M. *Inorg. Chem.* **2012**, *51*, 1963 – 1968. Copyright © **2012** American Chemical Society)

Abstract

1,1-Diamino-2,2-dinitroethene (FOX-7) reacts readily with copper nitrate in an aqueous solution of potassium hydroxide to form pea green $Cu(FOX)_2(H_2O)_2$ (**5**). FOX-7 complexes of copper and nickel supported by a variety of diamines including $Cu(en)_2(FOX)_2(H_2O)$ (**1**), $Cu(pn)_2(FOX)_2$ (**2**), $Cu(bipy)(FOX)_2(H_2O)_4$ (**3a**), $Cu(bipy)_2(FOX)_2(H_2O)_{2.5}$ (**3b**), $Cu(bipy)(FOX)_2(DMSO)_2 \cdot 2DMSO$ (**3c**), $Cu(phen)_3(FOX)_2(H_2O)_3$ (**4**), $(Ni)_2(phen)_6(FOX)_4(NO_3)_3(H_2O)_2$ (**6**), and Ni-$(bipy)_3(FOX)_2(H_2O)_4$ (**7a**) were obtained via metathesis reactions with potassium-FOX (KFOX). Surprisingly FOX-7, in the presence of Ni(II) and bipyridyl in a mixed solvent of methanol and dimethyl sulfoxide, gave a chelated FOX carbamate anion resulting in the compound $Ni(bipy)_2(FOX{-}CO_2)\cdot(DMSO)$ (**7b**). All metal salts were characterized by infrared, elemental analysis, and differential scanning calorimetry (DSC). Single-crystal X-ray diffraction structures

2.1 Introduction

Since the discovery of 1,1-diamino-2,2-dinitroethene (FOX-7) in 1998,[1] a considerable amount of attention has been directed toward this energetic compound as it was suggested as a potential replacement for the currently used secondary explosive cyclo-1,3,5-trimethylene-2,4,6-trinitramine (RDX) due to its higher threshold toward impact and friction sensitivity.[1−5] The unique structure of FOX-7, which has two electron-withdrawing nitro groups on the C1

carbon and two electron-donating amino groups on the C2 carbon, displays a "push−pull" alkene system,[1] giving rise to a fundamental chemistry of considerable interest.

Although the chemistry of FOX-7 is challenging, a wide scope of chemistry has been reported including alkylation, acylation, acetylation, halogenation, and nitration reactions.[1] However, the metal chemistry of FOX-7 has been less well studied.[6,7] The only reported metal compound of FOX-7 was its potassium salt,[6,8] K-FOX, until our recent work where we prepared the silver salt and silver and copper FOX-7 metal complexes stabilized with simple amines as ligands.[6,7] Investigation of the metal chemistry of FOX-7 highlights its characteristics as a possible ligand or an anionic species. The earlier metal complexes were shown to be thermally stable and insensitive to impact.[6,7] However, it is interesting to learn what roles FOX-7 might assume when competing with bidentate ligands to form coordination complexes with metals such as copper and nickel. Given its unique structure, FOX-7 does exhibit a variety of behaviors with metals in changing environments. More often than not, FOX-7 behaves in unpredictable ways including not reacting at all. Here, we report new chemistry of FOX-7 including the binary copper FOX-7 salt as well as additional copper and the first nickel complexes where bidentate ligands are utilized to stabilize the structure.

2.2 Results and Discussion

The syntheses of copper−FOX-7 complexes with various bidentate amines were accomplished by addition of K-FOX to a solution of copper(II) nitrate in an aqueous solution of the selected diamine (Scheme 2.1).

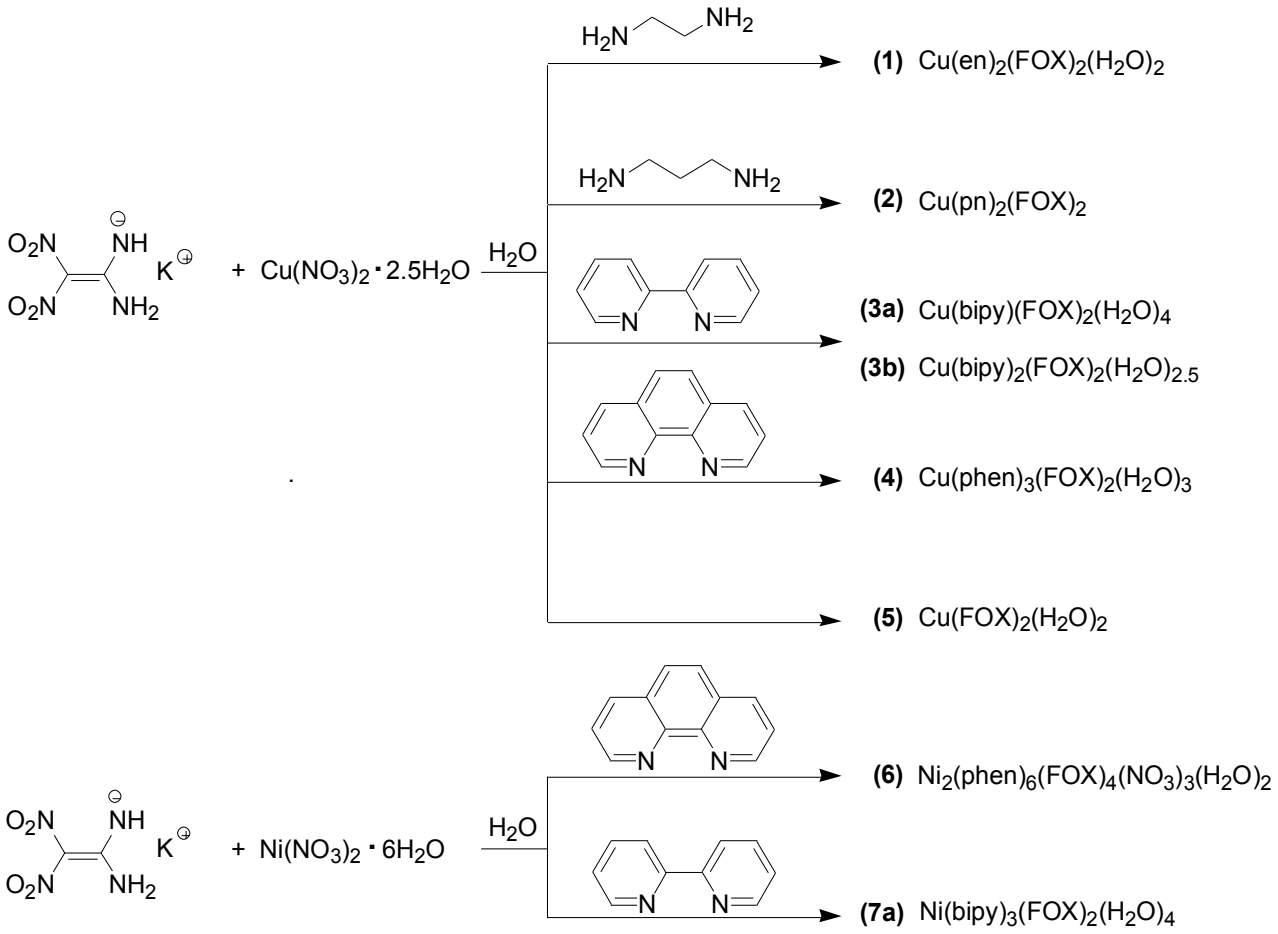

Scheme 2.1 Synthesis of copper and nickel complexes with K-FOX and various diamines.

Purple metallic crystals [ethylenediamine (en) and 1,3-propylenediamine (pn)] and green solids [bipyridyl (bipy) and phenanthroline (phen)] precipitated from aqueous solution. The purple crystals of copper FOX-7 ethylene diamine (**1**) and 1,3- propylenediamine (**2**) complexes were obtained by allowing the solutions to evaporate slowly after all reactants were dissolved. This resulted in formation of finely divided purple solids from which larger, better-formed crystals were obtained by allowing the solids to stand in the supernatant liquid. The same procedure was followed for the nickel complexes to give orange microcrystals. Compound **1** was obtained in comparable yield by substituting FOX-7 for K-FOX. It is likely that similar results would be the case for all compounds, but these reactions were not attempted. With the exception of reactions with bipyridyl and phenanthroline that were run at 90 °C, all reactions were carried out at 25 °C.

Single-crystal X-ray diffraction structures for the copper FOX-7 complexes (**1**, **2**, and **3c**) were obtained (Figures 1, 2, and 3, respectively). Crystallographic data are summarized in Table 1 (Experimental Section). Compound 1 crystallizes in the monoclinic crystal system (space group $P2_1/c$) with four molecules per unit cell (Figure 2.1).

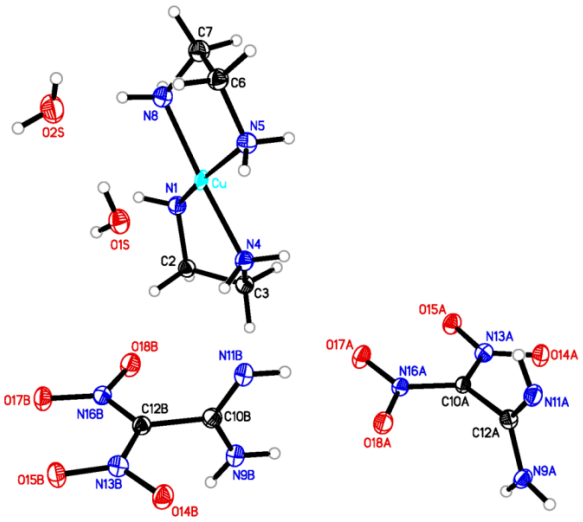

Figure 2.1 Thermal ellipsoid plot (30%) and labeling scheme for $Cu(en)_2(FOX)_2(H_2O)_2$ **(1).** Selected distances [Å] and angles [deg]: C(10B)–N(11B), 1.292(7); N(9B)–C(10B), 1.340(7); Cu–N(1), 2.004(5); Cu–N(8), 2.023(5); C(7)–N(8), 1.486(7); N(5)–C(6), 1.487(7); Cu–O(1S), 2.328(4); N(1)–Cu–N(4), 84.67(19); N(5)–Cu–N(8), 84.53(19); N(1)–Cu–N(8), 95.05(19); N(4)–Cu–N(5), 94.98(19); N(1)–Cu–N(5), 166.28(19); N(1)–Cu–O(1S), 99.99(17); N(5)–Cu–O(1S), 93.73(17).

The two ethylenediamine ligands surround the central copper(II) atom with one water molecule and one FOX molecule at a longer distance (viz., Cu−N (en) × 4, 2.023 Å; Cu−O (water), 2.328 Å; Cu−O (FOX), 3.045 Å) to give a six-coordinate octahedral coordination sphere (Figure 1). The N(1)−Cu−N(4) angle is 84.67°, which is somewhat smaller compared with the value for the N(1)−Cu−N(2) angle of 86.2° for $Cu(en)_2(NO_3)_2$.[7] The loss of a proton by FOX-7 to form the FOX-7 anion is supported by the fact that the C−NH bond is shorter than the C−NH_2 bond by 0.05 Å, which is good agreement with the values observed for monoamine complexes, $Cu(NH_3)_2(FOX)_2$ and $Cu(C_3H_7NH_2)_2(FOX)_2$.[7]

Compound 2 also crystallizes in a monoclinic crystal system (space group C2/m) with two molecules per unit cell (Figure 2.2). The two propylenediamine ligands coordinate to the

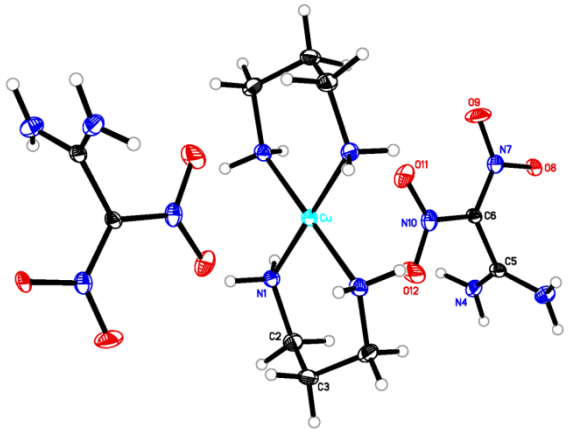

Figure 2.2 Thermal ellipsoid plot (30%) and labeling scheme for $Cu(pn)_2(FOX)_2$ **(2).** Selected distances [Å] and angles [deg]: Cu–N(1)#1 = Cu–N(1)#2 = Cu–N(1)#3 = Cu–N(1)#4, 2.024(2); N(4)–H(4B) = 0.906(19); N(4)–H(4A) = 0.901(18); N(1)#1–Cu–N(1)#2, 86.70(14); N(1)#1–Cu-N(1)#3, 93.30(14); N(1)#2–Cu-N(1)#3, 180.0; N(1)#1–Cu-N(1), 180.0.

central copper(II) atom with a concomitant interaction via the oxygen of the nitro group of FOX giving a six-coordinate octahedral coordination sphere, viz., Cu−N (pn) × 4, 2.023 Å; Cu−O (FOX) × 2, 2.798 Å.

The crystal structure of the FOX-7 moiety appears as if it has four protons; however, each FOX-7 anion has a charge of minus one with only three protons per moiety. This occurs because the hydrogen on N4 occupies each position only onehalf of the time (Figure 2). The system is highly hydrogen bonded between the N−H of the pn ligand which is coordinated to copper and the oxygen atom of the nitro group of FOX-7.

Recrystallization of 3a, 3b, and 4 was very difficult due to solubility problems. Green crystals of the 3b and 4 complexes were obtained by recrystallizing each from water. However, the crystals were not suitable for X-ray analysis. When the crystals remained in aqueous solution for an extended period, the complexes underwent slow hydrolysis resulting in formation of crystals of yellow FOX-7. This observation was also made in earlier attempts to characterize copper FOX-7 monodentate amine complexes.[7]

Suitable crystals of $Cu(bipy)(FOX)_2(DMSO)_2 \cdot 2DMSO$ (3c) were obtained by vapor diffusion of methanol into a solution of 3b in DMSO to give dark green crystals. Prior to recrystallization, elemental analysis data supported the product, 3b, consisting of one copper atom with two bipyridyl ligands and two FOX anions with 2.5 water molecules of

crystallization (Scheme 1). After recrystallization from methanol and DMSO, one of the bipyridyl ligands had been displaced by two DMSO molecules.[9] X-ray analysis and elemental analysis indicated the presence of a single bipyridyl ligand, two FOX ligands, and two DMSO moieties, **3c** (Scheme 2).

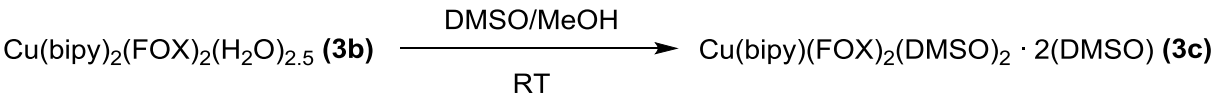

Scheme 2.2 Recrystallization of $Cu(bipy)_2(FOX)_2$ (**3b)** from DMSO/MeOH to form $Cu(bipy)(FOX)_2(DMSO)_2 \cdot 2$ DMSO (**3c)**.

Compound **3c** crystallizes in a monoclinic space group C2/c with four molecules in the unit cell (Figure 2.3). The distorted octahedral complex consists of a copper atom bonded to two FOX-7 anions, two molecules of DMSO, one bipy ligand, and two DMSO molecules of solvation with bond distances Cu−N (bipy) × 2, 2.041 Å; Cu−O (DMSO) × 2, 2.427 Å; Cu−N (FOX) × 2, 1.977 Å.

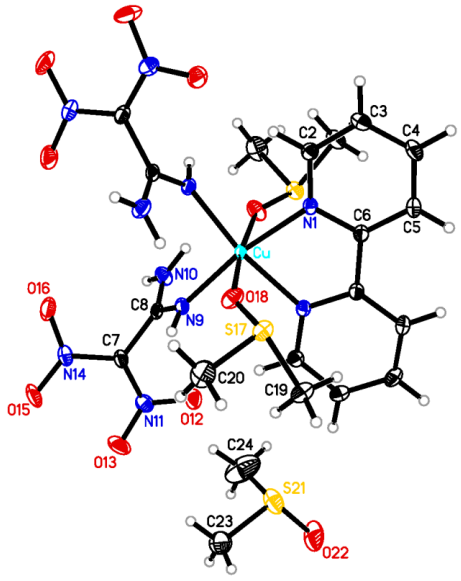

Figure 2.3 Thermal ellipsoid plot (30%) and labeling scheme for $Cu(bipy)(FOX)_2(DMSO)_2 \cdot 2$ DMSO **(3c).** Selected distances [Å] and angles [deg]: Cu–N(9), 1.9767(15); Cu–N(1), 2.0412(16); Cu-O(18)#1, 2.4270(14); C(8)–N(9), 1.299(2); C(8)–N(10), 1.330(2); N(9)–Cu–N(9)#1, 96.25(9); N(9)#1–Cu–N(1), 92.31(6); N(9)#1–Cu–N(1)#1, 170.34; N(9)–Cu–O(18)#1, 98.74(6); N(1)–Cu–O(18)#1, 86.47(5); N(1)–Cu–N(1)#1, 79.53(9); S(17)–O(18)–Cu, 148.99(9); C(20)–S(17)–C(19), 97.82(11).

Because one of the bipy ligands had been displaced from **3b** by two DMSO ligands, the complex consists of a metal environment which is similar to the monodentate cases described in our previous work.[7] The N(9)−Cu bond is shorter than the N(1)−Cu bond, which suggests that FOX is more tightly bonded to the Cu core than is the bipyridyl ligand. It is seen that C(8)−N(9) < C(8)−N10 in the FOX structure, supporting loss of a proton and formation of FOX as an anion, which was observed in structures of **1**, **2**, **3c**, **6**, and **7b**.

The only metal compound of FOX-7 was its potassium salt, K-FOX, until our recent work where we prepared the silver salt and silver and copper FOX-7 metal complexes stabilized with simple amine as ligands.[6,7] We now report the essentially quantitative precipitation of $Cu(FOX)_2(H_2O)_2$ (**5**), which was isolable as a stable pea green powder from a room temperature metathetical reaction of K-FOX in an aqueous solution of copper(II) nitrate.[6] The $Cu(FOX)_2(H_2O)_2$ salt is thermally decomposed at 171.6 °C but stable in air and supported by good elemental analysis. It is less stable thermally than FOX-7 or K-FOX but more thermally stable than the bidentate copper FOX complexes described in this work with the exception of **1**.

Single-crystal X-ray diffraction structures were obtained for nickel complexes **6** and **7b**. Compound **6** is a dimer, which crystallizes in a triclinic (P-1) crystal system with one molecule per unit system. The complex consists of three phenanthroline ligands forming an octahedral coordination sphere around each central nickel atom along with water molecules of crystallization and nitrate and FOX-7 anions (Figure 2.4).

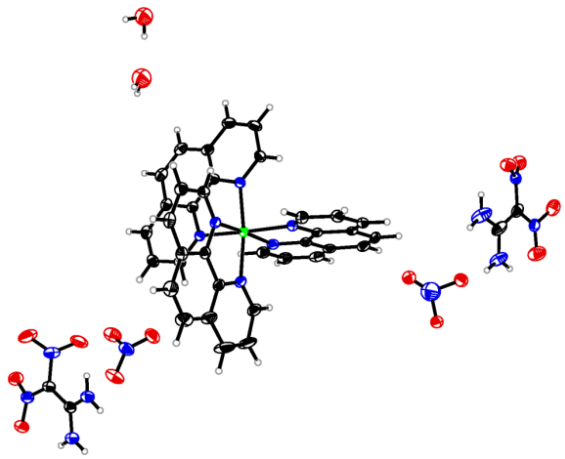

Figure 2.4 Thermal ellipsoid plot (30%) and labeling scheme for $(Ni)_2(phen)_6(FOX)_4(NO_3)_3(H_2O)_2$ (6)

Compound **7a** exists as orange microcrystals which were too small for X-ray analysis. The compound was confirmed by elemental analysis, IR, and DSC, which supported formation of $Ni(bipy)_3(FOX)_2(H_2O)_4$. While attempting to obtain suitable crystals for X-ray analysis, recrystallization of **7a** using DMSO/MeOH in the same manner as discussed for **3c** reproducibly gave crystals which were found by X-ray analysis to be compound **7b**. Interestingly, the crystal structure showed an unexpected transformation of the FOX-7 moiety such that addition of carbon bonded to two oxygen atoms to the amine functional group had taken place upon recrystallization in DMSO/MeOH. The complex crystallizes in a monoclinic space group of $P2_1/n$ with 4 molecules per unit cell. The central nickel atom is in a distorted octahedral configuration coordinated to two bipy ligands and one bidentate FOX-7−CO_2 moiety in which bonding to the metal is via the nitrogen of a FOX−NH group and the oxygen of the CO_2 group (Figure 2.5).

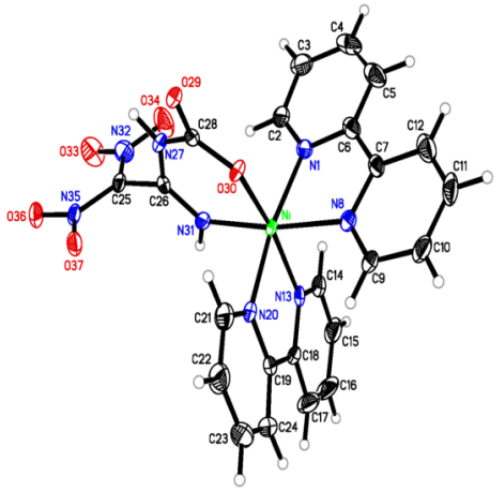

Figure 2.5 Thermal ellipsoid plot (30%) and labeling scheme for $Ni(bipy)_2(FOX\text{-}CO_2) \cdot (DMSO)$ (solvated DMSO not shown) **7b.** Selected distances [Å] and angles [deg]: Ni–N(31), 2.018(3); Ni–O(30), 2.037(3); Ni–N(1), 2.101(3); Ni–N(8), 2.108(3); C(28)–O(30), 1.276(4), C(28)–N(27),1.401(5); C(26)–N(27), 1.376(5); C(26)–N(31), 1.285(5); O(30)–C(28)–119.9(3); N(31)–Ni–O(30), 90.76(12); N(31)–Ni–N(20), 94.84(12); N(20)–Ni–N(1), 94.90(13); C(28)–Ni–O(30), 129.7(3); C(26)–N(31)–Ni, 127.5(3).

A molecule of DMSO is hydrogen bonded N(31) [N(31)−H(31)···O39#2]. Bond C(26)−N(31) is 0.09 Å shorter than C(26)−N(27), displaying the effect of the electronegative oxygen on the latter bond length.

Thermal Stabilities and Impact Sensitivity. Differential scanning calorimeter (DSC) data for all compounds were obtained. The copper complexes have thermal stabilities of 178.0 (**1**), 161.2 (**2**), 153.2 (**3a**), 156.4 (**3b**), 167.2 (**3c**), 169.5 (**4**), and 171.6 °C (**5**) . The nickel complexes decompose at 193.3 (**6**), 197.4 (**7a**), and 225.5 °C (**7b**). In general, the nickel complexes are thermally more stable than the analogous copper complexes. All decompose without explosion. Not unexpectedly, the impact sensitivities for all compounds which were determined with BAM Fallhammer tests[9] were found to be greater than 40 J.

2.3 Conclusion

Copper and nickel metal complexes of FOX-7 were synthesized with various bidentate diamine ligands in moderate yields. All compounds were characterized and analyzed via IR, elemental analysis, and differential scanning calorimetry (DSC). Singlecrystal X-ray diffraction data were obtained for compounds **1**, **2**, **3c**, **6**, and **7b**. These materials show thermal stabilities between 156 and 225 °C, which is slightly less stable than FOX-7 (~261 °C) and K-FOX (226 °C).[7] The new metal complexes presented in this paper are not energetic, and as expected, they are less sensitive to impact (≥40 J) than K-FOX (33 J). In **3c** and **7b**, the only two examples where the metal forms bonds with the nitrogen atoms of both bipy and FOX, it is seen the bond length is very slightly shorter for the FOX nitrogen.

2.4 Experimental

Caution: Although none of the compounds described herein has exploded or detonated in the course of this research, FOX-7 is an insensitive munition, and all of these materials should be handled with extreme care using proper safety practices.

General Methods. IR spectra were recorded as KBr pellets using a BIORAD model 3000 FTS spectrometer. DSC measurements were performed on a TA Q10 instrument over the range from 40 to 400 °C at a heating rate of 5 °C/min. Elemental analyses were performed on an Exeter CE440 element analyzer. Occasionally the agreement between experimental and theoretical values for carbon and hydrogen is outside of the acceptable range; this arises most

usually for hydrated species. The values obtained for nitrogen often are a function of the nitrogen percentage in the compound; a lower nitrogen content most frequently results in better agreement. K-FOX was prepared by reaction of FOX-7 with potassium hydroxide in water.[7,8] All other reagents were used as purchased and of reagent grade.

$Cu(NH_2CH_2CH_2NH_2)_2(FOX)_2\cdot 2H_2O$ (**1**). A solution of $Cu(NO_3)_2\cdot 2.5H_2O$ (0.232 g, 1.0 mmol in 3 mL of water) was added dropwise to a solution of ethylenediamine (78 mmol, 4.68 g in 3 mL of water) followed by addition of powdered K-FOX (0.374 g, 2 mmol) with stirring at 25 °C. After 5−10 min, a purple precipitate formed. It was removed by filtration and dried under vacuum (0.250 g, yield 49%). Purple crystals were formed by maintaining the unfiltered solution at 90 °C for 15 min and then allowing the solution to stand overnight. T_{dec} 178.6 °C. IR (KBr): ν = 3437, 3327, 3290, 3263, 2956, 2723, 2482, 2194, 1635, 1575, 1500, 1444, 1347, 1281, 1245, 1141, 1114, 1042, 893, 830, 745, 687, 663 cm^{-1}. Anal. Calcd for $C_8H_{26}CuN_{12}O_{10}$ (513.95); C, 18.70; H, 5.10; N, 32.17. Found: C, 18.71; H, 5.11; N, 32.44.

$Cu(NH_2CH_2CH_2CH_2NH_2)_2(FOX)_2$ (**2**). A solution of $Cu(NO_3)_2\cdot 2.5H_2O$ (0.232 g, 1.0 mmol in 3 mL of water) was added dropwise to a solution of 1,3-propylenediamine (78 mmol, 5.78 g in 3 mL of water) followed by addition of K-FOX (0.374 g, 2 mmol) as a solid powder. The reaction was stirred at room temperature. Within 5−10 min of stirring, a purple precipitate formed. The precipitate was filtered and dried under vacuum. Purple crystals of the product were formed by heating the unfiltered solution at 90 °C for 15 min and then allowing the solution to remain overnight (0.347 g, yield 69%). T_{dec} 161.2 °C. IR (KBr): ν = 3048, 3296, 3241, 3136, 3042, 2980, 2932, 2889, 2824, 2341, 1659, 1610, 1493, 1415, 1386, 1343, 1281, 1220, 1178, 1132, 1065, 1029, 923, 876, 830, 794, 743, 680 cm^{-1}. Anal. Calcd for $C_{10}H_{26}CuN_{12}O_8$ (505.97): C, 23.74; H, 5.18; N, 33.22. Found: C, 23.79; H, 5.21; N, 32.66.

$Cu(bipy)(FOX)_2(H_2O)_4$ (**3a**). 2,2′-Bipyridyl (0.5 mmol, 0.078 g) was added to a solution of $Cu(NO_3)_2\cdot 2.5H_2O$ (0.116 g, 0.5 mmol in 5 mL of water) and stirred until all the bipy dissolved. To the solution, K-FOX (0.093 g, 0.5 mmol) was then added as a powder. The reaction formed a precipitate almost immediately to give a turquoise green solid which was stirred for ∼30 min, and the precipitate was filtered and dried under vacuum (0.225 g, yield

77%). T_{dec} 153.2 °C. IR (KBr): ν = 3417, 3328, 3300, 1619, 1500, 1473, 1448, 1385, 1325, 1218, 1193, 1161, 1138, 1070, 1019, 860, 829, 789, 771, 755, 731, 625 cm^{-1}. Anal.Calcd for $C_{14}H_{22}CuN_{10}O_{12}$ (585.93): C, 28.70; H, 3.78; N, 23.91. Found: C, 28.88; H, 3.11; N, 22.96.

$Cu(bipy)_2(FOX)_2(H_2O)_{2.5}$ (3b). 2,2′-Bipyridyl (0.234 g, 1.5 mmol) was added to a solution of $Cu(NO_3)_2·2.5H_2O$ (0.116 g, 0.5 mmol in 5 mL of water) and stirred until all the bipy was dissolved. To the solution, powdered K-FOX (0.187 g, 1 mmol) was then added. The reaction formed a clear green solution which was stirred for an additional 30 min. The solvent was then removed by blowing air over the surface to give a sticky substance. This was then triturated with ∼5 mL of acetonitrile to give a light green solid, which was removed by filtration and air dried (0.220 g, yield 62%). T_{dec} 156.4 °C. IR (KBr): ν = 3424, 3401, 3329, 3296, 1626, 1600, 1518, 1505, 1474, 1389, 1331, 1194, 1163, 1138, 1064, 1018, 860, 793, 754, 622 cm^{-1}. Anal. Calcd for $C_{24}H_{27}CuN_{12}O_{10.5}$ (715.09): C, 40.31; H, 3.81; N, 23.50. Found: C, 40.54; H, 3.11; N, 22.91.

$Cu(bipy)(FOX)_2(DMSO)_2·2$ DMSO (3c). Compound 3c was obtained by dissolving a minimum amount of 3b in DMSO and placing it inside of a chamber which contained methanol to give crystals of 3c slowly. T_{dec} 167.2 °C. IR (KBr): ν = 3373, 3242, 3118, 3064, 2766, 2363, 2025, 1644, 1605, 1569, 1529, 1499, 1477, 1446, 1357, 1328, 1294, 1274, 1174, 1153, 1143, 1099, 1061, 1034, 858, 828, 773, 731, 639 cm^{-1}.

$Cu(phen)_3(FOX)_2(H_2O)_3$ (4). 1,10-Phenanthroline monohydrate (1.5 mmol, 0.297 g) was added to a solution of $Cu(NO_3)_2·2.5H_2O$ (0.116 g, 0.5 mmol in 3 mL of water) and placed into an oil bath at 85−90 °C until the phenanthroline dissolved. Powdered K-FOX (0.187 g, 1 mmol) was then added to the solution and stirred for ∼30 min in the oil bath. The turquoise precipitate was filtered and dried under vacuum (0.280 g, yield 59%). T_{dec} 169.5 °C. IR (KBr): ν = 3431, 3390, 3213, 3065, 2364, 2343, 1638, 1601, 1541, 1518, 1473, 1429, 1385, 1363, 1343, 1239, 1130, 1036, 1004, 952, 909, 869, 776, 766, 754, 723, 644, 629 cm^{-1}. Anal. Calcd for $C_{40}H_{36}CuN_{14}O_{11}$ (952.35): C, 50.45; H, 3.81; N, 20.59. Found: C, 50.15; H, 3.54; N, 19.72.

$Cu(FOX)_2(H_2O)_2$ (5). To a suspension of FOX-7 (1 mmol, 0.148 g) in 0.8 mL of water, a solution of potassium hydroxide, KOH (0.14 mL of 11.11 M), was added dropwise to give a clear dark yellow solution. An aqueous solution of copper(II) nitrate (0.5 mmol, 0.116 g in 0.5 mL) was then added dropwise. With the first drop, a pea green precipitate formed immediately. After addition is complete, the reaction was stirred for 24 h, filtered, and washed with a small amount of water (0.207 g, yield ~99%). T_{dec} 171.6 °C. IR (KBr): 3569, 3423, 3405, 3331, 3298, 3227, 2923, 2475, 2361, 2243, 1933, 1633, 1518, 1473, 1394, 1353, 1221, 1166, 1139, 1025, 859, 791, 752, 673, 622 cm^{-1}. Anal. Calcd for $C_4H_{10}CuN_8O_{10}$ (393.72): C, 12.20; H, 2.56; N, 28.46. Found: C, 12.01; H, 2.25; N, 26.03.

$(Ni)_2(phen)_6(FOX)_4(NO_3)_3(H_2O)_2$ (6). 1,10-Phenanthroline monohydrate (1.5 mmol, 0.297 g) was added to a solution of $Ni(NO_3)_2 \cdot 6H_2O$ (0.145 g, 0.5 mmol in 3 mL of water) and heated at 85−90 °C. Powdered K-FOX (0.187 g, 1 mmol) was added, and the mixture was stirred for 15 min. The solution was cooled slowly to 25 °C and orange crystals formed. They were filtered and dried under vacuum (0.390 g, yield 77%). T_{dec} 193.3 °C. IR (KBr): ν = 3396, 3058, 2931, 2461, 2292, 1982, 1625, 1583, 1517, 1491, 1423, 1384, 1337, 1317, 1237, 1132, 1101, 887, 849, 778, 748, 725, 669, 642 cm^{-1}. Anal. Calcd for $C_{80}H_{68.40}N_{31}Ni_2O_{27.70}$ (2024.68): C, 47.46; H, 3.41; N, 21.45. Found: C, 47.34; H, 3.43; N, 20.57.

$Ni(bipy)_3(FOX)_2(H_2O)_4$ (7a). 2,2′-Bipyridyl (1.5 mmol, 0.234 g) was added to a solution of $Ni(NO_3)_2 \cdot 6H_2O$ (0.145 g, 0.5 mmol in 3 mL of water) and placed into an oil bath at 85−90 °C to give a clear red solution. Powdered K-FOX (0.187 g, 1 mmol) was added, and the solution was stirred for 15 min in the oil bath. The solution was cooled slowly to 25 °C in which orange microcrystals formed overnight. The crystals were filtered and dried under vacuum (0.429 g, yield 96%). T_{dec} 197.4 °C. IR (KBr): ν = 3421, 3108, 3078, 2366, 2150, 1637, 1598, 1567, 1522, 1473, 1440, 1381, 1353, 1313, 1236, 1128, 1018,
908, 830, 777, 737, 650 cm^{-1}. Anal. Calcd for $C_{34}H_{38}N_{14}NiO_{12}$ (893.45): C, 45.71; H, 4.29; N, 21.95. Found: C, 45.49; H, 3.67; N, 21.56.

$Ni(bipy)_2(FOX\text{-}CO_2)\cdot(DMSO)$ (7b). In a 4 mL vial, 0.102 g of 7a was dissolved in 0.5 mL of DMSO and placed into a chamber of methanol (2.5 mL) in which orange crystals formed.

They were filtered and air dried to give 7b. T_{dec} 225.5 °C. IR (KBr): 3650, 3512, 3424, 3202, 3109, 3078, 2993, 2905, 1642, 1602, 1573, 1479, 1443, 1359, 1311, 1240, 1172, 1136, 1043, 1020, 970, 894, 803, 766, 737, 711, 651, 631 cm^{-1}. Anal. Calcd for $C_{25}H_{24}N_8NiO_7S$ (639.27): C, 46.97; H, 3.78; N, 17.53. Found: C, 46.49; H, 3.70; N, 17.96.

2.5 Supporting Information

2.5.1 X-ray Crystallography:

A purple plate (**1**) of dimensions 0.17 × 0.12 × 0.01 mm^3, a purple plate (**2**) of dimensions 0.40 × 0.28 × 0.04 mm^3, an irregular green crystal (**3c**) of dimensions 0.43 × 0.29 × 0.17 mm^3, a thin gold plate (**6**) of dimensions 0.29 × 0.19 × 0.04 mm^3, or an orange plate (**7b**) of dimensions 0.11 × 0.10 × 0.02 mm^3 was mounted on a MiteGen MicroMesh using a small amount of Cargille Immersion oil. Data were collected on a Bruker three-circle platform diffractometer equipped with a SMART APEX II CCD detector. Crystals were irradiated using graphite monochromated Mo Kα radiation (λ = 0.71073). An Oxford Cobra low-temperature device was used to maintain the crystals at a constant 100(2) K during data collection.

Data collection was performed, and the unit cell was initially refined using APEX2 [v2009.3-0].[10]Data reduction was performed using SAINT [v7.60A][11]and XPREP [v2008/2].[12] Corrections were applied for Lorentz, polarization, and absorption effects using SADABS [v2008/1].[13] The structure was solved and refined with the aid of the programs in the SHELXTL-plus [v2008/4] system of programs.[14] The full-matrix least-squares refinement on F^2 included atomic coordinates and anisotropic thermal parameters for all non-H atoms. The H atoms were included using a riding model. Details of the data collection and refinement are given in Table 1.

Table 2.1 Crystal Data and Structure Refinement for **1**, **2**, **3c**, **6**, and **7b**

	1	**2**	**3c**	**6**	**7b**
Formula	$C_8H_{26}CuN_{12}O_{10}$	$C_{10}H_{26}CuN_{12}O_8$	$C_{22}H_{38}CuN_{10}O_{12}S_4$	$C_{80}H_{68.4}0N_{31}Ni_2O_{27.70}$	$C_{25}H_{24}N_8NiO_7S$
Fw	513.95	505.97	826.4	2024.68	639.27
cryst size (mm^3)	0.17 × 0.12 × 0.01	0.40 × 0.28 × 0.04	0.43 × 0.29 × 0.17	0.23 × 0.11 × 0.05	0.11 × 0.10 × 0.02
cryst syst	Monoclinic	monoclinic	monoclinic	triclinic	monoclinic
space group	$P2_1/c$	C2/m	C2/c	P-1	$P2_1/n$
a (Å)	13.363(5)	17.461(3)	24.377(3)	9.9134(17)	11.195(3)
b (Å)	11.495(4)	6.7620(10)	11.7645(12)	14.553(2)	15.925(4)
c (Å)	12.708(5)	9.8590(10)	17.213(2)	16.056(3)	15.613(4)
α (deg)	90	90	90	66.395(2)	90
β (deg)	97.329(5)	123.609(10)	134.042(3)	84.118(2)	103.266(3)
γ (deg)	90	90	90	81.961(2)	90
V ($Å^3$)	1936.0(12)	969.5(2)	3548.4(7)	2099.0(6)	2709.2(10)
Z	4	2	4	1	4
D_c (g cm^{-3})	1.763	1.733	1.501	1.602	1.567
μ (mm^{-1})	1.208	1.198	0.921	0.553	0.855
T (K)	100(2)	100(2)	100(2)	100(2)	100(2)
$\lambda_{Mo\ K}\alpha$ (Å)	0.71073	0.71073	0.71073	0.71073	0.71073
reflns collected	15303	4057	15821	19392	23837
data/restraints/params	3558/194/298	978/2/92	3651/12/226	8633/74/683	5546/0/380
GOF on F^2	0.994	1.033	1.125	1.035	1.012
R_1 ($I > 2\sigma(I)$)	0.0598	0.039	0.0293	0.0473	0.0545
wR_2 ($I > 2\sigma(I)$)	0.1361	0.0762	0.0722	0.1217	0.1164
R (all data)	0.1058	0.0577	0.0338	0.057	0.1061
wR (all data)	0.1592	0.0825	0.0745	0.1291	0.1375
Δρmin and Δρmax (e/Å3)	0.596 and −1.053	0.389 and −0.528	0.761 and −0.659	2.549 and −1.066	1.024 and −0.912

2.5.2 References

(1) (a) Bellamy, A. J. FOX-7 (1,1-Diamino-2,2-dinitroethene). In High Energy Density Materials; Klapötke, T. M., Ed.; Springer-Verlag:Berlin, Heidelberg, 2007; Struct. Bond. 125, 1−33 and references cited therein. (b) Latypov, N. V.; Bergman, J.; Langlet, A.; Wellmar, U.; Bemm, U. Tetrahedron 1998, 54, 11525−11536. (c) Herve, G.; Jacob, G.; Latypov, N. Tetrahedron 2005, 61, 6743−6748.

(2) Agrawal, J. P.; Hodgson, R. D. Organic Chemistry of Explosives; John Wiley & Sons, Ltd.: Chichester, 2007; p 243.

(3) Krause, H. H. In Energetic Materials; Teipel, U., Ed.; VCH: Weinheim, 2005; pp 1−25.

(4) Klapötke, T. M. Chemistry of High-Energy Materials; Walter de Gruyter GmbH &

Co. KG: Berlin/New York, 2011; pp 179−184.
(5) Gao, H.; Shreeve, J. M. Chem. Rev. 2011, 111, 7377−7436.
(6) (a) Garg, S.; Gao, H.; Joo, Y.-H.; Parrish, D. A.; Shreeve, J. M. J. Am. Chem. Soc. 2010, 132, 8888−8890 and references cited therein. (b) Xu, K.-Z.; Chang, C.-R; Song, J.-R.; Zhao, F. Q.; Ma, H.-X.; Lu, X.Q.; Hu, R.-Z. Chin. J. Chem. 2008, 26, 495−499.
(7) (a) Garg, S.; Gao, H.; Parrish, D. A.; Shreeve, J. M. Inorg. Chem. 2011, 50, 390−395 and references cited therein. (b) Vo, T. T.; Shreeve, J. M.; Abstracts, 66th Northwest Regional Meeting of the American Chemical Society, Portland, OR, June 26−29, 2011; American Chemical Society: Washington, D.C., 2011; NORM-188.
(8) Anniyappan, M.; Talawar, M. B.; Gore, G. M.; Venugopalan, S.; Gandhe, B. R. J. Hazard. Mater. 2006, B137, 812−819.
(9) (a) www.bam.de. (b) A 15−20 mg portion of the copper or nickel complex of FOX-7 was subjected to a Bam Fallhammer test using a 10 kg weight: insensitive > 40 J; less sensitive ≥ 35 J; sensitive ≥ 4 J.; very sensitive ≤ 3J.
(10) Apex2, v2010.3-0; Bruker AXS Inc., Madison, WI, 2010.
(11) SAINT, v7.68A; Bruker AXS Inc., Madison, WI, 2009.
(12) XPREP, v2008/2; Bruker AXS Inc., Madison, WI, 2008.
(13) SADABS, v2008/1; Bruker AXS Inc., Madison, WI, 2009.
(14) SHELXTL, v2008/4; Bruker AXS Inc., Madison, WI, 2009.

Chapter 3

New Roles for FOX-7: Halogenated FOX-7 and Azo Bis(diahaloFOX) as Energetic Materials and Oxidizers

by

Thao T. Vo, Jiaheng Zhang, Damon A. Parrish, Brendan Twamley and Jean'ne M. Shreeve

Published in

Journal of American Chemical Society

(Vo, T. T.; Zhang, J.; Parrish, D. A.; Twamley, B.; Shreeve, J. M. *J. Am. Chem. Soc.* **2013**, *135*, 11787-11790. Copyright © **2013** American Chemical Society)

3.1 Abstract

The syntheses and full characterization of new halogenated FOX-7 compounds (**13** and **14)** and halogenated azo-bridged FOX-7 derivatives (**4**, **6**, and **7**) are described. Some of these new structures demonstrate properties that approach those of RDX (cyclo-1,3,5-trimethylene-2,4,6-trinitramine). All the compounds displayed hypergolic properties with common hydrazine based fuels and primary aliphatic amines (ignition delay times of 2 -53 ms). This is a new role that has yet to be reported for FOX-7 and its derivatives. Their physical and energetic properties have been investigated. All compounds were characterized by single-crystal X-ray crystallography, elemental analysis, infrared spectra, and differential scanning calorimetry (DSC). These new molecules as energetic materials and hypergolic oxidizers contribute to the expansion of the chemistry of FOX-7.

3.2 Introduction

Materials that can store and release large amounts of chemical energy on demand have a wide variety of applications.[1-4] These materials must possess properties that allow them to be handled safely, and to avoid accidents during transport, and storage. New energetic materials that are nitrogen-rich, and that have high density, high heat of formation and positive oxygen balance, are highly sought as they exhibit good detonation performance suitable for roles as propellants, pyrotechnics, or explosives. Superior energetic performances

may potentially be achieved by incorporation of explosophores thus increasing the nitrogen content. However, achieving a fine balance between high detonation performance and low sensitivity is an interesting, but challenging task as the detonation performance enhancements most often come at the expense of molecular stability.

1,1-Diamino-2,2-dinitroethene (FOX-7), (**1)** (Scheme 1) has captured a major role in energetic materials research. A key characteristic of the thermally stable FOX-7 is its insensitivity to impact and friction, while exhibiting a detonation performance comparable to that of the currently commonly used secondary explosive RDX (cyclo-1,3,5-trimethylene-2,4,6-trinitramine).[1-5] Perhaps the single most stimulating attribute of FOX-7 is that it is chemically unpredictable which makes its reaction behaviour extremely challenging. In spite of that, a rather broad range of chemical reactions has been reported including alkylation, acylation, acetylation, electrophilic halogenation, and nitration.[1,5] More recently, the metal chemistry of FOX-7 has been explored.[6-8a-c]

Pursuing our interests in extending the chemistry of FOX-7 and its derivatives and based on calculations which suggested it might be possible to improve the detonation performance properties relative to FOX-7 and RDX, we initiated work to develop azo-bridged FOX-7 derivatives.[5c, 8d] The reactions of FOX-7 with chlorine-based oxidizing reagents N-chlorosuccinimide, and trichloroisocyanuric acid (TCICA)[9] (**2)** were found to be very successful in converting a single diamine group in FOX-7 to a new azo bridged product, (*E*)-1,2-bis{(*E*)-2-chloro-1-(chloroimino)-2,2-dinitroethyl}diazene (**4**), in addition to the previously known dichloro substrate, 1-chloro-1,1-dinitro-2-(N-chloroamidino)-ethane **(3)**.[1c] Now we report some new fully characterized energized halogenated derivatives of FOX-7 – some with extraordinary properties.

3.3 Results and Discussion

When FOX-7 was reacted with a slight excess of **2** for two hours, dichloro compound **3**[1c] (major) and azo complex **4** (minor) were isolated. Extending the reaction time, e. g., to 24 hours, did not result in total conversion of **1** to **4.** However, using a larger excess (5 equivalents) of **2** with **1** led to the formation of **4** as the major product. It is likely that **3** is formed initially and subsequently reacts with **2** to generate **4** (Scheme 3.1). To verify this, it

was shown that when **3** was isolated and then reacted with additional amounts of **2,** compound **4** was formed as the major product.

Scheme 3.1 Synthesis of dichloro substrate **(3)** and compound **(4)**.

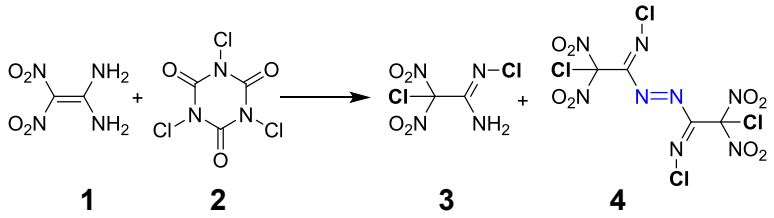

1 **2** **3** **4**

Based on these results, analogous reactions of dibromo substrate, 1-bromo-1,1-dinitro-2-(N-bromoamidino)-ethane **(5)**[1c] with **2** were explored and the products formed were a function of the quantity of **2** used (Scheme 2). The azo complex, (*E*)-1,2-bis{(*E*)-1-(bromoimino)-2-chloro-2,2-dinitroethyl}diazene **(6),** was obtained as the major product when a slight excess of **2** was reacted with **5**. When three equivalents of **5** was reacted with one equivalent of **2**, it was believed initially that three products, azo compounds **7** and **8** and the bromochloro compound **9** were formed; however, only **7**, (E)-1-{(E)-2-bromo-1-(bromoimino)-2,2-dinitroethyl-2-{(E)-2-bromo-1- (chloroimino)-2,2-dinitroethyl}diazene, could be isolated as determined by elemental analysis. Based on ^{13}C-NMR, there was an indication of a mixture of the starting material, **5** (δ 157.4 C-NH_2, δ 112.8 Br-C-NO_2), and **9** (δ 157.5 ppm C-NH_2, δ 114.3 ppm Br-C-NO_2). Due to similar polarities, it was not possible to separate the two compounds. As in the case with the preparation of **3** and **4**, the quantity of products formed was a function of the quantity of **2** used (Scheme 3.2). Compound **8** was not found.

Scheme 3.2 Synthesis of azo compounds **6** and **7.**

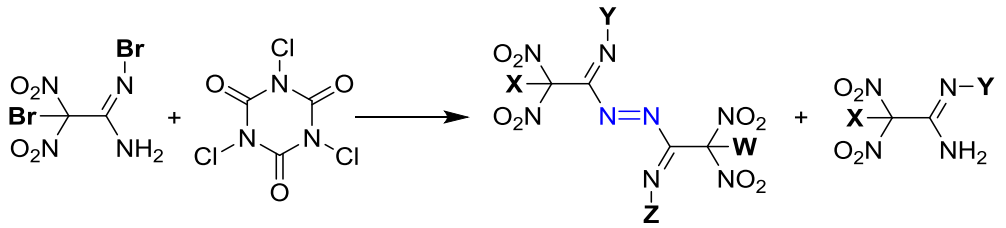

5 **2**

6: W, X = Br; Z = Cl
7: W, X, Y = Br; Z = Cl
8*: W, X, Y, Z = Br

9*: X = Br; Y = Cl

(* Not isolated)

Attempts to enhance the energetic performance of azo-bridged compounds via the incorporation of additional nitro groups, e. g., into **4** via reaction with 100% HNO_3/acetic anhydride (AA) or into substrate[1c] **10** via reaction with **2** to form **10b** failed (Scheme 3.3).

Scheme 3.3 Attempts to enhance the energy of azo substrate **4**.

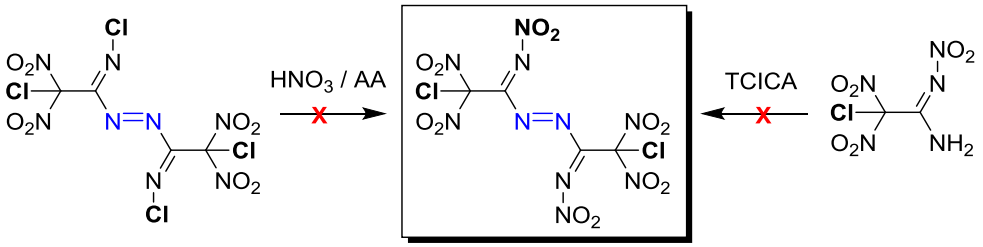

Based on this lack of success, no further efforts were made to nitrate the other halogenated FOX-7 derivatives. Due to the rather high impact sensitivity of azo compounds (vide infra), introduction of a methyl group would be expected to help stabilize the azo derivatives. However, when substrate **11**[10] was reacted with **2**, azo product **12** was not detected; rather only the chlorinated compounds, 2-chloro-N-methyl-2,2-dinitroacetimidamide (**13**) and (E)-N',2-dichloro-N-methyl-2,2-dinitroacetimidamide (**14**), resulted as a function of the quantity of **2** used (Scheme 3.4).

Scheme 3.4 Synthesis of chlorinated compounds **13** and **14**.

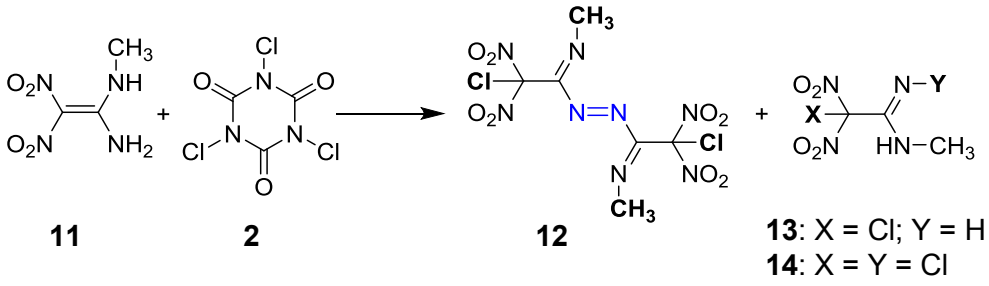

(* Not isolated)

The physical properties of the halogenated FOX-7 derivatives and the properties of some standard energetics for comparison are summarized in Table 3.1. The thermal

Table 3.1 Physical properties of FOX-7 derivatives.

Compd.	T_m[a] (°C)	T_d[b] (°C)	d[c]/ d[d] (g/cm^3)	ΔH_f[e] (kJ/mol) / (kJ/g)	P[f] (Gpa)	D[g] (ms^{-1})	IS[h] (J)	OB[i] (%)	I_{sp}[j] (s)
1[k]	-[l]	274	1.89	-53.1/-0.36	34.0	8930	60	0	-
3	91	127	1.86/1.84	274.1/1.26	32.5	8389	10	7.4	250
4	-[l]	139	1.97/1.99	1010.3/2.35	32.4	8348	3.5	14.9	246
5	70	128	2.47/2.48	872.8/2.85	36.7	7159	7.5	5.2	238
6	-[l]	136	2.08/2.10	1315.3/2.53	25.4	7102	< 2	12.3	234
7	-[l]	133	2.39/2.33	707.7/1.32	34.3	7403	< 2	11.4	238
10	129[m]	147	1.92/1.93	-42.2/-0.19	30.3	8406	≤ 9	21.1	235
13	131	136	1.70/1.74	-64.4/-0.33	22.9[n]	7382[n]	>40	-12.2	219
14	125	141	1.79/1.77	297.4/1.29	27.5	8013	32.0	-6.9	254
TNT	81	295	1.65	-67/-0.29	19.5	6881	15.0	-24.7	205[o]
PETN[o,p]	143	160	1.78	-502.8/-1.59	31.4	8564	2.9	15.2	-
RDX	206	230	1.82	92.6/0.42	35.2	8977	7.4	0	258
HMX[o,q]	282	287	1.94	116.1/0.39	41.5	9221	7.0	0	258

(a) Melting point. (b) Thermal decomposition temperature under nitrogen gas (DSC, 5 °C min^{-1}). (c) Density (measured). (d) Crystal density. (e) Heat of formation (Gaussian 03). (f) Detonation pressure (Cheetah 6.0). (g) Detonation velocity (Cheetah 6.0). (h) Impact sensitivity (BAM Drophammer –10 kg; Ref. (11). (i) Oxygen balance (% based on CO formation). (j) Specific impulse, calculated isobarically at 68 atm, (Cheetah 6.0). (k) Ref. (3). (l) Decomposed prior to melting. (m) Ref. 1c. (n) Detonation performance calculated by Explo 5.05. (o) Ref. (12). (p) Pentaerythritol tetranitrate (PETN). (q) Cyclotetramethylenetetranitramine (HMX).

decomposition temperatures of the halogenated FOX-7 derivatives range from 127 to 147 °C; thus, they are significantly less stable thermally than 1 (T_d 274 °C). The incorporation of bromine atoms tends to destabilize the azo complex relative to **4**.

Densities of the halogenated FOX-7 derivatives were determined at 25 °C using a gas pycnometer. Each compound was measured three times and the average value is reported in Table 3.1. Densities range from 1.70 g/cm^3 for **13** to 2.47 g/cm^3 for **5**. Although the halo compounds have densities that are ≥ **1**, the detonation performances for the derivatives are not competitive with **1**; however, they exceed those of TNT. The calculated detonation velocity values range from 8406 ms^{-1} for **10** to 7102 ms^{-1} for **6** and detonation pressures lie between 23 GPa for **13** to 37 Gpa for **5**, exceeding PETN (except **13** and **14**). Compounds **5** and **7** exceed RDX. The sensitivities of halogenated FOX-7 derivatives range from 2 to >40 J with the azo compounds having the highest sensitivity toward impact. The remaining compounds are less sensitive than PETN and RDX.

Oxygen balance is a measure of how much oxygen is required for complete combustion of hydrogen to water and carbon to carbon monoxide. A positive or negative

oxygen balance signifies that there is an excess of or a deficiency of oxygen in the molecule for complete combustion. Of the compounds, **10** has the highest and **13** the lowest oxygen balance. All halo FOX-7 derivatives compare well with TNT (-74.0%), but **1**, PETN, RDX and HMX have superior oxygen balance values relative to the methyl derivatives **13** and **14**.

All the compounds were structured by single crystal X-ray crystallography (see supporting information). Although **3** and **5** are previously known compounds, their crystal structures had not been obtained due to reported difficulty in obtaining crystals.[1c] We now have grown suitable crystals of these materials and for completeness their structures are reported. All the crystals were obtained by slow evaporation of a 50:50 mixture of hexane and dichloromethane. The azo compounds, **4** (Figure 3.1a) and **6** both crystallize as dark purple prisms consisting of a monoclinic P1 2_1/n1 space group with two molecules per unit cell while **7** crystallizes as dark green prisms with a monoclinic $P2_1/n$ space group with two molecules per unit cell. The absence of hydrogen bonding in these structures may contribute to their impact sensitivity. The azo -N=N- bond distances for azo complexes **4**, **6**, and **7** agree with the average bond distance for -N=N- (1.20 Å).[13] The bond angle of C-$(NO_2)_2$ is decreased in **4** (N7-C5-N10, 102.5°), **6** (N1-C1-N3, 102°), and **7 (**N1-C2-N2, 103°) compared to **3** and **5** (104°). This may be attributable to the steric repulsion of the nitro moieties and the chlorine atoms for both compounds. Compound **6** has some compositional disorder (85% / 15%). This is a common phenomenona in which different atoms can occupy the same site in different molecules in the crystal.[14]

Dichloro compound **14** crystallizes as colorless needles in a monoclinic space group Cc containing four molecules per unit cell (Figure 1b). As in chlorinated derivatives **3** and **13**, the C3-C6 bond distance in **14** is the expected average bond distance for C-C bonds. The sp^3 hybridized C6 atom is also observed (C3-C6-N8, 109°) as well as the deviation of the bond angle for C3-C6-Cl7 (115°) due to the steric replusion of the chlorine and nitro moieties similar to compounds **3** and **5**. Compression of the bond angle N8-C6-N11 (103° instead of 116°) is also observed. The bond angle of N4-C3-C6 (119°) is increased compared to the bond angle of N1-C1-C2 (115°) in **13** due to the presence of the additional chlorine atom on N2. Similar to **3**, **5**, and **13**, it is the hydrogen atom of the secondary amine that participates in hydrogen bonding with the nitrogen of the N-chloroamidino moiety.

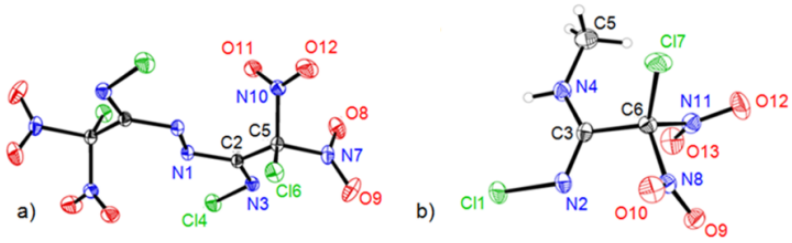

Figure 3.1 Thermal ellipsoids shown at 50% of (a) azo compound **4** and (b) chloro compound **14**.

One of the interesting features in this work was the discovery that the halo FOX-7 derivatives behaved as hypergolic oxidizers. While derivatives of FOX-7 have been studied extensively for their energetic properties, their role as oxidizers had yet to be explored. Hypergolicity is a term used to describe a spontaneous combustion reaction between a fuel and an oxidizer.[15]

Ongoing efforts continue in the development of new sources of fuels to replace the carcinogenic hydrazine and its derivatives; alternatives to commonly used oxidizers are of great interest due to the poor shelf life, highly corrosive nature and moisture sensitivity of ones in current use.[16, 17] Although much research has been and continues to be focused on fuels, less attention has been directed toward the development of new or improved oxidizers. However, while the oxidizing properties of halo FOX-7 moieties are of chemical interest, it is anticipated that the disadvantage of using solid oxidizers with liquid fuels should not be underestimated.

Reactions of the pure halogenated FOX-7 derivatives were examined with two common fuels, i. e., hydrazine hydrate (HH) and monomethyhydrazine (MMH), in order to determine if these materials were potential hypergolic oxidizers. Additionally it had been demonstrated that a variety of aliphatic amines are hypergolic with white fuming nitric acid (WFNA).[18] These hypergolic systems with ethylenediamine (EN) and tripropylamine (TPA) were determined to have ignition delay times (ID) (the time from when the fuel first comes into contact with the oxidizer until the initial flame appears) of 90 and 50 ms, respectively.[18] Therefore, these two amines were also investigated as fuels with the halogenated FOX-7 derivatives. The ID was measured by using a droplet test with a high-speed camera recording 500 frames per second. One drop of the fuel (HH, MMH, EN, TPA, or DAP (1,3-diaminopropane)) was dropped into a glass vial that contained 10 mg of the solid oxidant.

However, in our case, it was difficult to see the flame for some of the tests because the fuel pushed the solid oxidizer against the walls of the vial. Therefore, the first sign of smoke formation was used as the end point of the measurements. Thus, the times reported are not traditional ignition delay times but the precision of the recorded times which were measured three times for each halo FOX-7 compound with the average values given in Table 2 is very good. An example of the hypergolic testing can be found in Figure 2.

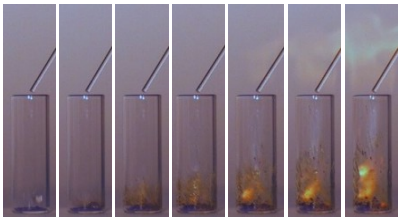

Figure 3.2 Hypergolic testing of azo substrate **4** with MMH.

Compounds **10**,[1c] **13**, and **14** are only hypergolic with MMH; this may arise from the absence of an electrophilic N-Clbond in compound **13** and the reduced electrophilicity of the N-Cl bond due to the presence of the methyl group in **14.** With the exception of **13**, all of the compounds displayed ID times that were significantly faster than WFNA with MMH and excluding **3,** for HH. The ID times ranged from 2 to 31 ms with the hydrazine based fuels tested.

Table 3.2 ID times for halo FOX-7 derivatives with HH, MMH, EN, and DAP

Compd.	HH (ms)	MMH (ms)	EN (ms)	DAP (ms)
3	20.7	3.3	53.3	53.3
4	13.3	4.6	14.7	14.7
5	4.7	2.7	4.7	8
6	4	2	2	3
7	6	2	6	5.3
10	NH[a]	10.7	NH	NH
13	NH	31.3	NH	NH
14	NH	10	NH	NH
WFNA[b]	19	20	90[c]	-

(a) Not hypergolic. (b) White fuming nitric acid (WFNA). (c) Ref. 18.

Similar to the hypergolic tests with HH and MMH, **10, 13**, and **14** are not hypergolic with the aliphatic amines tested. It has been reported that the ID times of hypergolic systems with unbranched aliphatic amines and WFNA are enhanced when the carbon chain is increased up to 5 carbons.[18] Thus, the expected trend was that the ID for TPA would be faster than EN. Interestingly, we observed no hypergolic reaction between TPA with **3** and **4**. Therefore, the remaining halo FOX-7 compounds were not investigated. Using simple primary aliphatic amines, DAP was predicted to exhibit better IDs compared to EN, based on literature data. However, the halo FOX-7 compounds that were hypergolic reacted at the same or faster rate with the shorter carbon chain (EN) than with the longer chain. EN and DAP have comparable IDs compared to HH and MMH for brominated azo compounds **6** and **7**. The IDs range from 2 to 53 ms for both fuels, exceeding the ID of WFNA with EN.

Derivatives of FOX-7 were not reported to behave as oxidizers earlier and the discovery of this behavior is a new chapter in the chemistry FOX-7. Although these compounds are not suggested as potential replacements for current hypergolic oxidizers, this is a worthwhile discovery in the chemical life and behavior of FOX-7.

3.4 Conclusion

In summary a series of new halogenated FOX-7 derivatives that are hydrolytically stable, have moderate thermal stability, and possess high densities and high heats of formation

has been synthesized and characterized. Structures **4**, **6**, and **7** represent the first azo derivatives of FOX-7. Calculations indicate the energetic performances of these exceed TNT, but are lower than that of the parent, FOX-7. The impact sensitivities of the compounds range between 2 and 40 J being at least competitive with or better than PETN. The new halo derivatives of FOX-7 have been found to behave as hypergolic oxidizers with common fuels helping to gain a new role and better understanding of the chemistry of FOX-7 itself.

ACKNOWLEDGMENT

The authors gratefully acknowledge the support of ONR (N00014-12-1-0536) and (N00014-11-AF-0-0002) – Dr. Clifford Bedford; and the Defense Threat Reduction Agency (HDTRA 1-11-1-0034). We are indebted to Dr. Illia Guzei, and Scott Economu for considerable assistance with crystal structuring.

3.5 References

(1) a) Bellamy, A. J. FOX-7 (1,1-Diamino-2,2-dinitroethene). In *High Energy Density Materials*; T. M. Klapötke, Ed.; Springer-Verlag: Berlin, Heidelberg, 2007; Struct. Bond., Vol. *125*, pp 1–33, and references cited therein. (b) Latypov, N. V.; Bergman, J.; Langlet, A.; Wellmar, U.; Bemm, U. *Tetrahedron* **1998**, *54*, 11525– 11536. (c) Hervé, G.; Jacob, G.; Latypov, N. *Tetrahedron* **2005**, *61*, 6743– 6748.

(2) Agrawal, J. P.; Hodgson, R. D. *Organic Chemistry of Explosives*, John Wiley & Sons, Ltd, Chichester, **2007**, pp. 243.

(3) Krause, H. H. in *Energetic Materials*, U. Teipel (Ed.), VCH, Weinheim, **2005**, pp. 1−25.

(4) Klapötke, T. M. *Chemistry of High-Energy Materials*, Walter de Gruyter GmbH & Co. KG, Berlin/New York, 2011, pp. 179–184.

(5) (a) Gao, H.; Shreeve, J. M. *Chem. Rev.* **2011**, *111*, 7377– 7436. (b) Gao, H.; Joo, Y.-H.; Parrish, D. A.; Vo, T.; Shreeve, J.M. *Chem. Eur. J.* **2011**, *17*, 4613 – 4618. (c) G. Hervé, *Propellants Explos. Pyrotech.* **2009**, *34*, 444– 451.

(6) Anniyappan, M.; Talawar, M. B.; Gore, G. M.; Venugopalan, S.; Gandhe, B. R. *J. Hazard. Mater.* **2006**, 137, 812– 819.

(7) (a) Garg, S.; Gao, H.; Joo, Y.-H.; Parrish, D.A.; Shreeve, J. M. *J. Am. Chem. Soc.* **2010**, *132*, 8888– 8890, and references cited therein. (b) Xu, K.-Z.; Chang, C.-R.; Song, J.-R.; Zhao, F. Q.; Ma, H.-X.; Lu, X.-Q.; Hu, X.-Q. *Chin. J. Chem.* **2008,** *26*, 495– 499.

(8) (a) Garg, S.; Gao, H.; Parrish, D. A.; Shreeve, J. M. *Inorg. Chem.* **2011**, *50*, 390– 395, and references cited therein. (b) Vo, T. T.; Shreeve, J. M. FOX-7 as a Coordinating Ligand or Anion in Metal Salts. Abstracts, 66th *Northwest Regional Meeting of the*

American Chemical Society, Portland, OR, June 26-29 (2011), NORM 188. (c) Vo, T. T.; Parrish, D. A.; Shreeve, J. M. *Inorg. Chem.* **2012**, *51*, 1963–1968, and references cited therein. (d) Chaoyang, Z.; Yuanjie, S.; Xiaodong, Z.; Haishan, D.; Xingeng, W. *J. Molecular Structure: THERMOCHEM*. **2005**, *728*, 129–134.

(9) Chavez, D. E.; Parrish, D. A.; Leonard, P. *Synlett*, **2012**, *23*, 2126– 2128.

(10) Xu, K.; Wang, F.; Ren, Y.; Li, W.; Zhao, F.; Chang, C.; Song, J. *Chin. J. Chem.* **2010**, *28*, 583–588.

(11) (a) www.bam.de. (b) A 15– 20 mg potion of sample was subjected to a Bam Fallhammer test using a 10 kg weight: insensitive > 40 J; less sensitive ≥ 35 J; sensitive ≥ 4 J; very sensitive ≤ 3 J.

(12) (a) Fischer, N.; Fischer, D.; Klapötke, T. M.; Piercey, D. G.; Stierstorfer, J. *J. Mater. Chem.* **2012**, *22*, 20418–20422. (b) Lee, J.-S.; Hsu, C.-K.; Chang, C.-L. *Thermochim. Acta*, **2002**, *392–393*, 173–176.

(13) Fischer, N.; Hüll, K.; Klapötke, T. M.; Stierstorfer, J.; Laus, G.; Hummel, M.; Froschauer, C.; Wurst, K.; Schottenberger, H. *Dalton Trans.* **2012**, *41*, 11201–11211.

(14) (a) Bürgi, H.B. *Annu. Rev. Phys. Chem.* **2000**, *51*, 275–296. (b) Ghosh, M.; Biswas, P.; Flörke, U.; Nag, K. *Inorg. Chem*. **2008**, *47*, 281–296. (c) Habgood, M.; Grau-Crespo, R.; Price, S. L. *Phys. Chem. Chem. Phys.* **2011**, *13*, 9590–9600 and references therein. (d) Hazen, R. M.; Navrotsky, A. *Am. Mineral.* **1996**, *81*, 1021–1035.

(15) Clark, J. D. *Ignition! An Informal History of Liquid Rocket Propellants,* Rutgers University Press, New Bruswick, **1972**.

(16) a) Schneider, S.; Hawkins, T.; Rosander, M.; Drake, G. *Energy Fuels*, **2008**, *22*, 2871–2872; b) Schneider, S.; Hawkins, T.; Rosander, M.; Mills, J.; Vaghjiani, G.; Chambreau, S. *Inorg. Chem.* **2008**, *47*, 6082– 6089; c) Schneider, S.; Hawkins, T.; Ahmed, Y.; Rosander, M.; Hudgens, L.; Mills, J. *Angew. Chem*. **2011**, *123*, 6008–6010; *Angew. Chem. Int. Ed.* **2011**, *50*, 5886–5888; d) Chambreau, S. D.; Schneider, S.; Rosander, M.; Hawkins, T.; Gallegos, C. J.; Pastewait, M. F.; Vaghjiani, G. L. *J. Phys. Chem. A* **2008**, *112*, 7816–7824.

(17) a) Zhang, Y.; Gao, H.; Joo, Y.-H.; Shreeve, J. M. *Angew. Chem.* **2011**, *123*, 9726–9734; *Angew. Chem. Int. Ed*. **2011**, *50*, 9554– 9563, and references cited therein; b) Zhang, Y.; Shreeve, J. M. *Angew. Chem*. **2011**, *123*, 965– 967; *Angew. Chem. Int. Ed.* **2011**, *50*, 935– 937; c) Thottempudi, V.; Forohor, F.; Parrish, D. A.; Shreeve, J. M. *Angew. Chem.* **2012**, *124*, 10019–10023; *Angew. Chem. Int. Ed*. **2012**, *51*, 9881–9885, and references cited therein); d) Maciejewski, J. P.; Gao, H.; Shreeve, J. M. *Chem Eur. J.* **2013**, *19*, 2947–2950.

(18) Rapp, L. R.; Strier, M. P. *J. Jet Propulsion*, **1959**, *27*, 401–404.

3.6 Supporting information

New Roles for FOX-7: Halogenated FOX-7 and Azo Bis(dihaloFOX) as Energetic Materials and Oxidizers

Thao T. Vo[†], Jiaheng Zhang[†], Damon A. Parrish[‡], Brendan Twamley[†], and Jean'ne M. Shreeve*[,†]

Department of Chemistry

University of Idaho

Moscow, ID 83844-2343

FAX (+1)208-885-9176

E-mail: jshreeve@uidaho.edu

Table of Contents

(Compounds are numbered as in the paper)

General methods: ^{1}H spectra were recorded on a 300 (Bruker AVANCE 300) nuclear magnetic resonance spectrometer operating at 300.13, and 75.48 MHz , and a 500 MHz (Bruker AVANCE 500) nuclear magnetic resonance spectrometer operating at 50.69 MHz for ^{13}C spectra, respectively. [D_6]CD_3CN was used as a locking solvent unless otherwise stated. Chemical shifts in ^{1}H and ^{13}C spectra were reported relative to Me_4Si. The melting and decomposition points were recorded on a differential scanning calorimeter (DSC, TA Instruments Q10) at a scan rate of 5 ºC min^{-1} in closed aluminum containers. IR spectra were recorded using KBr pellets for solids on a BIORAD model 3000 FTS spectrometer. Densities were measured at room temperature using a Micromeritics Accupyc 1330 gas pycnometer.

Elemental analyses were obtained on a CE-440 elemental analyzer (EAI Exeter Analytical). The ignition delay times were recorded at 500 frames s^{-1} by using an Olympus *i*-Speed camera.

Safety Precautions: While we have experienced no difficulties in syntheses and characterization of these materials, proper protective measures should be used. Manipulations must be carried out in a hood behind a safety shield. Eye protection and leather gloves must be worn. Caution should be exercised at all times during the synthesis, characterization, and handling of any of these materials, and mechanical actions involving scratching or scraping must be avoided.

3.6.1. X-ray crystallography:

A colorless plate crystal of 0.04 x 0.06 x 0.43 mm^2 (**3**), a purple prism plate crystal of dimensions 0.17 x 0.26 x 0.27 mm^3 (**4**), a colorless plate crystal of dimensions 0.82 x 0.10 x 0.07 mm^3 (**5**), a purple prism plate crystal of 0.10 x 0.25 x 0.30 mm^3 (**6**), a green prism plate crystal of dimensions 0.83 x 0.71 x 0.12 mm^3 (**7**) a colorless needle of dimensions 0.11 x 0.24 x 0.62 mm^3 (**13**), and a colorless needle of dimensions 0.25 x 0.22 x 0.05 mm^3 (**14**). Data were collected on a Bruker three-circle platform diffractometer equipped with a SMART APEX II CCD detector. The crystals were irradiated using graphite monochromated MoK_α radiation (λ = 0.71073). An Oxford Cobra low temperature device was used to keep the crystals at a constant 293(2) K during data collection.

Data collection was performed, and the unit cell was initially refined using APEX2 [v2009.3-0].[1] Data Reduction was performed using SAINT [v7.60A][2]and XPREP [v2008/2].[3] Corrections were applied for Lorentz, polarization, and absorption effects using SADABS [v2008/1].[4] The structure was solved and refined with the aid of the programs in the SHELXTL-plus [v2008/4] system of programs.[5] The full-matrix least-squares refinement on F^2 included atomic coordinates and anisotropic thermal parameters for all non-H atoms. The H atoms were included using a riding model. Details of the data collection and refinement are given in Table S1.

Table 3.S1 Crystallographic data for **3 – 6**.

	3	**4**	**5**	**6**
Formula	$C_2H_2Cl_2N_4O_4$	$C_2Cl_4N_8O_8$	$C_2H_2Br_2N_4O_4$	$C_2Br_2Cl_2N_8O_8$
MW	216.96	429.89	305.90	518.84
CCDC	935020	935018	935019	935023
T (K)	100(2)	150(2)	150(2)	150(2)
Wavelength (Å)	0.71073	0.71073	0.71073	0.71073
Crystal system	Orthorhombic	Monoclinic	Orthorhombic	Monoclinic
Space group	Pbcn	Pl 2l/nl	Pbcn	P1 2l/n1
a (Å)	9.7378(12)	7.8266(10)	10.1648(10)	7.9255(8)
b (Å)	10.5173(13)	7.0676(9)	10.6545(10)	7.1177(7)
c (Å)	14.3679(17)	12.7622(16)	14.6781(13)	12.8665(12)
α (°)	90	90	90	90
β (°)	90	101(2)	90	102(10)
γ (°)	90	90	90	90
Volume ($Å^3$)	1471.5(3)	692.0(15)	1589.7(3)	709.6(12)
Z	4	2	8	2
Density (calculated) (g cm^{-3})	1.959	2.083	2.556 (-123) 2.480 (20)	2.447
Absorption coefficient (mm^{-1})	0.864	0.918	10.182	6.150
F(000)	864	432	1152	504
Crystal size (mm^3)	0.040 x 0.060 x 0.430	0.170 x 0.260 x 0.270	0.82 x 0.10 x 0.07	0.100 x 0.250 x 0.300
Theta range for data collection (°)	2.84 to 28.85	2.83 to 33.14	2.77 to 26.36	2.78 to 28.29
Index ranges	-13<=h<=13, -14<=k<=14, -19<=l<=19	-11<=h<=11, -10<=k<=10, -18<=l<=19	-10<=h<=12, -13<=k<=13, -18<=l<=18	-10<=h<=10, -9<=k<=9, -17<=l<=17
Reflections collected	19982	11969	12861	9333
Independent reflections	1938 [R(int) = 0.1183]	2524 [R(int) = 0.0343]	1623 [R(int) = 0.0427]	1768[R(int) = 0.0472]
Absorption correction	Numerical	Multi-scan	Semi-empirical from equivalents	Multi-scan
Max. And Min. Transmission	0.9696 and 0.7077	0.8595 and 0.7883	0.5359 and 0.0438	0.5898 and 0.2642
Refinement method	Full-matrix least squares on F^2	Full-matrix least squares on F^2	Full-matrix least squares on F^2	Full-matrix least-squares on F^2
Data / restraints / parameters	1938 / 0 / 109	2524 / 0 / 109	1623 / 0 / 109	1768 / 0 / 109
Goodness-of-fit on F2	1.006	1.033	1.031	1.125
Final R indices [I>2sigma(I)]	R1 = 0.0386, wR2 = 0.0675	R1 = 0.0228, wR2 = 0.0622	R1 = 0.0534, wR2 = 0.1085	R1 = 0.0584, wR2 = 0.1905
R indices (all data)	R1 = 0.0805, wR2 = 0.0825	R1 = 0.0253, wR2 = 0.0633	R1 = 0.0622, wR2 = 0.1126	R1 = 0.0620 wR2 = 0.1949
Largest diff. Peak and hole (e $Å^{-3}$)	0.431 and -0.404	0.552 and -0.196	2.273 and -2.980	2.605 and -1.295

Table 3.S1 continued. Crystallographic data for **7**, **13**, and **14**.

	7	**13**	**14**
Formula	$C_2Br_{2.4}Cl_{1.6}N_8O_8$	$C_3H_5ClN_4O_4$	$C_3H_4Cl_2N_4O_4$
MW	536.58	196.55	231.00
CCDC	935022	938317	935021
T [K]	173(2)	150(2)	150(2)
Wavelength (Å)	0.71073	0.71073	0.71073
Crystal system	Monoclinic	Monoclinic	Monoclinic
Space group	P 2l/n	P1 2_1/n1	Cc
a (Å)	7.9800(7)	8.0235(12)	5.9328(12)
b (Å)	7.1271(7)	9.8310(15)	16.786(3)
c (Å)	12.9548(12)	10.1811(15)	8.4872(17)
α (°)	90	90	90
β (°)	103(10)	111(2)	100(2)
γ (°)	90	90	90
Volume ($Å^3$)	718.8(12)	747.5(19)	831.2(3)
Z	2	4	4
Density (calculated) (g cm^{-3})	2.481	1.747	1.846 (-123 C) 1.775 (20 C)
Absorption coefficient	7.122	0.494	0.771
F(000)	511	400	464
Crystal size (mm^3)	0.83 x 0.71 x 0.12	0.11 x 0.24 x 0.62	0.25 x 0.22 x 0.05
Theta range for data collection (°)	2.75 to 29.00	2.79 to 30.54	2.43 to 26.56
Index ranges	-10<=h<=10, -9<=k<=9, -17<=l<=17	-11<=h<=11, -14<=k<=14, -14<=l<=14	-7<=h<=7, -20<=k<=20, -10<=l<=10
Reflections collected	9700	11335	3717
Independent reflections	1909 [R(int) = 0.0379]	2276 [R(int) = 0.0245]	1653[R(int) = 0.0150]
Absorption correction	Semi-empirical from equivalents	Multi-scan	Semi-empirical from equivalents
Max. And Min. Transmission	0.4870 and 0.0670	0.7461 and 0.6309	0.9625 and 0.8307
Refinement method	Full-matrix least squares on F^2	Full-matrix least squares on F^2	Full-matrix least squares on F^2
Data / restraints / parameters	1909 / 4 / 117	2276 / 0 / 115	1653 / 2 / 120
Goodness-of-fit on F2	1.115	1.049	1.048
Final R indices [I>2sigma(I)]	R1 = 0.0269, wR2 = 0.0704	R1 = 0.0341 wR2 = 0.0883	R1 = 0.0178, wR2 = 0.0454
R indices (all data)	R1 = 0.0305, wR2 = 0.0722	R1 = 0.0403, wR2 = 0.0922	R1 = 0.0181, wR2 = 0.0457
Largest diff. Peak and hole (e $Å^{-3}$)	1.153 and -0.662	0.411 and -0.422	0.234 and -0.142

3.6.2 Single Crystal X-ray structures of 3, 5, 6, 7, and 13:

The chloro and bromo compounds (**3**) and (**5**) both crystallize as colorless crystals with an orthorhombic crystal system and a Pbcn space group (Figure 3.S1).

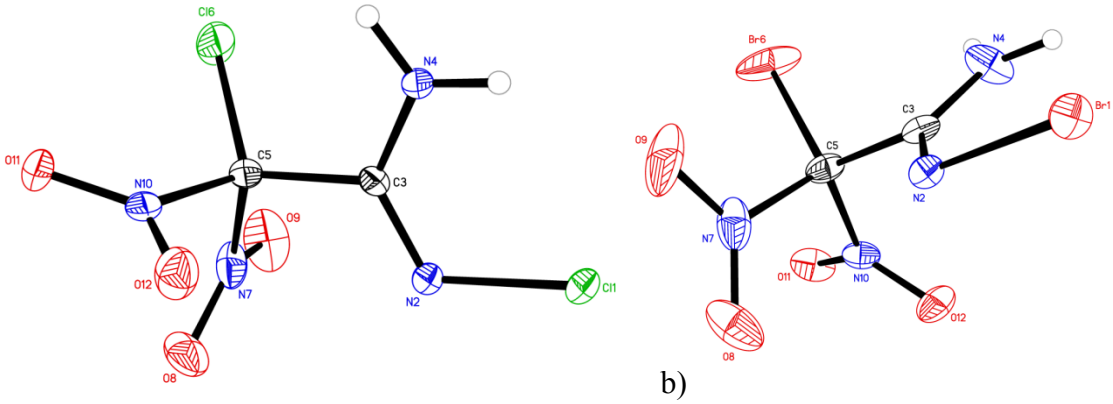

a) b)

Figure 3.S1 Thermal ellipsoids shown at 50% of a) dichloro FOX (**3**) and b) dibromo FOX (**5**).

The unit cell of **3** has four molecules while **5** has eight. The C3-C5 bond distance of **3** (1.51 Å), and **5** (1.52 Å), agree with the average bond distance for C-C single bonds (1.53 Å).[6] That the carbon C5 is sp^3 hybridized is indicated by the bond angle of 109° for C3-C5-N7 (**3**) and 110 ° for C3-C5-N10 for (**5**). This was also observed in the reported structure of chloronitro FOX (**10**).[6] The bond angle of C3-C5-Cl6 deviates slightly from the normal sp^3 bond angle (114° for both **3** and **5**) potentially due to steric repulsion of the halo atoms and the nitro moieties which was also reported similarly for the C2-C1-Cl bond angle of **10** (113° rather than 109°).[6] The bond angle of N7-C5-N10 of C-$(NO_2)_2$ in both **3** and **5** are more compressed (103°) compared to FOX-7 (**1**) (116°) due to the presence of the chlorine or bromine atom at the C5 position (Figures 1a and 1b). Hydrogen bonding exists between the hydrogen atoms of the amine and the nitrogen of the C=N moiety for both compounds as well (Figures 3.S2 and 3.S3).

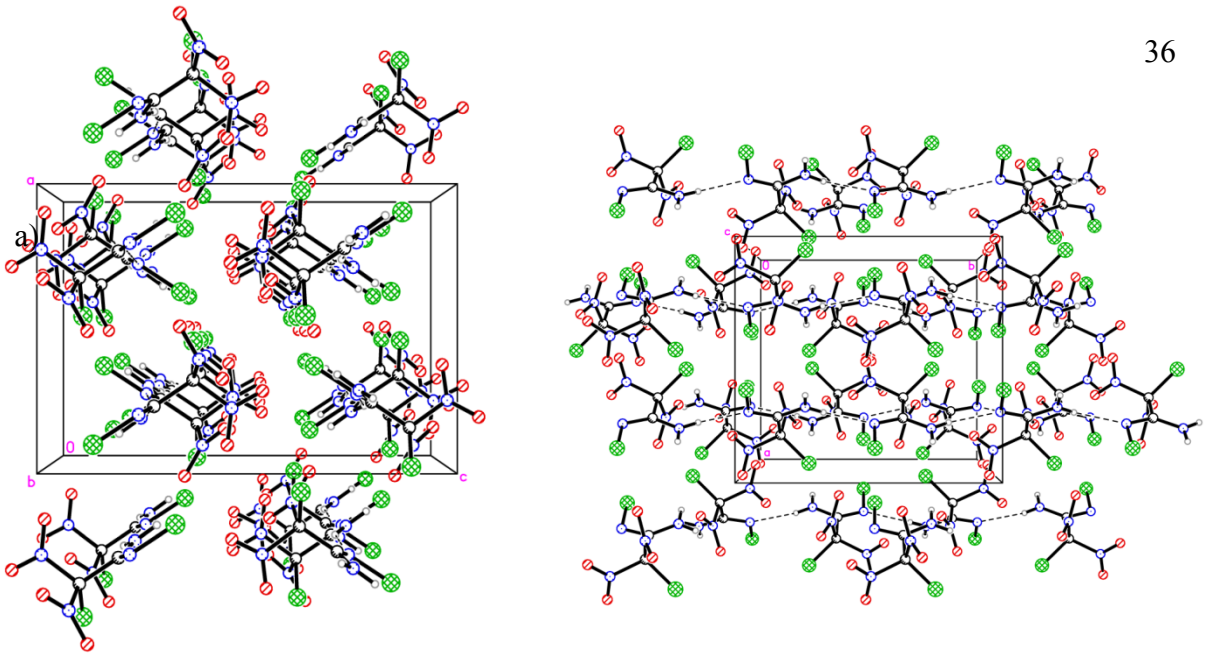

a) b)

Figure 3.S2 a) Ball and stick packing diagram of **3**. b) Dashed lines indicate hydrogen bonding.

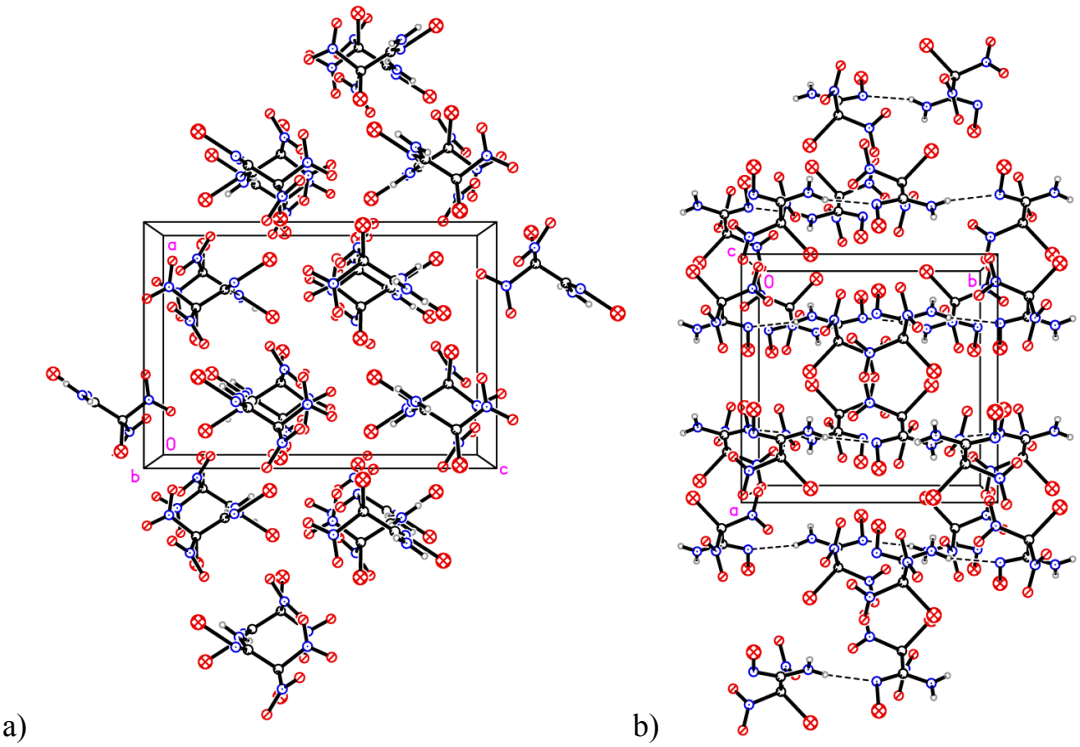

a) b)

Figure 3.S3 a) Ball and stick packing diagram of **5**. b) Dashed lines indicate hydrogen bonding.

Based on elemental analysis, **7** was found to have a ratio of 3 Br:1 Cl atoms. However, upon single crystal X-ray crystallography, it was found that **7** also displayed some compositional disorder similar to **6** (Figure 3.S4). Compound (**7**) was refined to consist of a ratio 2.4 Br: 1.6 Cl atoms.

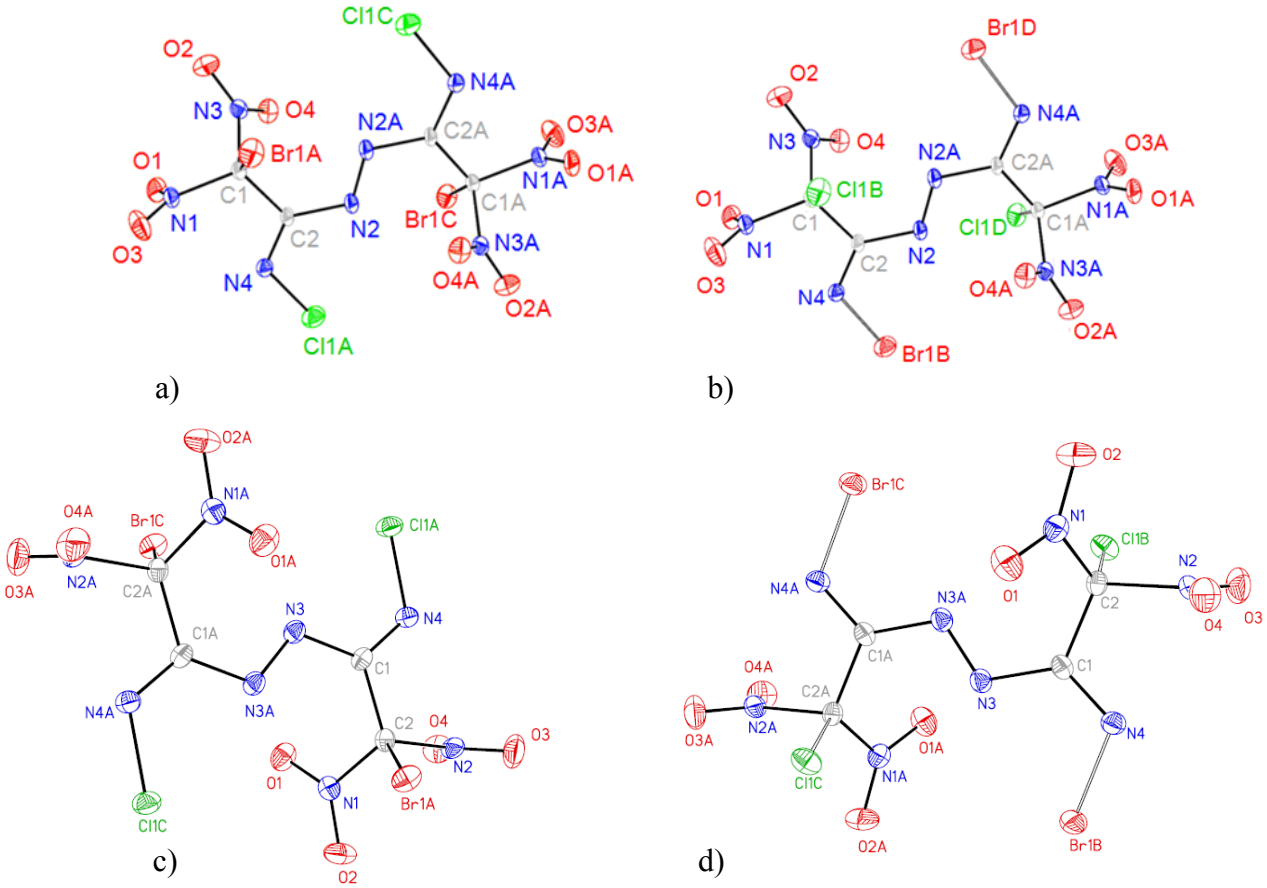

Figure 3.S4 Thermal ellipsoids displaying compositional disorder of compound **6** (85%:15%); **(**a) major disordered moiety shown (occupancy 85%); (b) minor disordered moiety shown (occupancy = 15%). Thermal ellipsoids displaying compositional disorder of compound **7**; (c) major disordered site occupancy (Br1A 97% and Cl1A 77%); (d) minor disordered site occupancy (Br1B 23% for the Cl1a site and Cl1B 3% for the Br1A site).

Halides Br1A and Cl1A were modeled with part occupancy of 97 and 77% respectively. Loose restraints were utilized between C2-Br1A, N4-Cl1A as well as N4-Br1B and C2-Cl1B of 1.89±0.02Å and 1.75±0.02Å respectively. The largest residual is ca. 1.4Å from the disordered Br1A/Cl1B site.

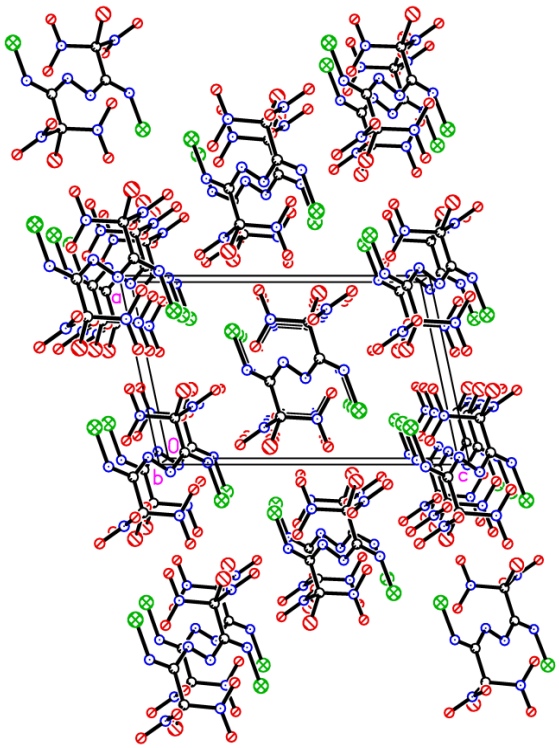

Figure 3.S5 Ball and stick packing diagram of **7**.

Chloro compound (**13**) crystallizes as colorless needles with a monoclinic space group P1 2_1/N1 consisting of four molecules per unit cell (Figures 3.S6 and 3.S7).

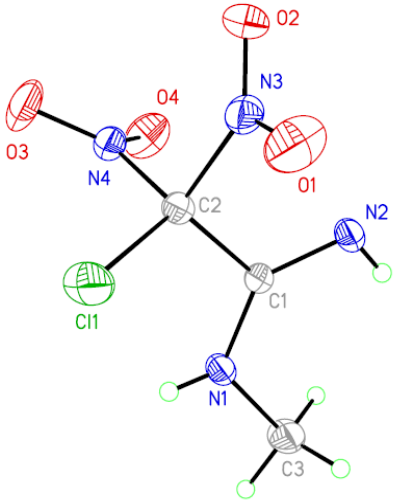

Figure 3.S6 Single crystal X-ray structure of chloromethyl FOX (**13**).

The C1-C2 bond distance (1.53 Å) is similar to the chloro and bromo compounds (**3**) and (**5**) with the expected average bond distance for C-C bonds. The C2 carbon displays sp^3 hybridization as observed in the previous compounds with the bond angle of 108° for C1-C2-N3. Again, the C1-C2-Cl1 bond deviates from the typical sp^3 bond angle due to steric repulsions of the surrounding chlorine and nitro moieties.

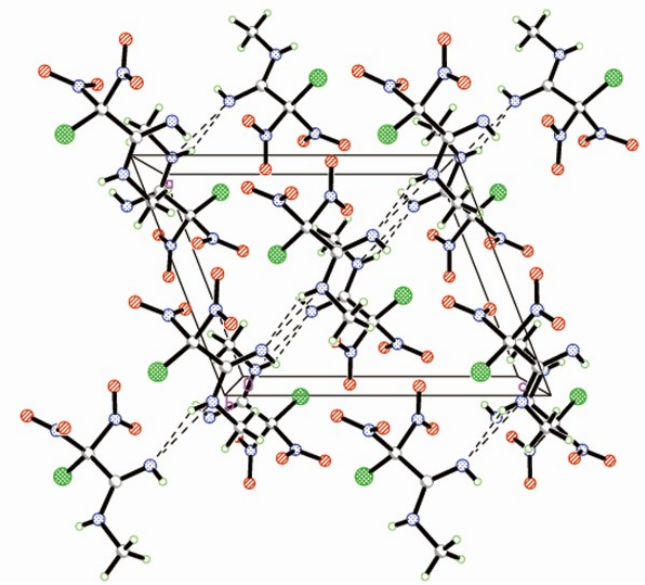

Figure 3.S7 Ball and stick packing diagram of compound (**13**).

3.6.3 Experimental

Note: N-bromosuccinimide (NBS) and N-chlorosuccinimide (NCS) were recrystallzied in water prior to use.

1-Chloro-1,1-dinitro-2-(N-chloroamidino)-ethane[6] **(3)**:

Prepared according to the literature with some slight modifications.[6] FOX-7, 2.0 g (13.5 mmol), was suspended in 120 mL MeOH. In one portion, NCS, 3.6 g (27.2 mmol), was added quickly and the suspension was stirred vigorously for 1.5 h. Dichloromethane (DCM) (360 mL) was then added to the solution and the organic phase was washed with a solution of aqueous sodium bicarbonate (0.4 M) to remove the acid byproduct (6 x 120 mL). The collected organic phase was then dried with anhydrous magnesium sulfate and concentrated to

obtain compound (**3**) without further purification (81% yield). Crystals for single crystal X-ray analysis were grown from a slowly evaporating solution of hexane and DCM (1:1) to obtain colorless needles.

1-Bromo-1,1-dinitro-2-(N-bromoamidino)-ethane[6] (**5**):

The same procedure as for **3** except NBS 4.84 g (27.2 mmol) replaced NCS to give colorless microcrystalline compound (**5**) (76% yield). The compound is stable after several weeks to a month before some yellow discoloration appears. Crystals for single crystal X-ray analysis were grown in a similar fashion as for **3** resulting in colorless needles.

Formation of **(*E*)-1,2-Bis{(*E*)-2-chloro-1-(chloroimino)-2,2-dinitroethyl}diazene)** (**4**) from **3**:

Dichloro compound **(3**) 2.16 g (10 mmol) was dissolved in 100 mL MeCN. Then 4.18 g (18 mmol) TCICA (**2**) was added as a solid in small portions over 10 minutes at room temperature. The color of the solution changed from yellow to colorless as the addition finished. The solution was then stirred for 2 hours. DCM (300 mL) was then added to the solution and the organic phase was washed with a solution of aqueous sodium bicarbonate (0.4 M) (6 x 120 mL) to remove the cyanuric acid by-product. The collected organic phase was then dried with anhydrous magnesium sulfate and concentrated to obtain azo compound (**4**), (11% recrystallized yield). These were recrystallized for single crystal X-ray analysis by slow evaporation from a solution of hexane and DCM (1:1) to obtain dark purple prisms. Elemental analysis: ($C_4Cl_2N_8O_8$, 429.89) Calcd: C, 11.18%; N, 26.07%. Found: C, 11.22%; N, 24.73%. IR (KBr): 3443, 2924, 2362, 2341, 1599, 1336, 1294, 1207, 1099, 1020, 942, 887, 834, 794, 725, 694, 657, 614 cm^{-1}.

Formation of **(*E*)-1,2-Bis{(*E*)-1-(bromoimino)-2-chloro-2,2-dinitroethyl}diazene** (**6**) from compound (**5**):

The same procedures were followed as for **4** except **5** [3.05 g (10 mmol)] was used in place of **3** to obtain pale purple prisms azo compound (**6**), (8%, recrystallized yield). These were recrystallized for single crystal X-ray analysis by slow evaporation from a solution of hexane and DCM (1:1) to obtain dark purple crystalline plates.Elemental analysis: ($C_4Br_2Cl_2N_8O_8$,

518.80) Calcd: C, 9.26%; N, 21.60%. Found: C, 9.70%; N, 21.38%. IR (KBr): 3448, 2920, 2887, 2364, 2342, 1596, 1336, 1294, 1205, 1020, 1000, 941, 921, 886, 831, 792, 724, 692, 653, 611 cm^{-1}.

Formation of **(E)-1-{(E)-2-bromo-1-(bromoimino)-2,2-dinitroethyl-2-{(E)-2-bromo-1-(chloroimino)-2,2-dinitroethyl}diazene** (**7**) from **5**:

The same procedures as for **6** were followed except 0.77g (3.33 mmol) of TCICA was used and added in one portion. The reaction was stirred at room temperature for six days to obtain a mixture of dark green prisms of **7** and colorless crystals of **5** and **9**. Compound (**7**) could be isolated by recrystallization; however, **5** and **9** were difficult to separate from each other. The verification of **9** was completed by ^{13}C-NMR. Compound (**7**) was recrystallized for single crystal X-ray analysis by slow evaporation from a solution of hexane and DCM (1:1) (9% recrystallized yield). Elemental analysis: ($C_4Br_{2.4}Cl_{1.6}N_8O_8$, 536.58) Calcd: C, 8.95%; N, 20.88%. Found: C, 8.85%; N, 19.37%. IR (KBr): 3505, 3430, 2926, 2884, 1594, 1336, 1293, 1188, 1103, 1012, 994, 941, 920, 886, 829, 790, 721, 690, 667, 651 cm^{-1}.

Formation of **2-chloro-N-methyl-2,2-dinitroacetimidamide** (**13**):

Compound (**11**)[10] (0.81g, 5 mmol) was dissolved in 50 mL MeCN. Then 0.385 g (1.66 mmol) TCICA (**2**) was added in small portions over a period of 10 minutes. The reaction was stirred for 2 hours. DCM (150 mL) was added to the solution and the organic phase was washed with a solution of aqueous sodium bicarbonate (0.4 M) (6 x 120 mL) to remove the cyanuric acid by-product. The collected organic phase was dried with anhydrous magnesium sulfate and concentrated to obtain chloro product (**13**), (71 % recrystallized yield). These were recrystallized for single crystal X-ray analysis by slow evaporation from a solution of hexane and DCM (1:1) to obtain colorless needles. Elemental analysis: ($C_3H_5ClN_4O_4$, 196.55) Calcd: C, 18.33%; H, 2.56%; N, 28.51%. Found: C, 18.01%; H, 2.33%; N, 27.34%. IR (KBr): 3441, 3323, 3232, 3014, 2966, 1645, 1596, 1522, 1454, 1413, 1354, 1311, 1182, 1153, 1117, 1082, 1007, 934, 833, 792, 754, 650, 632 cm^{-1}.

Formation of **(E)-N',2-dichloro-N-methyl-2,2-dinitroacetimidamide** (**14**):

The same procedure as for **13** was followed except 0.42 g (2.5 mmol) **11** was dissolved in 26 mL MeCN and 1.08 g (4.64 mmol) TCICA (**2**) was used. The organic phase was washed with a solution of aqueous sodium bicarbonate (0.4 M) (6 x 60 mL); chloro product (**14**), (90 % recrystallized yield). These were recrystallized for single crystal X-ray analysis by slow evaporation from a solution of hexane and DCM (1:1) to obtain colorless needles. Elemental analysis: ($C_3H_4Cl_2N_4O_4$, 230.99) Calcd: C, 15.60%; H, 1.75%; N, 24.26%. Found: C, 15.93%; H, 1.79%; N, 23.27%. IR (KBR): 3497, 3306, 2954, 2895, 2627, 2368, 1611, 1591, 1471, 1451, 1415, 1367, 1327, 1300, 1160, 1103, 1001, 936, 898, 827, 791, 735, 699, 650, 630, 579 cm^{-1}.

3.6.4 Theoretical studies

Energetic performances were calculated using Cheetah 6.0 and Explo 5.05. The heats of formation for all the compounds were calculated using Gaussian 03 (Revision D. 01).[6]The geometric optimization of the structures was based on single-crystal structures, and frequency analyses were carried out using the B3LYP functional with 6-31+G** basis set. Single-point energies were calculated at the MP2/6-311++G** level.[7] Atomization energies for compounds (**3**), (**5**), (**9**), and (**10**) were calculated using the G2 ab initio method.[8] All of the optimized structures were characterized to be true local energy minima on the potential energy surface without imaginary frequencies. The heats of formation for compound (**14**) and the other halogenated azo-bridge FOX-7 derivatives were determined using isodesmic reactions (Scheme 3.S1).

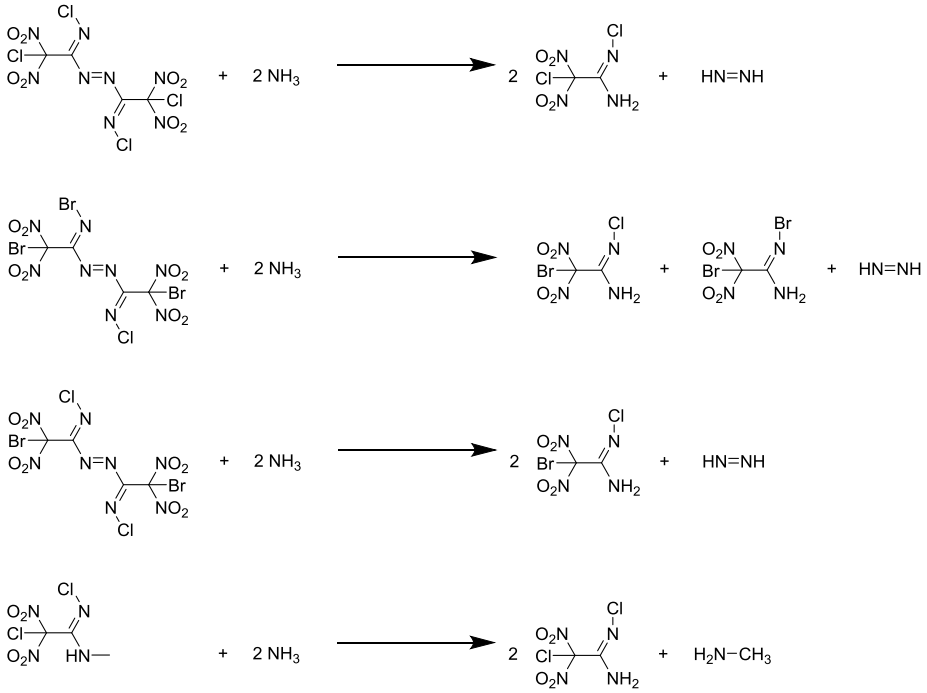

Scheme 3.S1 Isodesmic reactions for calculating heats of formation for compounds (**4)**, (**6)**, (**7**), and (**14)**.

The molar heats of formation for all the halogenated FOX-7 derivatives except for **10** and **13** are positive and exceed those of TNT, PETN, and RDX.

3.6.5 Infrared Spectra of 4.

Figure 3.S8 IR of Compound **4**.

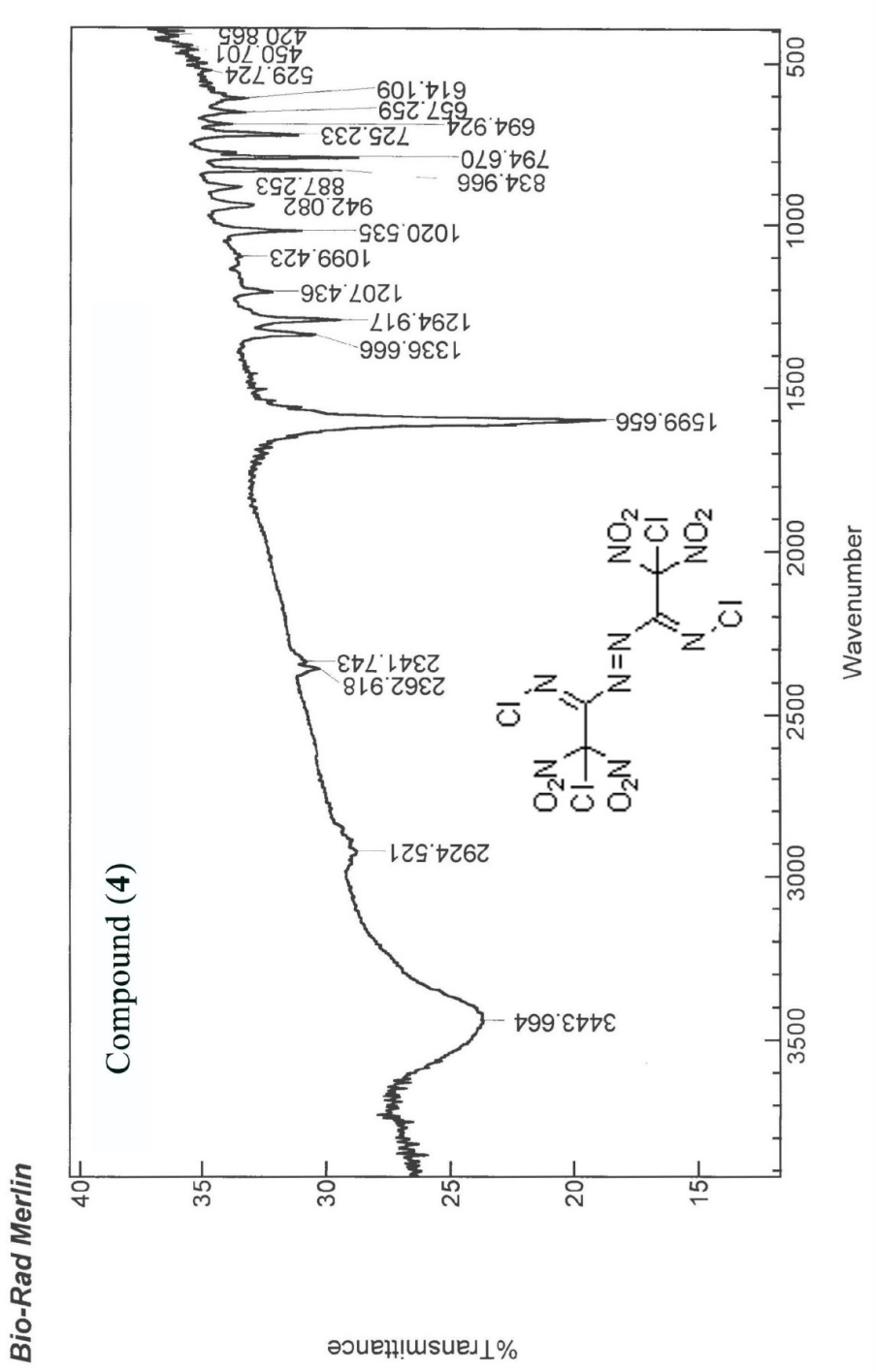

Figure 3.S9 IR of Compound **6**.

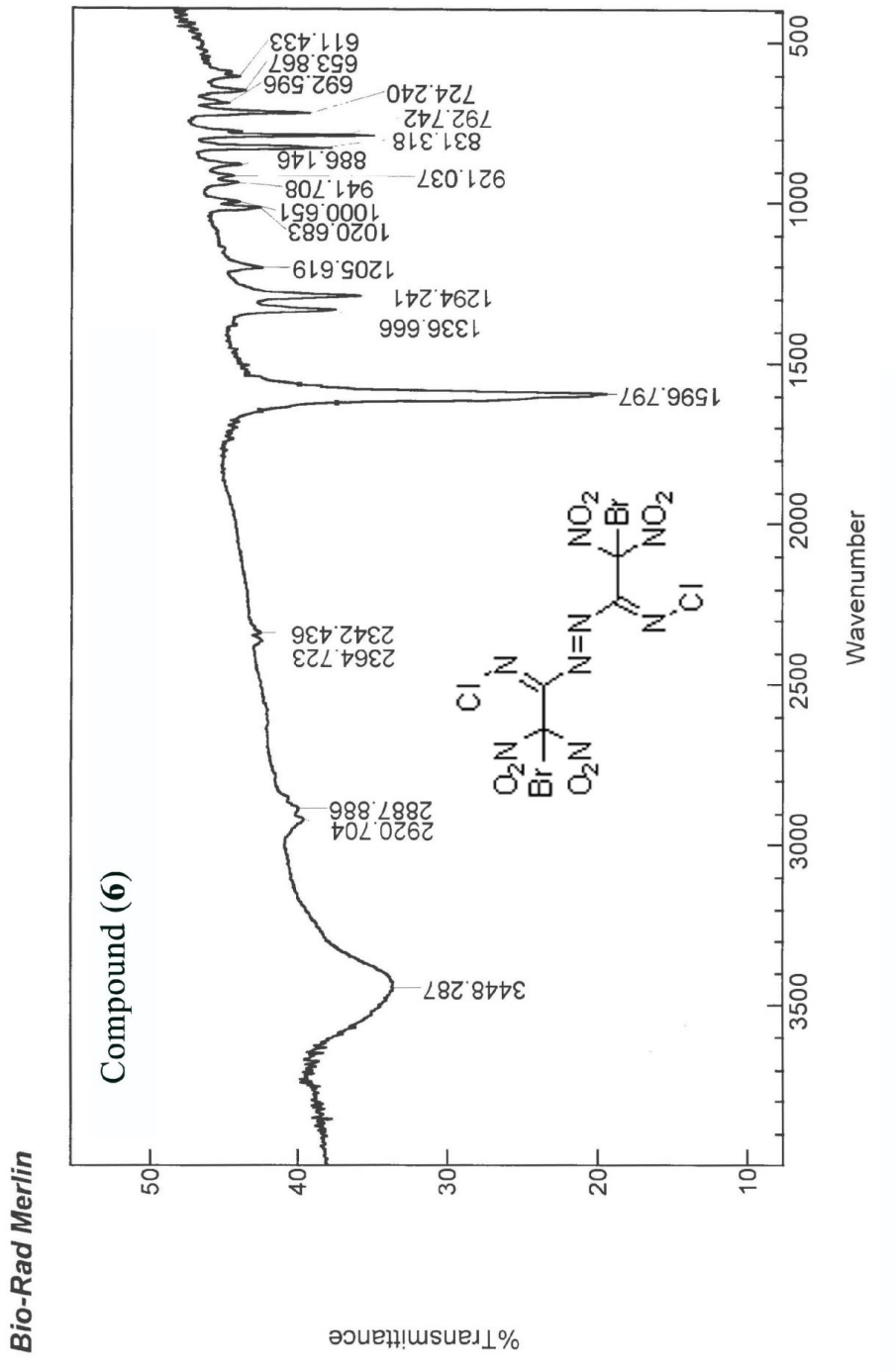

Figure 3.S10 IR of Compound **7**.

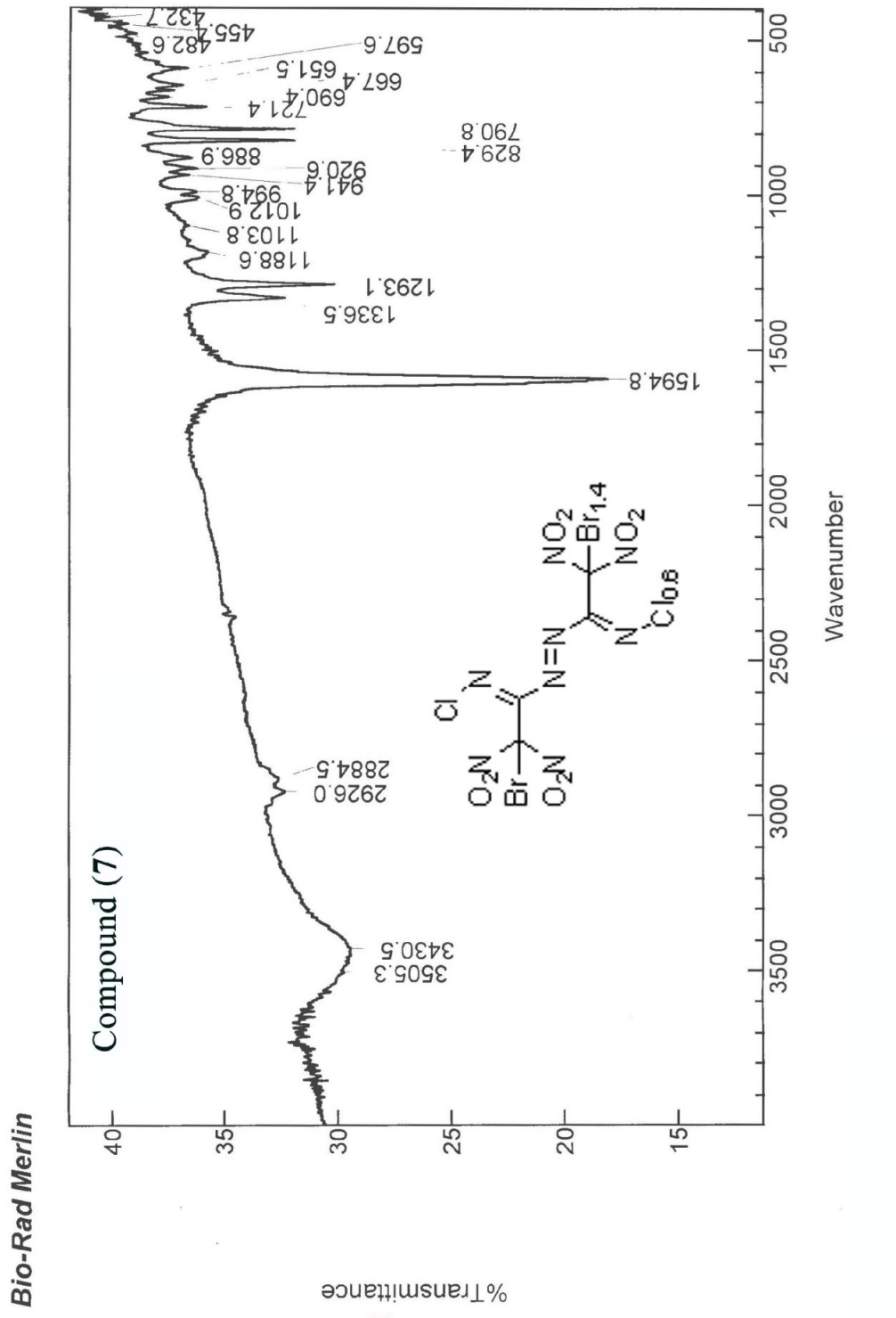

Figure 3.S11 IR of Compound **13**.

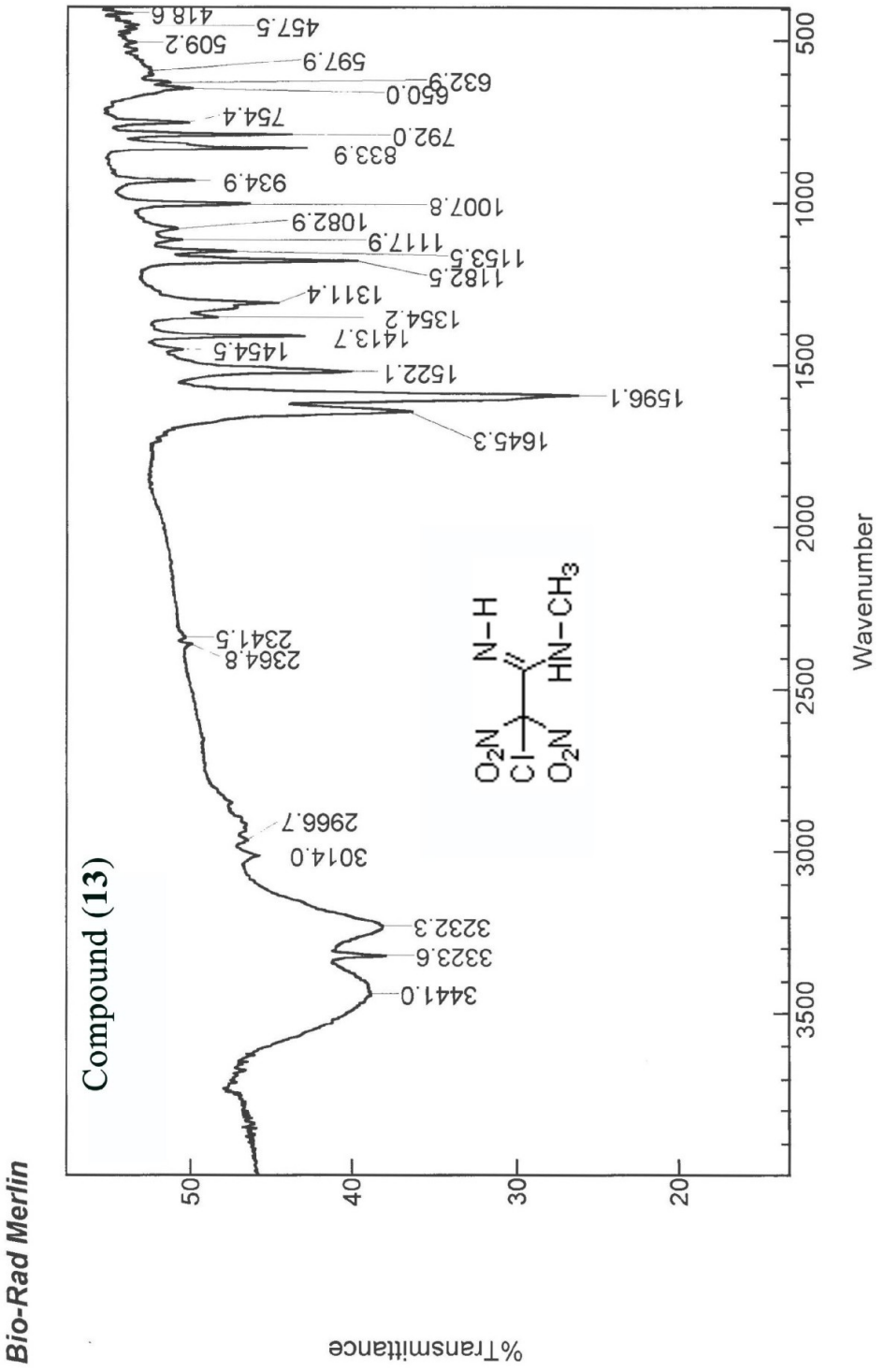

Figure 3.S12. IR of Compound **14**.

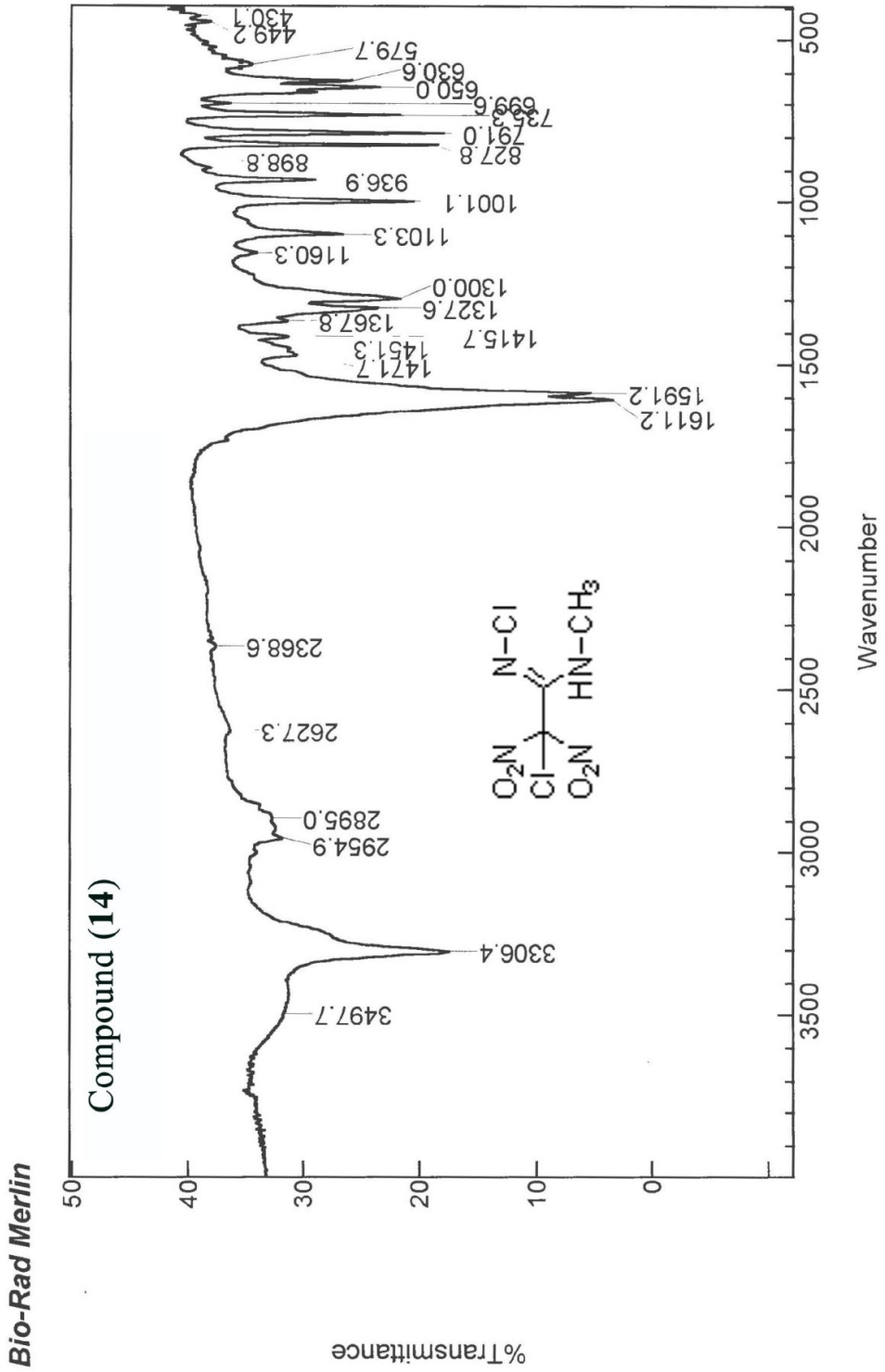

3.6.6 Differential Scanning Calorimetry (DSC) 5 °C /min:

Figure 3.S13. DSC of Compounds **3**, **5**, **13**, and **14**.

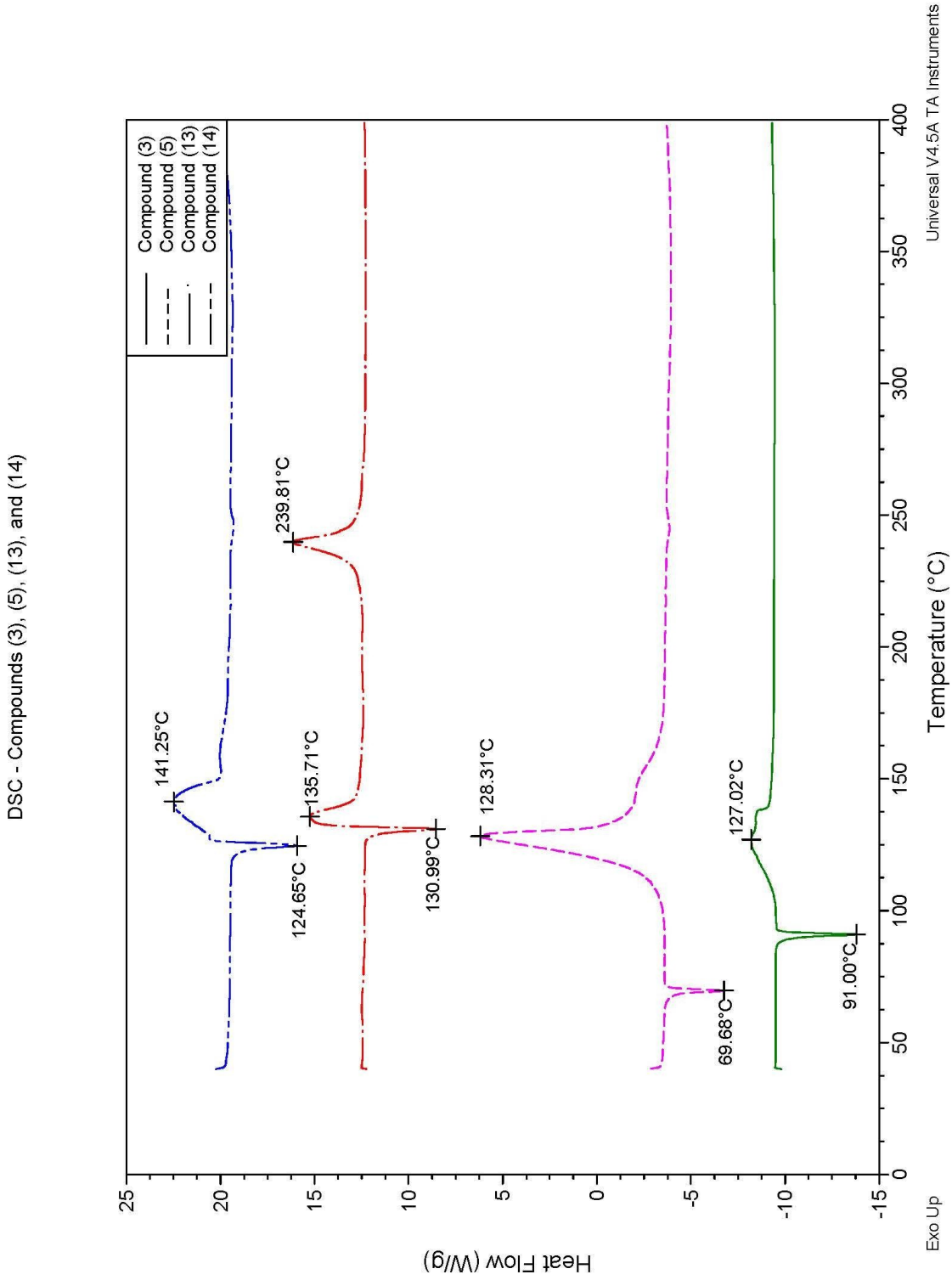

Figure 3.S14. DSC of Compounds 4, 6, and 7.

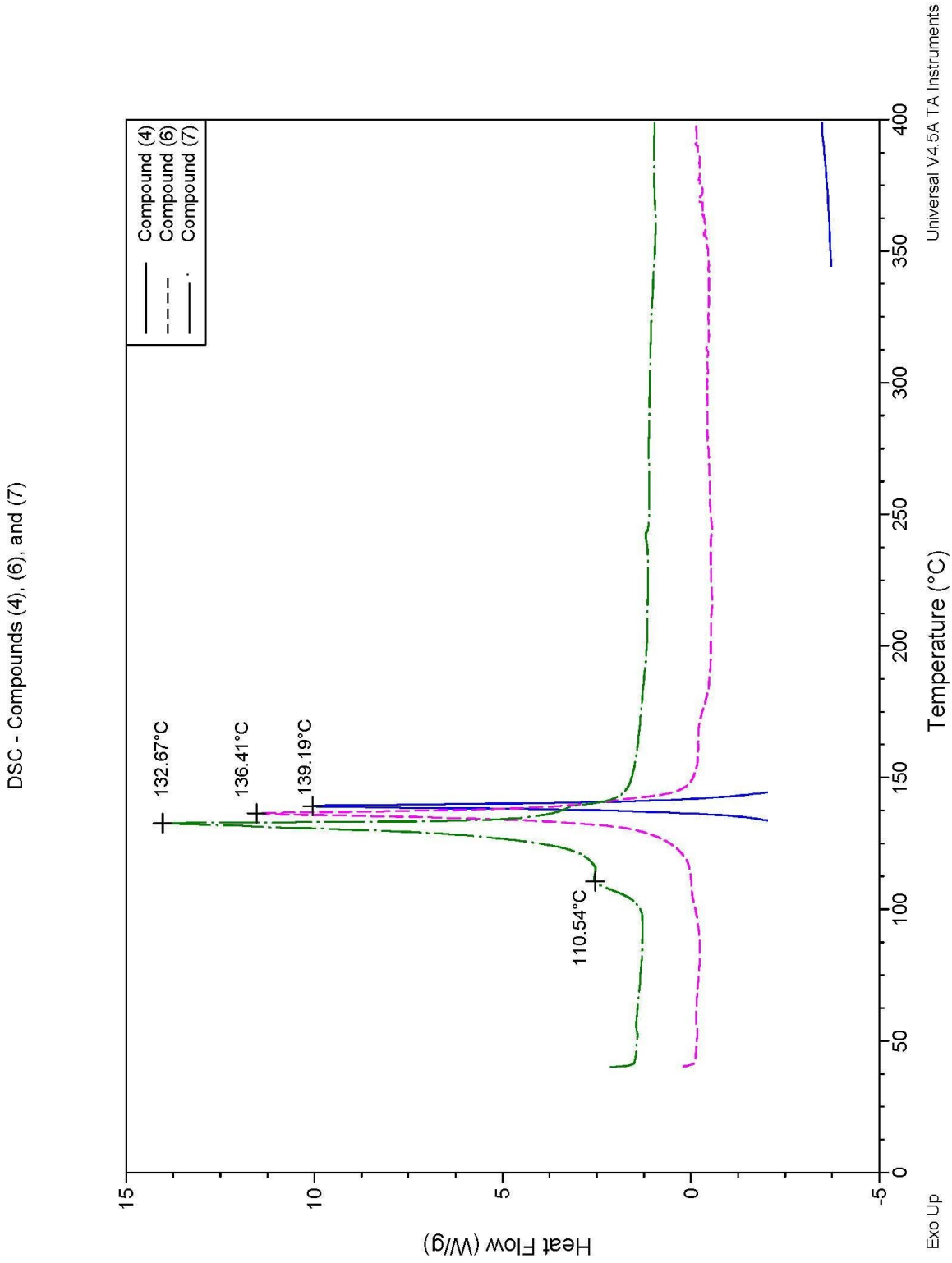

3.6.7 References

(1) Bruker (**2010**). Apex2 v2010.3-0. Bruker AXS Inc., Madison, Wisconsin, USA.

(2) Bruker (**2009**). SAINT v7.68A. Bruker AXS Inc., Madison, Wisconsin, USA.

(3) Bruker (**2008**). XPREP v2008/2. Bruker AXS Inc., Madison, Wisconsin, USA.

(4) Bruker (**2009**). SADABS v2008/1. Bruker AXS Inc., Madison, Wisconsin, USA.

(5) Bruker (**2009**). SHELXTL v2008/4. Bruker AXS Inc., Madison, Wisconsin, USA.

(6) Hervé, G.; Jacob, G.; Latypov, N. *Tetrahedron* **2005**, *61*, 6743– 6748.

(7) M. J. Frisch, G. W. Trucks, H. B. Schlegel, G. E. Scuseria, M. A. Robb, J. R. Cheeseman, J. A. Montgomery, T. V. Jr., K. N. Kudin, J. C. Burant, J. M. Millam, S. S. Iyengar, J. Tomasi, V. Barone, B. Mennucci, M. Cossi, G. Scalmani, N. Rega, G. A. Petersson, H. Nakatsuji, M. Hada, M. Ehara, K. Toyota, R. Fukuda, J. Hasegawa, M. Ishida, T. Nakajima, Y. Honda, O. Kitao, H. Nakai, M. Klene, X. Li, J. E. Knox, H. P. Hratchian, J. B. Cross, V. Bakken, C. Adamo, J. Jaramillo, R. Gomperts, R. E. Stratmann, O. Yazyev, A. J. Austin, R. Cammi, C. Pomelli, J. W. Ochterski, P. Y. Ayala, K. Morokuma, G. A. Voth, P. Salvador, J. J. Dannenberg, V. G. Zakrzewski, S. Dapprich, A. D. Daniels, M. C. Strain, O. Farkas, D. K. Malick, A. D. Rabuck, K. Raghavachari, J. B. Foresman, J. V. Ortiz, Q. Cui, A. G. Baboul, S. Clifford, J. Cioslowski, B. B. Stefanov, A. L. G. Liu, P. Piskorz, I. Komaromi, R. L. Martin, D. J. Fox, T. Keith, M. A. Al-Laham, C. Peng, A. Nanayakkara, M. Challacombe, P. M. W. Gill, B. Johnson, W. Chen, M. Wong, C. Gonzalez, J. A. Pople, *Gaussian 03, Revision D. 01*, Gaussian, Inc., Wallingford, CT, 2004.

(8) R. G. Parr, W. Wang, Density Functional Therory of Atoms and Molecules, Oxford University Press, New York 1989.

Chapter 4

1,1-Diamino-2,2-dinitroethylene (FOX-7) and 1-Amino-1-hydrazino-2,2-dinitroethene (HFOX) as Amphotères: Bases with Strong Acids

by

Thao T. Vo, Damon A. Parrish, and Jean'ne M. Shreeve

Has been submitted for publication to

Journal of American Chemical Society

Abstract:

The exciting discovery of the first cations based on 1,1-diamino-2,2-dinitroethene (FOX-7) and its hydrazine derivative, 1-amino-1-hydrazino-2,2-dinitroethene (HFOX), along with their syntheses and full characterization is described. The oxygen rich content of these cations lends to their potential as promising precursors for energetic salts. A variety of acids including triflic, perchloric, and hydrochloric acids were found to react with FOX-7 and HFOX to give rise to the following salts: 1-amino-2,2-dinitroethaniminium triflate (**3a**), 1-amino-2,2-dinitroethaniminium perchlorate (**3b**), 1-amino-1-hydrazino-2,2-dinitroethaniminium triflate (**4a**), and1-amino-1-hydrazino-2,2-dinitroethaniminium chloride (**5**). Additionally, it was also learned that HFOX reacts with acetone to generate the corresponding hydrazone derivative, 2,2-dinitro-1-(2-(propan-2-ylidene)hydrazinyl)-ethenamine (**9**). The structures of the salts (except **5**) and hydrazone **9** are supported by single crystal X-ray analysis. These compounds have thermal stabilities ranging between 74 °C – 147 °C and crystal densities between 1.53 gcm^{-3}–1.94 gcm^{-3}. The isolation of these novel FOX-7 and HFOX cations are interestingly important as it: 1) extends the chemistry of FOX-7 and HFOX, 2) demonstrates the amphoteric properties of FOX-7 and HFOX, and 3) gives rise to new forms of FOX-7 and HFOX, which opens to study their potential as promising precursors for energetic salts. All the salts were found to have energetic properties that exceed that of TNT and some are comparable to FOX-7 and RDX, indicating that the cations of FOX-7 and HFOX may contribute to more energetic salts if parlayed with appropriate counter anions. The significance of this work demonstrates that the chemistry of FOX-7 continues to be profound and worthwhile.

4.1 Introduction

The development of efficient and environmentally friendly energetic materials tailored for applications such as propellants, pyrotechnics, and explosives has long been at the forefront of energetic materials research. The balance between high energy and safety constitutes a challenging task for scientists and researchers worldwide. A major breakthrough was the development of 1,1-diamino-2,2-dinitroethene (FOX-7), an insensitive high explosive exhibiting excellent energetic properties including high density, high thermal stability and high detonation performance.[1-5] The extensive hydrogen bonding displayed by FOX-7 leads to the stabilization of this molecule resulting in insensitivity towards external stimuli – an ideal characteristic of safety for an energetic material.

Significant interest in FOX-7 stems from its potential to replace some currently used explosives that suffer from high sensitivity and are deemed environmentally toxic. FOX-7's lack of reaction predictability has also captured interest among academic and industrial chemists. Its poor solubility in most organic solvents contributes to the many challenges of studying FOX-7. Therefore, studies of its reaction chemistry are still quite limited, which suggests that this field is far from being fully explored. Physicochemical properties of FOX-7 including the thermodynamic, mechanical, and explosive properties have been vigorously examined with the aim of gaining a deeper understanding of the chemical reactivity and feasibility of synthesizing new FOX-7- based susbtrates.[1, 5-8]

Considerable effort has been made by our group to expand the chemistry of FOX-7 and its derivatives. Prior to our work, the only known metal chemistry of FOX-7 was its potassium salt.[7a,8a-c] We initiated the synthesis of a series of FOX-7 based metal complexes (silver,[7a] copper,[7a,8a-b] and nickel[8b-c]) in order to understand its reaction behavior. These metal complexes demonstrated that FOX-7 behaved either as an inner-sphere or outer-sphere ligand, depending on the amine additive used to stabilize the complex. In our more recent work, a series of halogenated azo-bridged FOX-7 derivatives were synthesized by the reactions of FOX-7 with chlorine-based oxidizing reagents such as N-chlorosuccinimide or trichloroisocyanuric acid (TCICA).[8d] One of the most exciting aspects of these new halogenated derivatives of FOX-7 is the promising potential application as hypergolic oxidizers in the field of propellants. The azo-bridged substrates represent the first isolated

azo-derivatives of FOX-7 and the first example of FOX-7 derivatives displaying hypergolic properties (as hypergolic oxidizers).

In continuing efforts to extend the study of FOX-7, it was realized that the chemistry of FOX-7 (**1**) and its hydrazine derivative, 1-amino-1-hydrazino-2,2-dinitroethene (HFOX, **2**), with bases to generate the corresponding anionic substrates (**1b** and **2b**) was well established (Scheme 4.1). However, to our surprise, limited reports were found that describe the studies of **1** and **2** with acids to obtain the corresponding cationic substrates.[9] A protonated form of the HFOX species (**2c** in Scheme 4.1) had been suggested to form at pH values < 2; however,

Scheme 4.1. Different forms of FOX-7 and HFOX under varying pH conditions.

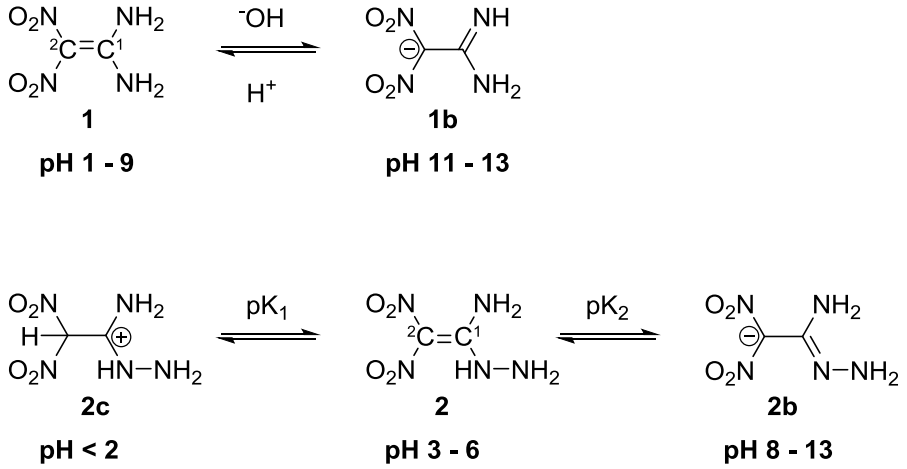

this was only observed in UV studies and the material was never isolated. Protonated FOX-7 was not mentioned. The isolation of such species is of great interest due to the opportunity to study a new form of FOX-7 and these cation-containing molecules have potential as promising precursors that may enhance the properties of energetic salts. Our initial calculations indicated the potential of FOX-7 and HFOX cations as suitable ions for energetic salts. For example, when counter anions such as nitrate, trinitromethanide, dinitroamide, and 3-nitro-1,2,4-triazol-5-one (NTO) were considered, the detonation performances were found to exceed that of FOX-7 and some standard explosives such as RDX (cyclo-1,3,5-trimethylene-2,4,6-trinitramine) and TNT (trinitrotoluene) (see Supporting Information).

Now we describe our study to extend the chemistry of FOX-7 by the syntheses of salts containing the first cationic species of both FOX-7 and HFOX. These salts were synthesized by reacting the parent compounds with a variety of strong acids to illustrate the amphoteric properties of **1** and **2**. The syntheses, full characterization, and theoretical investigation of these new salts were carried out in order to determine their properties and usefulness as building blocks for energetic salts.

4.2 Results and Discussion

The reactions of **1** and **2** with acids having acid dissociation constant values (pKa) ranging between ~0.17 to -15 were examined. It was found that acids with pKa values more negative than or equal to -10 were sufficiently acidic to protonate **1**. In contrast, the protonation of **2** occurs more readily due to the basic hydrazine group in the molecule, and the protonated salt is easily formed by acids with pKa values more negative than -7. For the protonated products of **1**, there are two possible forms (**1a** and **1b**); however, three possible cationic structures (**2a-c**) could be produced upon the protonation of **2** (Scheme 4.2). Based on single crystal X-ray analysis (see discussion vide infra), it was learned that the proton was

Scheme 4.2. a) Possible protonation sites of FOX-7 (1a – 1b).

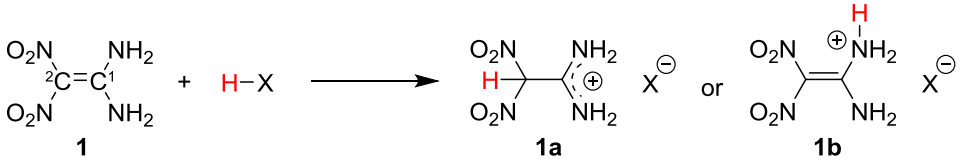

b) Possible protonation sites of HFOX (2a – 2c).

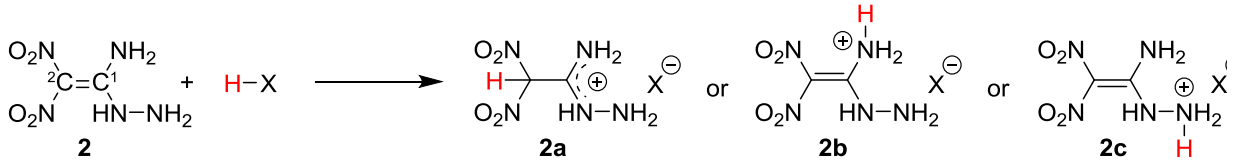

introduced at the C2 carbon for both **1** and **2**, leading to the formation of only salts **1a** and **2a**.

Compounds **1** and **2** were first treated with an excess of triflic acid (CF_3SO_3H; pKa = -15) under neat conditions at 25 °C to yield salts (white powders), **3a** and **4a** (Scheme 4.3).

Scheme 4.3. Reaction of FOX-7 and HFOX with triflic and perchloric acid.

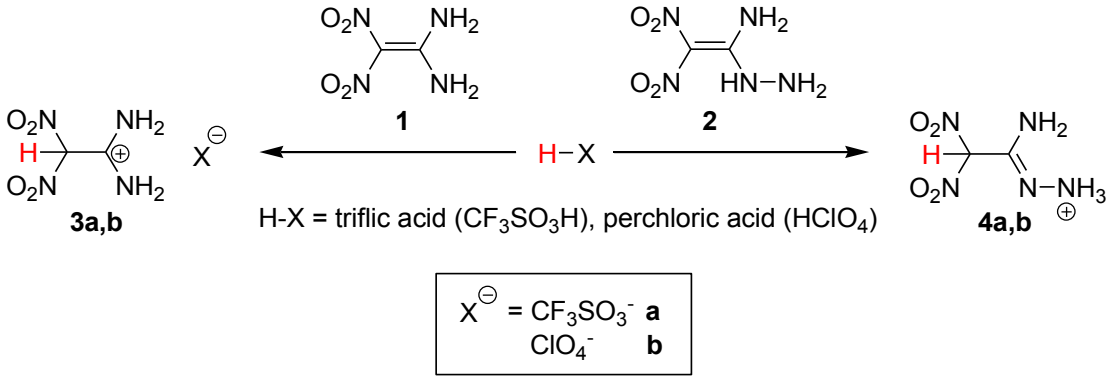

The addition of anhydrous acetonitrile to the reaction mixture resulted in colorless prisms after the solvent was removed under vacuum (Figure 4.1a). Both of these salts are highly

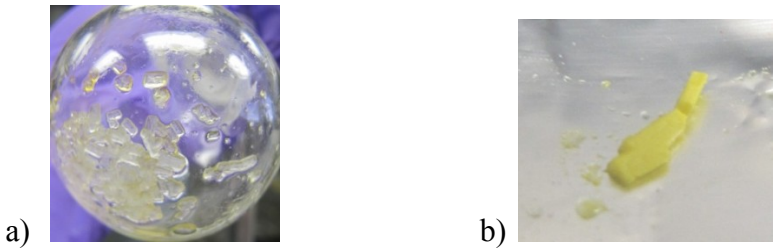

Figure 4.1. a) Crystals of salt **3a;** and b) crystals after exposure to air to form FOX-7 (**1**).

hygroscopic (typical of triflate salts),[10] but can be handled under nitrogen in hexane and stored for several months in hexane at -20 °C without decomposition. Exposure to moisture causes both salts to revert to **1**. This was confirmed when the colorless salt **3a** became yellow upon being exposed briefly to moisture (Figure 4.1b). The yellow solid was identified as FOX-7 based on infrared spectroscopy. The same phenomenon was observed for salt **4a**. Structural

identification of the triflate salts **3a** and **4a** are supported by single crystal X-ray analysis, IR, and differential scanning calorimetry (DSC).

Due to the lack of compatibility of perchloric acid ($HClO_4$) with organic solvents, the reactions of **1** and **2** with $HClO_4$ (pKa = -10) were carried out neat. Substrates **1** and **2** were suspended in an excess of $HClO_4$, and heated gently at 80 ºC briefly until each one had dissolved. The reaction was continued at this temperature for an additional two minutes and the mixture was allowed to stir at room temperature for 10 – 15 minutes. After removal of the majority of the excess acid in vacuo over an extended period, the perchlorate salts **3b** (supported by single crystal X-ray analysis) and **4b** were isolated as colorless crystals (Scheme 4.3). Crystals of **3b** were more stable to handling at room temperature than the HFOX perchlorate salt, **4b,** which is believed to have formed, but because of low stability, verification of its structure by X-ray analysis was not possible. Based on spectral and thermal analysis (see discussion vide infra), it was concluded that salt **4b** may have been formed initially, but rapidly decomposed to ammonium perchlorate (shown by X-ray crystal structure analysis). Similar to the triflate salts, these perchlorate salts began to change from solids to liquids within half an hour when stored at room temperature with or without a nitrogen atmosphere. The perchlorate salt **3b** can be stored at -20 °C over several months without decomposition while the perchlorate salt **4b** begins to undergo decomposition within ~ 24 hours after formation regardless of temperature.

Compounds **1** and **2** were also treated with an excess of 12 M hydrochloric acid (HCl). The reaction of **1** dissolved in dry acetonitrile with concentrated HCl (pKa = -7), as well as with HCl_g in anhydrous methanol, did not result in the isolation of the corresponding chloride salt. When the excess acid and solvent were removed, **1** was recovered. The unsuccessful formation of the desired salt may be that hydrochloric acid is not sufficiently acidic to protonate **1** or the salt is too unstable to be isolated. Thus protonation of **1** was observed only with acids having pKa values more negative than or equal to -10.

An excess of HCl_g was bubbled into the yellow suspension of **2** in anhydrous methanol under nitrogen. Within ten minutes with stirring, the solution became colorless and a white suspension formed. Upon removal of the excess acid and solvent in vacuo, pale yellow salt **5** was formed. It is believed that the chloride salt (**5**) formed based on elemental analysis, DSC, and IR spectra. Salt **5** has poor solubility in common organic solvents, is

sensitive to water, and was found to be unstable similar to **2** – very often spontaneously combusting within ~12 hours after forming. Therefore, extreme caution should be observed while attempting to synthesize **5**, even on a small scale. NMR spectral analysis and suitable crystals of salt **5** were difficult to obtain due to its poor solubility and unstable nature. Indirect attempts to confirm **5** were made via the metathesis of salt **5** with silver FOX-7 (**6**)[8a] (Scheme 4.4).

An equal molar amount of **6** was added to a suspension of **5** in anhydrous methanol under nitrogen. The reaction was protected from light due to the light sensitivity of **6**. After stirring for four hours, the suspension was filtered and analyzed to be a mixture of a product, unreacted starting material and silver chloride (**8**) which was verified via powder X-ray analysis. The filtrate was concentrated to give a yellow solid believed to be **7**. Different reactions resulted in **7** forming either as a powder or microcrystals that were not suitable for X-ray analysis. The composition of **7** was initially suggested by the confirmation of **8**, DSC and IR. However, attempts to obtain a suitable crystal for X-ray analysis from solvents such as DMSO, dichloromethane, and methanol were unsuccessful. In DMSO, **1** and **2** were isolated (Scheme 4). Recrystallization in acetone gave rise to crystals of hydrazone **9** [2,2-dinitro-1-(2-(propan-2-ylidene)hydrazinyl)ethenamine]. It is proposed that in solution, some **2** formed and further reacted with acetone leading to **9**. A control was carried out in which **2**

Scheme 4.4. Attempted synthesis of salt 7 and the synthesis of hydrazone 9.

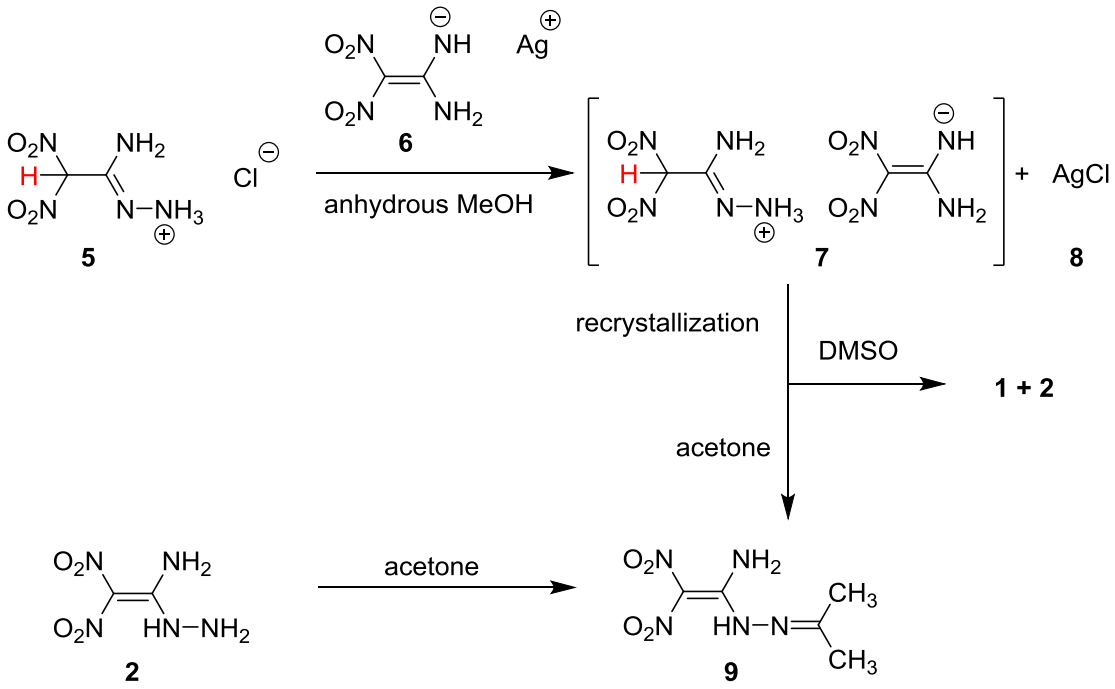

was dissolved in acetone and the solution was allowed to evaporate slowly overnight. Yellow prisms formed which were verified to be **9** by elemental analysis, IR, DSC and single crystal X-ray analysis (Scheme 4.4). Reaction of **2** with DMSO has not been reported. Typical analysis of **2** and its derivatives are carried out via NMR in d_6-DMSO.[5] Salt **7** may have formed; however, the salt may have undergone proton exchange to generate the more stable neutral compounds **1** and **2**. The isolation and identification of silver chloride (**8**) further lends support to the formation of salts **5** and **7**.

Single crystal X-ray analyses were used to verify all the new compounds excluding salts **4b**, **5** and **7**. All salts crystallized as colorless prisms and compound **9** as yellow prisms. The crystal structures of triflate salts **3a** and **4a** are given in Figure 2. Salt **3a** crystallizes in the monoclinic space group P1 2_1/c1 with four molecules per unit cell and has a crystal density of 1.94 g/cm^3 (Figure 4.2a). The C2 carbon bearing the nitro groups is protonated rather than either of the amine moieties. The cationic C-C bond distance (1.52 Å) agrees with the reported average bond distance for C-C (1.54 Å) single bonds. However, the C-N bond lengths in salt **3a** (C1-N3, 1.30 Å; C1-N4, 1.31 Å) are shorter than the average C-N single bond (1.47 Å) and longer than the average C=N double bond (1.22 Å).[12]This indicates that the

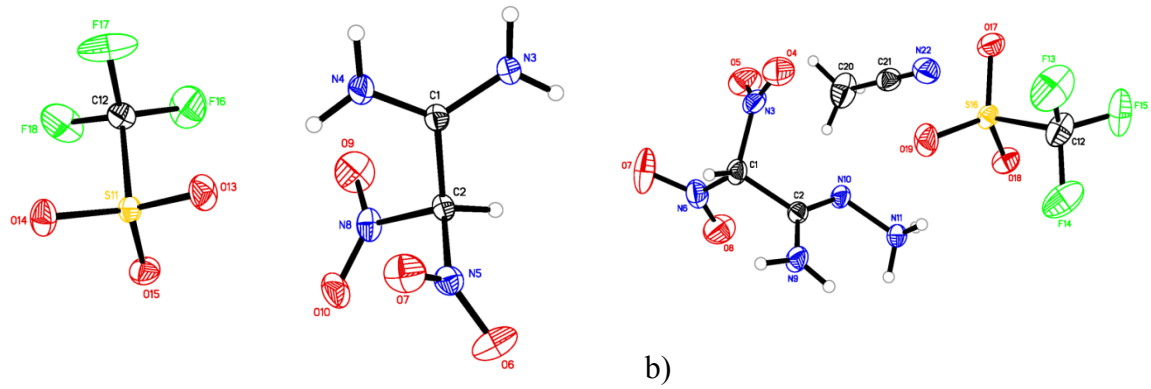

a) b)

Figure 4.2. Thermal ellipsoids plots shown at 50% a) triflate salt **3a;** and b) triflate salt **4a** with one molecule of acetonitrile.

positive charge is delocalized over the atoms N4-C1-N3. The bond angle of $-C(NO_2)_2$ [N5-C2-N8, 108°] in **3a** is significantly compressed compared to the $-C(NO_2)_2$ of **1** (N11-C1-N12, 116°) due to the incorporation of the proton at the C2 position.[11] This also results in the compression of the bond angle of C1-C2-N8 (111°) and C1-C2-N5 (112°) compared to the corresponding angles in **1** [C1-C2-N11 (124°) and C1-C2-N12 (120°)].[11] An effect of that compression leads to the slight expansion of the $-C(NH_2)_2$ bond angle (N3-C1-N4, 124°) compared to the corresponding $-C(NH_2)_2$ bond angle of FOX-7 (N21-C2-N22, 118°).[11]

Salt **4a** crystallizes with one molecule of acetonitrile in the triclinic space group P-1 system (Figure 4.2b). It is composed of two molecules per unit cell and has a crystal density of 1.68g/cm^3. The C-C single bond distance (1.51 Å) of the HFOX cation has significantly increased from the C=C double bond distance (1.34 Å) in **2** and agrees with the reported average bond distance for C-C single bonds. Similar to salt **3a**, the C-N bond length in **4a** (C2-N9, 1.32 Å; C2-N10, 1.29 Å) is between that of a single C-N and double C=N bond, which supports the positive charge being delocalized over the atoms N9-C2-N10.[12] As observed in **3a**, the $-C(NO_2)_2$ bond angle in **2** (N4-C2-N4A, 124°) is also compressed in **4a** (N3-C1-N6, 108°) with the addition of the proton. The bond angle of N9-C2-N10 (132°) is opened compared to **2** (N1-C1-N3, 122°) due to the proton shift of N10 to N11.

Perchlorate salt **3b** crystallizes in the triclinic P-1 space group with twelve molecules per unit cell (Figure 4.3a) and a crystal density of 1.94 g/cm^3. There are six unique ionic pairs

with one displaying some disorder (Figure 4.3b). The single bond distance of C1A-C2A (1.51 Å) is consistent with the reported average value and the FOX-7 cation in **3a**. The single bond

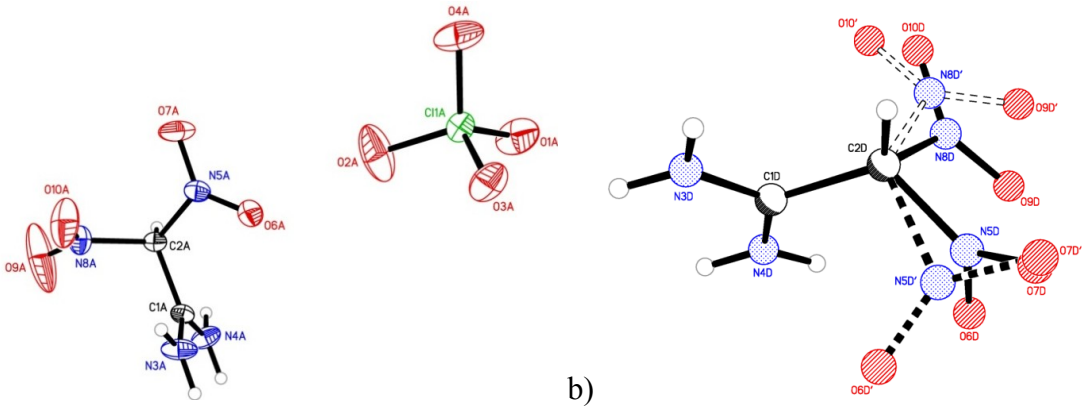

a) b)

Figure 4.3. Thermal ellipsoids shown at 50% a) perchlorate salt of FOX-7 **3b;** and b) the disorder of cation **3b**.

distance of C1A-C2A (1.51 Å) is consistent with the reported average value and the FOX-7 cation in **3a**. The bond angle of N5A-C2A-N8A (108º) is also in agreement with the $-C(NO_2)_2$ moiety in **3a**. The delocalized positive charge over N3A-C1A-N4A is supported by the observed C-N bond length (C1A-N3A, 1.31 Å; C1A-N4A, 1.30 Å).

The instability of **4b** was further observed during attempts to obtain X-ray analysis. Collecting crystal data for this salt was very difficult. Aside from its sensitivity to moisture and its instability for extended periods at room temperature, crystals of salt **4b** reacted immediately upon contact with the mounting material (paratone oil). When the crystals were mounted with glue, they were stable and the analysis showed that **4b** had decomposed to form ammonium perchlorate. Suitable crystals of **7** were difficult to obtain since the salt reacted with most solvents. As mentioned vide supra, attempts to recrystallize **7** in acetone led to the formation and isolation of the hydrazone, **9**, which was further verified by a control reaction. Compound **9** crystallizes in the triclinic P-1 space group with two molecules per unit cell and has a crystal density of 1.53 g/cm^3 (Figure 4.4). Each molecule is stacked in alternative orientations as can be seen in the packing diagram. Hydrogen bonding between the amino moiety and NH of the hydrazine substituent with the oxygen atoms from one of the nitro groups helps stabilize the system.

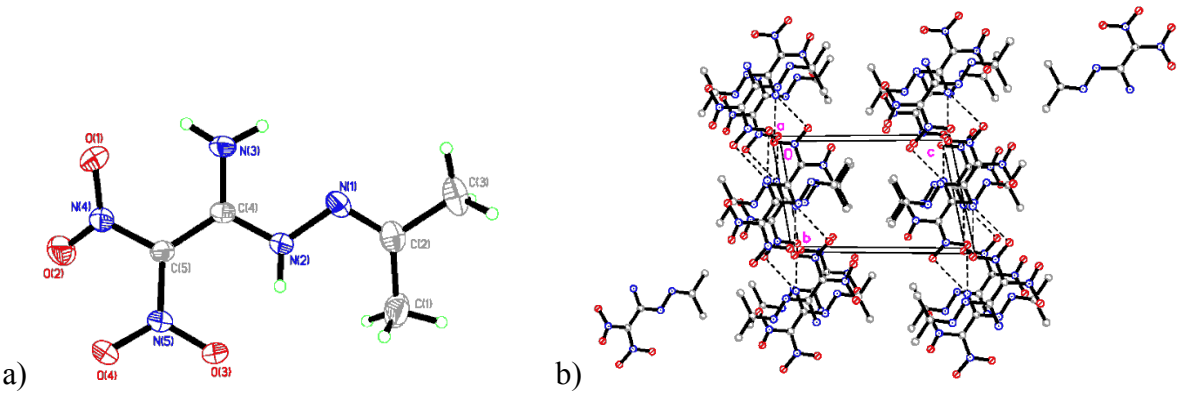

Figure 4.4. Thermal ellipsoids shown at 50% a) compound **9;** and b) the packing diagram of compound **9** along the a-axis where the dotted lines represent hydrogen bonding.

The physical properties for all the structures and standard energetic properties for comparison are reported in Table 4.1. The thermal stability (onset temperature) of all compounds presented were evaluated via differential scanning calorimetry (DSC). All the compounds are less thermally stable than **1** and decompose without melting. An observable trend among the salts shows that those containing FOX-7 cations are less thermally stable (**3a**, T_{dec} = 74 °C; **3b**, T_{dec} = 76 °C) than those containing HFOX cations (**4a**, T_{dec} = 118 °C; **4b**, T_{dec} = 120 °C; **5**, T_{dec} = 60 °C,) with the exception of salt **5** (Table 4.1). As mentioned earlier, the chemical instability of **4b** made the structural verification via crystal structure difficult as the product decomposed to the more stable ammonium perchlorate. It is believed that **4b** was isolated initially due to the observed onset decomposition temperature at 120 °C and subsequently decomposed to ammonium perchlorate. The onset decomposition of **4b** was observable along with peaks belonging to ammonium perchlorate[13,14](T_{dec} = 350 °C). Infrared spectroscopy also supports the observation of salt **4b** decomposing to ammonium perchlorate. Compound **9** (T_{dec} = 147 °C) was found to be more thermally stable than **2**. The increased thermal stability is to be expected due to the additional stabilization effect of the methyl groups.

For energetic materials, density is one of the most important physical properties.[1,5]The densities range from 1.53 gcm^{-3} for **9** to 1.98 gcm^{-3} for **4a**. The crystal densities of **4b** and **5** were not obtained and therefore calculated using a reliable method published by our group.[15a] For comparison, densities of salts **3a**, **3b**, and **4a** were calculated using this method and the results were found to be significantly close to the calculated crystal densities (Table 4.1).

Table 4.1. Physical properties of salts 3a, 3b, 4a, 4b, and 5.

	FOX-7 cation salts		**HFOX cation salts**			**Standard explosives**[a]		
	3a	**3b**	**4a**	**4b**	**5**	**TNT**[b]	**FOX-7**	**RDX**[c]
ρ^d (gcm^{-3})	1.94	1.94	1.98[e]	-	-	1.65	1.88	1.82
ρ^f (gcm^{-3})	1.94	1.94	1.98	1.84	1.64	-	-	-
T_d^g (°C)	74	76	118	120	60	295[h]	274[h]	230[h]
OB[i] (%)	-10.7	12.9	-12.8	9.1	-20.0	-74.0	-21.6	-21.6
$\Delta H_{f(cation)}{}^j$ (kJ/mol)	-659.7	-659.7	799.5	799.5	799.5	-	-	-
$\Delta H_{f(anion)}{}^k$ (kJ/mol)	-244.3	-1411.1	-244.3	-1411.1	-230.3[l]	-	-	-
$\Delta H_f{}^m$(kJ/mol) / (kJ/g)	-1230.1/ -4.13	-86.1/ -0.35	-1086.6/ -3.47	67.8/ 0.26	61.1/ 0.31	-59.3/ -0.26	-134.1/ -0.91	70.3/ 0.32
P^n (GPa)	19.3	32.6	21.9	32.0	23.7	21.3	35.2	35.8
D^o (ms^{-1})	6784	8485	7219	8482	7657	7304	8771	8864
Isp[p] (s)	202	249	213	263	250	211	240	267

a) Properties were obtained and calculated from Explo5 v6.01. b) Trinitrotoluene (TNT). c) Cyclo-1,3,5-trimethylene-2,4,6-trinitramine (RDX). d) Crystal density. e) Corrected density by subtracting the volume of an acetonitrile molecule [v(MeCN) 87 $Å^3$].[15]f) Calculated density [ref. 15]. g) Thermal decomposition temperature (onset temperature). h) [ref. 8d]. i) Oxygen balance (OB). j) Cation heat of formation. k) Anion heat of formation. l) [ref 15c]. m) Heat of formation. n) Detonation pressure. o) Detonation velocity. p) Specific impulse [calculated at an isobaric pressure of 70 bar and initial temperature of 3,300 K].

Therefore it can be concluded that the calculated densities of salts **4b** and **5** are reliable. The densities of **3a**, **3b**, **4a**, and **4b** are greater than **1**, TNT and RDX, and that of **5** is comparable to TNT.

Using the densities and calculated heats of formation (see Supporting Information), the energetic properties of all the new salts were calculated using the program Explo5 v6.01. In addition, the energetic properties of **1**, TNT, and RDX were also calculated for comparison. The detonation pressures of the salts ranged from 19.3 GPa to 32.6 GPa. With the exception of **3a**, the detonation pressures of all salts exceed TNT and the perchlorate salts **3b** and **4b** are close to **1** and RDX. The detonation velocities of the salts range from 6784 ms^{-1} to 8485 ms^{-1}. Salts **3b**, **4a**, **4b**, and **5** are either comparable to or exceed TNT and salt **3b** is close to that of **1**

and RDX. The specific impulse (Isp), a measure of a propellant's efficiency (in seconds), was also calculated for all the salts. The Isp ranged from 202s to 257 s, with all salts (except **3a**) exceeding TNT. Salts **3b**, **4b**, and **5** have Isp values greater than **1**. Among all the salts, the detonation velocities, detonation pressures and Isp values of **3b** and **4b** are the most promising as energetic salts since their energetic performance is close to that of **1**, demonstrating the potential of FOX-7 and HFOX cations as good counter ions for energetic salts.

4.3 Conclusion

In summary, we report the exciting discovery of the first isolated cationic FOX-7 and HFOX salts (**3a**, **3b**, **4a**, and **5**) as well as hydrazone **(9)** that have been synthesized and fully characterized by single crystal x-ray analysis (except **5**). These compounds have thermal stabilities ranging from 74 °C – 147 °C and crystal densities ranging between 1.53 gcm^{-3} – 1.94 gcm^{-3}. Although their hygroscopic nature makes handling difficult, the isolation of the cationic derivatives of **1** and **2** is of great importance in demonstrating the amphoteric properties of FOX-7 and HFOX. The advantage of the cations based on **1** and **2** includes increased oxygen content for energetic precursors. These oxygen rich cations may aid in enhancement of future energetic performance if they can be parlayed with an appropriate counter anion that will further stabilize the cations. All the salts have been calculated to have energetic properties that exceed TNT and some are comparable to **1** and RDX showing the great potential of these energetic salts based on cations of **1** and **2**. The discovery of these new cationic structures contributes significantly to the expansion and understanding of the chemistry of FOX-7, demonstrating there is still much to learn!

ASSOCIATED CONTENT

Supporting Information

Experimental procedures, characterization data (single crystal X-ray), heat of formation calculations and energetic performances for salts containing counter anions - nitrate, trinitromethanide, dinitroamide, and 3-nitro-1,2,4-triazol-5-one (NTO). This material is available free of charge via the Internet at http://pubs.acs.org.

AUTHOR INFORMATION

Corresponding Author

jshreeve@uidaho.edu

Notes

The authors declare no competing financial interest.

ACKNOWLEDGMENTS

The authors gratefully acknowledge the support of ONR (N00014-12-1-0536 and N00014-11-AF-0-0002), Dr. Clifford Bedford, and the Defense Threat Reduction Agency (HDTRA 1-11-1-0034). We are indebted for Mr. Scott Economu and Dr. Brendan Twamley for considerable assistance with crystal structuring.

4.4 References

(1) (a) Latypov, N. V.; Bergman, J.; Langlet, A.; Wellmar, U.; Bemm, U. *Tetrahedron* **1998**, *54*, 11525-1153. (b) Hervé, G.; Jacob, G.; Latypov, N. *Tetrahedron* **2005**, *61*, 6743– 6748. (c) Bellamy, A. J. FOX-7 (1,1-Diamino-2,2-dinitroethene). In *High Energy Density Materials*; Klapötke, T. M., Ed.; Structure and Bonding 125; Springer-Verlag: Berlin/Heidelberg, **2007**; pp 1–33 and references cited therein.

(2) Agrawal, J. P.; Hodgson, R. D. *Organic Chemistry of Explosives*; John Wiley & Sons, Ltd.: Chichester, **2007**; p 243.

(3) Krause, H. H. In *Energetic Materials*; Teipel, U., Ed.; VCH: Weinheim, **2005**; pp 1–25.

(4) Klapötke, T. M. *Chemistry of High-Energy Materials*; Walter de Gruyter GmbH & Co. KG:Berlin/New York, **2011**; pp 179–184.

(5) (a) Gao, H.; Shreeve, J. M. *Chem. Rev.* **2011**, *111*, 7377–7436. (b) Gao, H.; Joo, Y.-H.; Parrish, D. A.; Vo, T.; Shreeve, J. M. *Chem. Eur. J.* **2011**, *17*, 4613–4618. (c) Hervé, G. *Propellants Explos. Pyrotech.* **2009**, *34*, 444–451.

(6) Anniyappan, M.; Talawar, M. B.; Gore, G. M.; Venugopalan, S.; Gandhe, B. R. *J. Hazard. Mater.* **2006**, *137*, 812–819.

(7) (a) Garg, S.; Gao, H.; Joo, Y.-H.; Parrish, D. A.; Shreeve, J. M. *J. Am. Chem. Soc.* **2010**, *132*, 8888–8890 and references cited therein. (b) Xu, K.-Z.; Chang, C.-R.; Song, J.-R.; Zhao, F. Q.; Ma, H.-X.; Lu, X.-Q.; Hu, X.-Q. *Chin. J. Chem.* **2008**, *26*, 495–499.

(8) (a) Garg, S.; Gao, H.; Parrish, D. A.; Shreeve, J. M. *Inorg. Chem.* **2011**, *50*, 390–395 and references therein. (b) Vo, T. T.; Shreeve, J. M. FOX-7 as a Coordinating Ligand or Anion in Metal Salts. Abstracts from the 66th Northwest Regional Meeting of the American Chemical Society, Portland, OR, June 26–29, **2011**; NORM 188. (c) Vo, T. T.; Parrish, D. A.; Shreeve, J. M. *Inorg. Chem.* **2012**, 51, 1963–1968 and references

cited therein. (d) Vo, T. T.; Zhang, J.; Parrish, D. A.; Twamley, B.; Shreeve, J. M. *J. Am. Chem. Soc.* **2013**, *135*, 11787-11790. (e) Xu, K. Z.; Qiu, Q. Q.; Pang, J. Y.; Ma, H. X.; Song, J. R.; Wang, B. Z.; Zhao, F. Q. *Journal of Energetic Materials* **2013**, *31*, 273–286.

(9) Sandberg, C.; Latypov, N. V.; Goede, P.; Tryman, R.; Bellamy, A. J. New Trends Res. Energ. Mater., Proc. Semin. 5th, **2002**, 292–299.

(10) Howells, R.D.; Mc Cown, J. D. *Chem. Rev.*, **1997**, *77*, 69 – 92.

(11) Abboud, K.A.; Irvin, D. J.; Reynolds, J.R. *Acta Cryst.***1998**, *C54*, 199–1999.

(12) Allen, F. H.; Kennard, O.; Watson, D. G.; Brammer, L.; Orpen, A. G.; Taylor, R. *J. Chem. Soc. Perkin Trans. II*. **1987**, S1–S19.

(13) a) Rajić, M.; Sućeska, M. *J. Thermal Analysis and Calorimetry*, **2001**, *63*, 375–386. c) Boldyrev, V. V. *Thermochimica Acta*, **2006**, *443*, 1–36.

(14) Keenan, A. G.; Siegmund, R. F. Office of Naval Research *Special Report No. 6 (Contract Nonr-4008(07);* **1968**, 1 – 49.

(15) a) Ye, C.; Shreeve, J. M. *J. Phys. Chem. A.* **2007**, *111*, 1456–1461. b) Jenkins, H. D. B.; Tudela, D.; Glasser, L. *Inorg. Chem.* **2002**, *41*, 2364–2367. c) Gao, H.; Ye, C.; Piekarski, C. M.; Shreeve, J. M. *J. Phys. Chem. C*, **2007**, *111*, 10718 – 10731 and references cited therein.

4.5 Supporting Information

1,1-Diamino-2,2-dinitroethylene (FOX-7) and 1-Amino-1-hydrazino-2,2-dinitroethene (HFOX) as Amphotères: Bases with Strong Acids

Thao T. Vo [§], Damon A. Parrish[‡], and Jean'ne M. Shreeve[*,§],

[§] Department of Chemistry, University of Idaho, Moscow, Idaho 83833-2343 United States

[‡] Naval Research Laboratory, 4555 Overlook Avenue, Washington, D. C. 20375 United States

E-mail: jshreeve@uidaho.edu

Table of Contents

(Compounds are numbered as in the paper)

4.5.1 Experimental

1. General experimental methods: ^{1}H, ^{13}C, and ^{19}F spectra were recorded on a 300 MHz (Bruker AVANCE 300) nuclear magnetic resonance spectrometer operating at 300.1 MHz, 75.47 MHz, and 282.40 MHz respectively. Analysis of ^{13}C, ^{19}F, and ^{14}N were also recorded on a 500 MHz (Bruker AVANCE 500) nuclear magnetic resonance spectrometer operating at 125.76 MHz, 470.59 MHz, and 36.14 MHz, respectively. CD_3CN was used as a locking solvent unless otherwise stated. Chemical shifts in ^{1}H and ^{13}C spectra were reported relative to Me_4Si. The melting and decomposition points were recorded with a differential scanning calorimeter (DSC, TA Instruments Q10) at a scan rate of 5 ºC min^{-1} in closed aluminum containers. IR spectra were recorded using KBr pellets for solids on a BIORAD model 3000 FTS spectrometer. Elemental analyses were obtained on a CE-440 elemental analyzer (EAI Exeter Analytical).

Safety Precautions: While we have experienced no difficulties in syntheses and characterization of these materials, proper protective measures should be used. Manipulations must be carried out in a hood behind a safety shield. Eye protection and leather gloves must be worn. Caution should be exercised at all times during the synthesis, characterization, and handling of any of these materials, and mechanical actions involving scratching or scraping must be avoided.

Note: Acetonitrile was dried over molecular sieves (3Å) prior to use.[1a] FOX-7 and HFOX were synthesized according to literature procedures.[1b-c] HFOX should be handled with extreme caution as it may spontaneously combust.[2] Dry methanol was freshly distilled with elemental sodium (0.1g Na : 100 mL MeOH) prior to use.

2. 1-Amino-2,2-dinitroethaniminium triflate (3a):

To a round bottomed flask charged with 0.22 g (1.5 mmol) of FOX-7, 0.44 mL of triflic acid was added drop wise. The reaction vessel was capped and allowed to stir until all of the starting material dissolved to give a clear colorless solution. One mL of dry acetonitrile was then added and the mixture was stirred for 5 minutes (to obtain crystals). The majority of the

excess acid and solvent was then removed under vacuum overnight to give colorless prisms that could be quickly filtered (~ 99% yield). The crystals were then washed with hexane to remove the residual acid. Structural identification was completed by single crystal X-ray analysis. ^{13}C NMR: δ = 155.40 (C-NH_2), [127.44, 123.23, 119.03, 114.82] ($CF_3SO_3^-$), 104.79 (C-NO_2). ^{19}F NMR: δ = -79.35. IR (KBr): $\tilde{\nu}$ = 3425, 3333, 3301, 1638, 1610, 1522, 1474, 1395, 1352, 1248, 1171, 1030, 858, 791, 751, 642, 622, 577, 521cm^{-1}. Elemental analysis ($C_3H_5F_3N_4O_7S$, 298.15): Calcd. C, 12.09%; H, 1.69%; N, 18.79%. Found C, 11.77%; H, 1.77%; N, 16.58%

3. 1-Amino-2,2-dinitroethaniminium perchlorate (3b):

To a 10 mL round bottomed flask charged with 0.22 g (0.5 mmol) FOX-7, 0.4 mL HClO4 (60-62%) was added dropwise. The suspension was then heated gently at 80 °C until the suspension was dissolved to give a yellow solution and stirred for an additional ~2 minutes. The reaction was then capped and allowed to stir at room temperature for 10-15 minutes. The majority of the excess acid was removed under vacuum to give colorless prisms which were suitable for single crystal X-ray analysis. The crystals were isolated by filtration and washed with a small amount of hexane to remove the residual acid (~ 99% yield). IR (KBr): $\tilde{\nu}$ = 3408, 3332, 3300, 3227, 1637, 1609, 1521, 1474, 1394, 1353, 1238, 1140, 1081, 1026, 940, 858, 790, 751, 675, 626, 578, 536, 522 cm^{-1}. Elemental analysis ($C_2H_5ClN_4O_8$, 248.53): the crystals were too unstable to obtain elemental analysis data.

4. 1-Amino-1-hydrazino-2,2-dinitroethaniminium triflate (4a):

The same procedures were followed as for **3a** except 0.08g (0.5 mmol) HFOX was used instead of FOX-7 to give colorless prism crystals (~ 99 yield). Salt **4a** crystallizes with one molecule of acetonitrile. ^{13}C NMR: δ = 153.16 (C-NH_2), [127.22, 123.01, 118.80, 114.60] ($CF_3SO_3^-$), 105.93 (C-NO_2). ^{19}F NMR: δ = -79.27. IR (KBr): 3433, 3346, 3261, 1704, 1627, 1604, 1535, 1479, 1413, 1259, 1181, 1147, 1032, 925, 779, 767, 755, 740, 642, 580, 519 cm^{-1}. Elemental analysis ($C_3H_6F_3N_5O_7S$, 313.16): the crystals were too unstable to obtain elemental analysis data.

5. 1-Amino-1-hydrazino-2,2-dinitroethaniminium chloride (5):

To a 25 mL round bottomed flask with 0.08g (0.5 mmol) HFOX suspended in dry methanol, HCl gas (generated from H_2SO_4 and NaCl) was bubbled into the solution in which the suspension dissolved to give clear yellow solution. The gas was continued bubbling through the solution for approximately 30 minutes after a cloudy white solution formed. The solvent was then removed under vacuum overnight to give a pale yellow solid **6** (~99% yield). It is important to utilize extreme caution when synthesizing this salt as it spontaneously combusts. The salt was observed to decompose violently within 12 hours after forming. It is best to synthesize on a small scale and use immediately. IR (KBr): 3431, 3344, 3257, 3150, 2866, 2515, 1851, 1699, 1626, 1535, 1478, 1411, 1325, 1282, 1265, 1188, 1140, 923, 847, 773, 752, 741, 592 cm^{-1}. Elemental analysis ($C_2H_6N_5O_4Cl$, 199.55): Calcd. C, 12.04%; H, 3.03%; N, 35.10%. Found: C, 12.84%; H, 3.44%; N, 34.17%.

6. 2,2-dinitro-1-(2-(propan-2-ylidene)hydrazinyl)ethenamine (9):

To a round bottomed flask charged with 0.08g (0.5 mmol) HFOX, 40 mL of acetone was added and the solution was allowed to stir ~ 6 hours in which a clear yellow solution formed. The solution was allowed to concentrate slowly overnight to give yellow prism crystals of **9** (0.150g). IR (KBr): 3443, 3325, 3208, 1719, 1608, 1564, 1533, 1487, 1420, 1368, 1350, 1277, 1204, 1134, 1114, 1051, 1021, 862, 831, 787, 750, 686, 626, 593 cm^{-1}. Elemental analysis ($C_5H_9N_5O_4$, 203.16): Calcd. C, 29.56%; H, 4.47%; N, 34.47%. Found: C, 29.51%; H, 4.42%; N, 33.00%.

4.5.2 X-ray crystallography:

A colorless prism of dimensions 0.44 x 1.01 x 1.28 mm^3 (**3a**), a colorless prism of 0.37 x 0.14 x 0.11 mm^3 (**3b**), a colorless plate crystal of dimensions 0.82 x 0.10 x 0.07 mm^3 (**4a**), and a yellow plate of 0.27 x 0.23 x 0.07 mm^3 (**9**) were mounted with a MiteGen MicroMesh and a small amount of Cargille Immersion Oil (for salts **3a**, **3b**, and **4a**) or a Nylon loop with paratone oil (compound **9**). For all salts, data were collected on a Bruker three-circle platform diffractometer equipped with a SMART APEX II CCD detector. The crystals were irradiated using graphite monochromated MoK_α radiation (λ = 0.71073). An Oxford Cobra low temperature device was used to keep the crystals at a constant 124(2) K [**3a** and **3b**], and 150(2) K [**4a**] during data collection. For compound **9**, data were collected using

a Bruker CCD (charge coupled device) based diffractometer equipped with an Oxford Cryostream low-temperature apparatus operating at 173 K. Data were measured using omega and phi scans of 1.0° per frame for 30 s. The total number of images was based on results from the program COSMO[3] where redundancy was expected to be 4.0 and completeness to 0.83 Å to 100%.

For all the salts, data collection was performed, and the unit cell was initially refined using APEX2 [v2009.3-0].[4] Data reduction was performed using SAINT [v7.60A][5] and XPREP [v2008/2].[6] Corrections were applied for Lorentz, polarization, and absorption effects using SADABS [v2008/1].[7] The structure was solved and refined with the aid of the programs in the SHELXTL-plus [v2008/4] system of programs (**3a**, **3b**, and **4a**).[8] The full-matrix least-squares refinement on F^2 included atomic coordinates and anisotropic thermal parameters for all non-H atoms. The H atoms were included using a riding model. Details of the data collection and refinement are given in Table S1.

4.5.3 Crystal data and structural refinement:

Table 4.S1. Crystallographic data for salts **3a**, **3b**, **4a**, and compound **9**

	3a	**3b**	**4a**	**9**
Formula	$C_3H_5F_3N_4O_7S$	$C_2H_5N_4O_8Cl$	$C_5H_9F_3N_6O_7S$	$C_5H_9N_5O_4$
MW	298.17	248.55	354.24	203.17
CCDC	1008326	1008327	1008328	1008325
T [K]	150 (2)	150 (2)	150 (2)	174 (2)
Wavelength (Å)	0.71073	0.71073	0.71073	1.54178
Crystal system	Monoclinic	Triclinic	Triclinic	Triclinic
Space group	P 121/c1	P-1	P-1	P-1
a (Å)	7.5409(4)	10.3533(11)	6.2235(9)	6.68570(10)
b (Å)	11.4812(6)	13.0615(14)	10.5855(15)	6.89930(10)
c (Å)	12.3048(6)	20.060(2)	11.8361(17)	10.2681(2)
α (°)	90	107.534(2)	111.318(2)	76.7114(10)
β (°)	106.8020(10)	94.518(2)	93.653(2)	79.0212(10)
γ (°)	90	95.584(2)	102.778(2)	75.8661(10)
Volume ($Å^3$)	1019.85(9)	2557.6(5)	699.44(17)	442.447(13)
Z	4	12	2	2
Density (calculated; gcm^{-3})	1.942	1.936	1.682	1.525
Absorption coefficient	0.404	0.489	0.313	1.147
F(000)	600	1512	360	212
Crystal size (mm^3)	0.44 x 1.01 x 1.28	0.37 x 0.14 x 0.11	0.60 x 0.27 x 0.25	0.27 x 0.23 x 0.07
Theta range for data collection (°)	2.48 to 30.52	1.99 to 30.56	1.87 to 26.47	4.47 to 71.81
Index ranges	-10<=h<=10, -16<=k<=16, -17<=l<=17	-14<=h<=14, -18<=k<=18, -28<=l<=28	-7<=h<=7, -13<=k<=12, -14<=l<=14	-8 ≤ h ≤ 8, -7 ≤ k ≤ 8, -12 ≤ l ≤ 12
Reflections collected	16143	41318	6266	6216
Independent reflections	3116 [R(int) = 0.0591]	15578 [R(int) = 0.1209]	2825 [R_{int} = 0.0169]	1680

Table 4.S1 (continued). Crystallographic data for salts **3a**, **3b**, **4a**, and compound **9**

	3a	**3b**	**4a**	**9**
Absorption correction	Multi-scan	Multi-scan	Semi-empirical from equivalents	Multi-scan
Max. and Min. Transmission	0.8423 and 0.6259		0.9258 and 0.8344	0.7535 and 0.6458
Refinement method	Full-matrix least-squares on F^2	Full-matrix least-squares on F^2	Full-matrix least-squares on F^2	Full-matrix least-squares on F^2
Data/restraints/parameters	3116/0/163	15578/53/870	2825/0/215	1680/0/141
Goodness-of-fit on F2	1.058	1.024	1.039	1.052
Final R indices [I>2sigma(I)]	R1 = 0.0335, wR2 = 0.0877	R1 = 0.0481, wR2 = 0.1275	R_1 = 0.0338, wR_2 = 0.0875	R_1 = 0.0323, wR_2 = 0.0854
R indices (all data)	R1 = 0.0365, wR2 = 0.0896	R1 = 0.0592, wR2 = 0.1366	R_1 = 0.0388, wR_2 = 0.0910	R_1 = 0.0401, wR_2 = 0.0900
Largest diff. peak and hole (e $Å^{-3}$)	0.499 and -0.463	1.158 and -0.915	0.587 and -0.375	0.24 and -0.17

For hydrazone **9**, cell parameters were retrieved using APEX II software[9] and refined using SAINT on all observed reflections. Data reduction was performed using the SAINT software[10] which corrects for Lp. Scaling and absorption corrections were applied using SADABS[11] multi-scan technique, supplied by George Sheldrick. The structures are solved by the direct method using the SHELXS-97 program and refined by least squares method on F^2, SHELXL-97[12a], which are incorporated in OLEX2[12b]. The structure was solved in the space group $P\bar{1}$ (# 2). All non-hydrogen atoms are refined anisotropically. Hydrogens were calculated by geometrical methods and refined as a riding model.

4.5.4 Selected bond lengths and bond angles:

Salt **3a**

Table 4.S2. Bond lengths (Å) of **3a.**

C1-N4	1.3032(15)	N8-O10	1.2107(15)
C1-N3	1.3068(14)	S11-O15	1.4405(9)
C1-C2	1.5179(15)	S11-O13	1.4436(9)
C2-N5	1.5111(15)	S11-O14	1.4539(9)
C2-N8	1.5164(14)	S11-C12	1.8358(12)
N5-O7	1.2119(14)	C12-F17	1.3108(15)
N5-O6	1.2158(14)	C12-F16	1.3167(16)
N8-O9	1.2082(16)	C12-F18	1.3186(14)

Table S3. Bond angles (°) of **3a**

N4-C1-N3	123.79(11)	O13-S11-C12	104.18(6)
N4-C1-C2	120.39(10)	O14-S11-C12	104.77(6)
N3-C1-C2	115.82(10)	F17-C12-F16	108.54(12)
N5-C2-N8	107.67(9)	F17-C12-F18	107.62(12)
N5-C2-C1	112.17(9)	F16-C12-F18	107.81(12)
N8-C2-C1	110.89(9)	F17-C12-S11	111.21(9)
O7-N5-O6	126.09(12)	F16-C12-S11	110.30(9)
O7-N5-C2	117.87(10)	F18-C12-S11	111.23(9)
O6-N5-C2	116.04(10)		
O9-N8-O10	127.54(11)		
O9-N8-C2	114.47(11)		
O10-N8-C2	117.95(10)		
O15-S11-O13	115.32(6)		
O15-S11-O14	114.15(6)		
O13-S11-O14	113.24(6)		
O15-S11-C12	103.47(6)		

Salt **3b**

Table 4.S3. Bond lengths (Å) of **3b.**

C1A-N4A	1.298(2)	N5D-O6D	1.204(4)
C1A-N3A	1.308(2)	N5D'-O6D'	1.190(7)
C1A-C2A	1.516(2)	N5D'-O7D'	1.259(8)
C2A-N5A	1.517(2)	O6D'-O6D'#1	1.797(10)
C2A-N8A	1.520(2)	N8D-O9D	1.198(5)
N5A-O7A	1.2151(17)	N8D-O10D	1.201(7)
N5A-O6A	1.2161(17)	N8D'-O10'	1.203(5)
N8A-O9A	1.189(2)	N8D'-O9D'	1.214(4)
N8A-O10A	1.192(2)	C1E-N3E	1.299(2)
C1B-N3B	1.292(2)	C1E-N4E	1.3049(19)
C1B-N4B	1.309(2)	C1E-C2E	1.518(2)
C1B-C2B	1.5179(19)	C2E-N5E	1.509(2)
C2B-N8B	1.509(2)	C2E-N8E	1.517(2)
C2B-N5B	1.515(2)	N5E-O7E	1.211(2)
N5B-O7B	1.2054(19)	N5E-O6E	1.218(2)
N5B-O6B	1.209(2)	N8E-O9E	1.2156(18)
N8B-O9B	1.212(2)	N8E-O10E	1.218(2)
N8B-O10B	1.231(3)	C1F-N4F	1.298(2)
C1C-N3C	1.298(2)	C1F-N3F	1.3060(19)
C1C-N4C	1.3077(19)	C1F-C2F	1.5159(19)
C1C-C2C	1.514(2)	C2F-N8F	1.506(2)
C2C-N5C	1.511(2)	C2F-N5F	1.5259(19)
C2C-N8C	1.523(2)	N5F-O6F	1.2120(19)
N5C-O6C	1.2119(19)	N5F-O7F	1.216(2)
N5C-O7C	1.222(2)	N8F-O10F	1.215(2)
N8C-O10C	1.206(2)	N8F-O9F	1.2163(19)
N8C-O9C	1.211(2)	Cl1A-O4A	1.4329(14)
C1D-N4D	1.288(2)	Cl1A-O2A	1.4341(15)
C1D-N3D	1.2983(19)	Cl1A-O1A	1.4344(14)
C1D-C2D	1.517(2)	Cl1A-O3A	1.4363(13)
C2D-N8D	1.376(4)	Cl1B-O3B	1.4283(13)
C2D-N5D	1.440(3)	Cl1B-O2B	1.4368(14)
C2D-N8D'	1.627(4)	Cl1B-O1B	1.4434(14)

Table 4.S3 (continued). Bond lengths (Å) of **3b.**

C2D-N5D'	1.648(5)	Cl1B-O4B	1.4459(15)
N5D-O7D	1.137(7)	Cl1C-O4C	1.4305(14)
Cl1C-O2C	1.4341(14)	Cl1E-O1E	1.4341(14)
Cl1C-O3C	1.4392(13)	Cl1E-O4E	1.4441(12)
Cl1C-O1C	1.4414(14)	Cl1E-O2E	1.4476(12)
Cl1D-O2D	1.4232(13)	Cl1F-O2F	1.4264(14)
Cl1D-O4D	1.4386(13)	Cl1F-O3F	1.4292(16)
Cl1D-O3D	1.4403(12)	Cl1F-O4F	1.4328(15)
Cl1D-O1D	1.4493(14)	Cl1F-O1F	1.4403(13)
Cl1E-O3E	1.4299(13)		

Table 4.S4. Bond angles (°) of **3b.**

N4A-C1A-N3A	124.15(14)	O9B-N8B-C2B	115.1(2)
N4A-C1A-C2A	116.72(13)	O10B-N8B-C2B	116.92(16)
N3A-C1A-C2A	119.12(14)	N3C-C1C-N4C	124.07(14)
C1A-C2A-N5A	111.49(11)	N3C-C1C-C2C	116.37(13)
C1A-C2A-N8A	109.31(13)	N4C-C1C-C2C	119.56(14)
N5A-C2A-N8A	108.60(12)	N5C-C2C-C1C	113.52(13)
O7A-N5A-O6A	126.55(15)	N5C-C2C-N8C	107.10(13)
O7A-N5A-C2A	116.01(12)	C1C-C2C-N8C	109.34(12)
O6A-N5A-C2A	117.41(12)	O6C-N5C-O7C	126.85(18)
O9A-N8AO10A	125.52(18)	O6C-N5C-C2C	115.70(16)
O9A-N8A-C2A	115.13(16)	O7C-N5C-C2C	117.38(14)
O10A-8AC2A	119.31(14)	O10C-N8C-O9C	127.06(18)
N3B-C1B-N4B	123.36(13)	O10C-N8C-C2C	118.46(16)
N3B-C1B-C2B	115.69(13)	O9C-N8C-C2C	114.48(17)
N4B-C1B-C2B	120.95(14)	N4D-C1D-N3D	124.17(16)
N8B-C2B-N5B	106.93(13)	N8D-C2D-N8D'	20.42(19)
N8B-C2B-C1B	112.53(13)	N8D-C2D-N5D'	109.7(3)
N5B-C2B-C1B	111.60(11)	N5D-C2D-N5D'	26.21(16)
O7B-N5B-O6B	127.38(16)	N5D'-O6D'-	131.7(5)
O7B-N5B-C2B	118.06(14)	O6D'#1O9D-N8D-	128.5(5)
O6B-N5B-C2B	114.51(14)	O10D	
		O9D-N8D-C2D	123.6(4)

Table 4.S4 (continued). Bond angles (°) of **3b.**

O9B-N8B-O10B	127.8(2)
O10'-N8D'-O9D'	127.3(4)
O10'-N8D'-C2D	115.7(3)
O9D'-N8D'-C2D	117.0(3)
N3E-C1E-N4E	124.18(14)
N3E-C1E-C2E	115.42(13)
N4E-C1E-C2E	120.39(14)
N5E-C2E-N8E	106.20(13)
N5E-C2E-C1E	112.38(12)
N8E-C2E-C1E	110.34(12)
O7E-N5E-O6E	126.81(16)
O7E-N5E-C2E	116.73(15)
O6E-N5E-C2E	116.47(14)
O9E-N8E-O10E	127.28(16)
O9E-N8E-C2E	115.88(14)
O10E-N8E-C2E	116.80(13)
N4F-C1F-N3F	123.83(14)
N4F-C1F-C2F	121.11(13)
N3F-C1F-C2F	115.06(14)
N8F-C2F-C1F	113.70(12)
N8F-C2F-N5F	106.75(11)
C1F-C2F-N5F	111.19(12)
O6F-N5F-O7F	127.87(15)
O6F-N5F-C2F	117.38(14)
O7F-N5F-C2F	114.59(13)
O10F-N8F-O9F	126.11(16)
O10F-N8F-C2F	117.24(14)
O9F-N8F-C2F	116.62(14)
O4A-Cl1A-O2A	109.24(11)
O4A-Cl1A-O1A	108.74(9)
O2A-Cl1A-O1A	109.56(11)
O4A-Cl1A-O3A	110.41(9)
O2A-Cl1A-O3A	108.84(9)
O1A-Cl1A-O3A	110.03(8)
O3B-Cl1B-O2B	110.21(8)
O10D-N8D-C2D	107.8(4)
O2B-Cl1B-O1B	111.28(9)
O3B-Cl1B-O4B	109.79(10)
O2B-Cl1B-O4B	108.94(9)
O1B-Cl1B-O4B	107.69(9)
O4C-Cl1C-O2C	110.60(10)
O4C-Cl1C-O3C	110.05(9)
O2C-Cl1C-O3C	108.74(9)
O4C-Cl1C-O1C	108.97(9)
O2C-Cl1C-O1C	109.58(9)
O3C-Cl1C-O1C	108.88(8)
O2D-Cl1D-O4D	110.59(8)
O2D-Cl1D-O3D	110.96(9)
O4D-Cl1D-O3D	108.94(8)
O2D-Cl1D-O1D	108.61(9)
O4D-Cl1D-O1D	108.49(10)
O3D-Cl1D-O1D	109.21(8)
O3E-Cl1E-O1E	110.07(9)
O3E-Cl1E-O4E	109.92(9)
O1E-Cl1E-O4E	109.32(8)
O3E-Cl1E-O2E	109.62(8)
O1E-Cl1E-O2E	109.86(9)
O4E-Cl1E-O2E	108.02(8)
O2F-Cl1F-O3F	108.84(10)
O2F-Cl1F-O4F	109.94(9)
O3F-Cl1F-O4F	108.63(12)
O2F-Cl1F-O1F	111.06(9)
O3F-Cl1F-O1F	109.16(9)
O4F-Cl1F-O1F	109.18(10)
O3B-Cl1B-O1B	108.90(8)

Salt **4a**

Table 4.S5. Bond lengths (Å) of **4a.**

C(1)-N(3)	1.507(2)	C(1)-C(2)	1.514(2)
C(1)-N(6)	1.516(2)	C(1)-H(1)	1.0000
C(2)-N(10)	1.292(2)	C(2)-N(9)	1.325(2)
N(3)-O(5)	1.209(2)	N(3)-O(4)	1.213(2)
N(6)-O(8)	1.202(2)	N(6)-O(7)	1.221(2)
N(9)-H(9A)	0.84(2)	N(9)-H(9B)	0.83(2)
N(10)-N(11)	1.4482(19)	N(11)-H(11C)	0.88(2)
N(11)-H(11B)	0.84(2)	N(11)-H(11A)	0.88(2)
C(12)-F(15)	1.318(2)	C(12)-F(13)	1.325(2)
C(12)-F(14)	1.326(2)	C(12)-S(16)	1.8202(18)
S(16)-O(17)	1.4352(12)	S(16)-O(19)	1.4404(12)
S(16)-O(18)	1.4473(12)	C(21)-N(22)	1.130(2)
C(21)-C(20)	1.450(3)	C(20)-H(20A)	0.9800
C(20)-H(20B)	0.9800	C(20)-H(20C)	0.9800

Table 4.S6. Bond angles (Å) of **4b**.

N(3)-C(1)-C(2)	109.80(13)	N(3)-C(1)-N(6)	107.87(13)
C(2)-C(1)-N(6)	113.06(14)	N(3)-C(1)-H(1)	108.7
C(2)-C(1)-H(1)	108.7	N(6)-C(1)-H(1)	108.7
N(10)-C(2)-N(9)	131.67(16)	N(10)-C(2)-C(1)	113.51(14)
N(9)-C(2)-C(1)	114.81(14)	O(5)-N(3)-O(4)	126.67(16)
O(5)-N(3)-C(1)	119.00(15)	O(4)-N(3)-C(1)	114.32(14)
O(8)-N(6)-O(7)	126.33(18)	O(8)-N(6)-C(1)	119.30(15)
O(7)-N(6)-C(1)	114.37(17)	C(2)-N(9)-H(9A)	117.4(14)
C(2)-N(9)-H(9B)	120.5(14)	H(9A)-N(9)-H(9B)	122(2)
C(2)-N(10)-N(11)	112.75(13)	N(10)-N(11)-H(11C)	112.9(13)
N(10)-N(11)-H(11B)	106.1(14)	H(11C)-N(11)-H(11B)	108.1(19)
N(10)-N(11)-H(11A)	109.9(14)	H(11C)-N(11)-H(11A)	111.7(18)
H(11B)-N(11)-H(11A)	107.8(18)	F(15)-C(12)-F(13)	108.67(17)
F(15)-C(12)-F(14)	108.49(16)	F(13)-C(12)-F(14)	107.91(16)
F(15)-C(12)-S(16)	110.85(13)	F(13)-C(12)-S(16)	110.85(13)
F(14)-C(12)-S(16)	109.99(13)	O(17)-S(16)-O(19)	115.82(8)
O(17)-S(16)-O(18)	115.24(7)	O(19)-S(16)-O(18)	112.79(8)
O(17)-S(16)-C(12)	103.69(8)	O(19)-S(16)-C(12)	104.22(8)
O(18)-S(16)-C(12)	103.00(8)	N(22)-C(21)-C(20)	179.4(2)
C(21)-C(20)-H(20A)	109.5	C(21)-C(20)-H(20B)	109.5
H(20A)-C(20)-H(20B)	109.5	C(21)-C(20)-H(20C)	109.5
H(20A)-C(20)-H(20C)	109.5	H(20B)-C(20)-H(20C)	109.5

Compound **9**

Table 4.S7. Bond lengths (Å) of **9**

O(1)-N(4)	1.2431(16)	N(3)-C(4)	1.3157(18)
O(2)-N(4)	1.2177(16)	N(4)-N(5)	1.4295(18)
O(3)-N(5)	1.2640(15)	N(5)-C(5)	1.3892(18)
O(4)-N(5)	1.2342(15)	C(1)-C(2)	1.492(2)
N(1)-N(2)	1.3908(16)	C(2)-C(3)	1.499(2)
N(1)-C(2)	1.283(2)	C(4)-C(5)	1.4462(18)
N(2)-C(4)	1.3360(18)		

Table 4.S8. Bond angles (°) of **9.**

C(2)-N(1)-N(2)	114.81(12)	N(1)-C(2)-C(3)	116.29(14)
C(4)-N(2)-N(1)	117.83(11)	C(1)-C(2)-C(3)	119.04(14)
O(1)-N(4)-C(5)	117.83(11)	N(2)-C(4)-C(5)	119.75(11)
O(2)-N(4)-O(1)	122.09(12)	N(3)-C(4)-N(2)	117.86(12)
O(2)-N(4)-C(5)	120.04(12)	N(3)-C(4)-C(5)	122.38(12)
O(3)-N(5)-C(5)	118.39(11)	N(4)-C(5)-C(4)	120.52(11)
O(4)-N(5)-O(3)	120.29(11)	N(5)-C(5)-N(4)	116.58(11)
O(4)-N(5)-C(5)	121.27(12)	N(5)-C(5)-C(4)	122.86(12)
N(1)-C(2)-C(1)	124.67(13)		

4.5.5 Theoretical studies:

Energetic performances were calculated using Explo5 v6.01. The heats of formation for all the compounds were calculated using Gaussian 03 (Revision D. 01).[13]The geometric optimization of the structures was based on single-crystal structures, and frequency analyses were carried out using the B3LYP functional with 6-31+G** basis set. Single-point energies were calculated at the MP2/6-311++G** level.[14] Atomization energies for compounds (**3a**), (**3b**), (**4a**), and (**4b**) were calculated using the G2 ab initio method.[15] All of the optimized structures were characterized to be true local energy minima on the potential energy surface without imaginary frequencies. The standard heats of formation of the salts were calculated based on the Born-Haber energy cycle (Scheme 4.S1) and Equation (1).[1c]

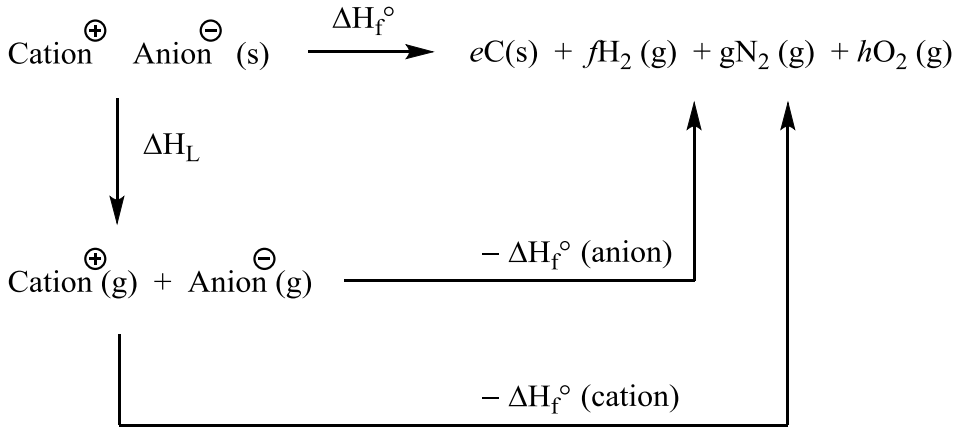

("e, f, g, h" represent the number of moles of each product)*

Figure 4.S1. Born-Haber cycle for formation of energetic salts.

$$\Delta H_f^\circ \text{ (salt, 298K)} = \Delta H_f^\circ \text{ (cation, 298K)} + \Delta H_f^\circ \text{ (anion, 298K)} - \Delta H_L \qquad (1)$$

The lattice energy (ΔH_L) of the salts A_pB_q are calculated using Equation (2) suggested by Jenkins, et al.[16]:

$$\Delta H_L = U_{POT} + [p(n_M/2\text{-}2) + q(n_x/2\text{-}2)]RT \qquad (2)$$

where n_M and n_x are dependent on the ions of A^{p+} and B^{q-} (q and p represent the charges on the cation and anion) and assigned values 3 for monoatomic ions, 5 for linear polyatomic ions,

and 6 for nonlinear polyatomic ions. The lattice potential energy, U_{POT}, (reported as kJ mol^{-1}) can be calculated from Equation (3):

$$U_{POT} = \gamma[\rho_m(M_m)^{1/3} + \delta \qquad (3)$$

where ρ_m is the density (gcm^{-3}), M_m is the chemical formula mass of the ionic material (g), and the coefficients γ (kJ mol^{-1}cm) and δ (kJ mol^{-1}) values are obtained from the literature.[17,18]

The densities were calculated according to a reliable method by our group.[19] The volume of FOX-7 and HFOX were calculated by taking the reported volume of the parent compounds from their crystal structure reports and adding 7Å (volume for a hydrogen bonded to carbon) to the volume to incorporate the added proton for the cations according (FOX-7 cation vol. = 136.98, HFOX cation vol. = 155.75).[19] The volumes for the following anions were taken from the literature: (trinitromethanide, dinitroamide, nitrate, triflate, and perchlorate)[19]and NTO[20].

As mentioned in the manuscript, our initial investigation began with calculations of energetic salts containing FOX-7 and HFOX cations. Salts containing counter anions such as nitrate (**10a**, **11a**), trinitromethanide (**10b**, **11b**), dinitroamide (**10c**, **11c**), and 3-nitro-1,2,4-triazol-5-one (NTO; [**10d**, **11d**]) were examined (Figure 4.S2).

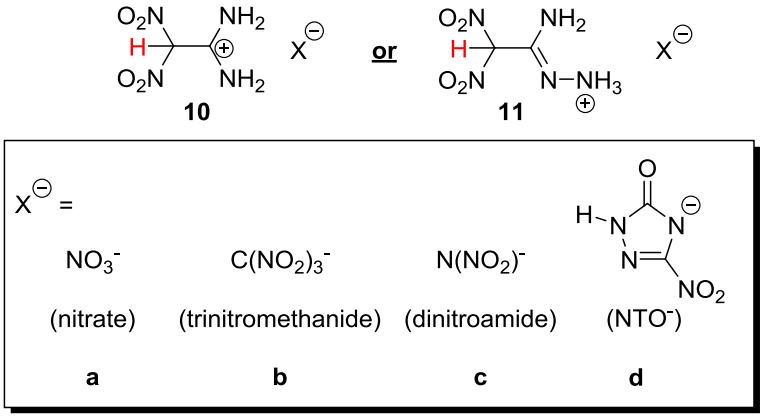

Figure 4.S2. Salts based on HFOX and FOX-7 cations with varying anions.

The calculated energetic properties were found to exceed that of TNT, FOX-7 and RDX, which supports the usefulness of FOX-7 and HFOX cations as building blocks for energetic

salts (Table 4.S9). Salt **11c** (8907 ms^{-1}) has the highest detonation velocity among the salts, exceeding the values of TNT, FOX-7 and RDX. The remaining salts all exceed TNT while salts **10c-d** and **11b-d** are either comparable or slightly better than FOX-7. With the exception of **11a**, the detonation pressures of the salts are close to that of FOX-7 and RDX.

Table 4.S9. Calculated energetic properties of salts based on HFOX and FOX-7 cations with varying anions.

	Compd.	ρ^a	Vol.[b]	$\Delta H_{f(cation)}$ [c]	$\Delta H_{f(anion)}$ [d]	ΔH_f [e]	P[f]	D[g]	Isp[h]
FOX-7	**10a**	1.753	199.98	659.7	-300.5	-150.8	31.8	8670	262
cation	**10b**	1.793	276.98	659.7	-287.0	-96.0	31.5	8605	257
salts	**10c**	1.811	233.98	659.7	-156.2	14.0	32.9	8793	259
	10d	1.784	258.98	659.7	63.9	246.8	33.9	8728	267
HFOX	**11a**	1.595	219.75	799.5	-300.5	1.50	26.2	8163	274
cation	**11b**	1.758	296.75	799.5	-287.0	52.0	32.4	8706	266
salts	**11c**	1.767	253.75	799.5	-156.2	164.0	33.8	8907	270
	11d	1.746	278.75	799.5	63.9	395.5	33.5	8750	274
Standard	**TNT**	1.65	-	-	-	-59.3	21.3	7304	211
energetics	**FOX-7**	1.88	-	-	-	-134.1	35.2	8771	240
	RDX	1.82	-	-	-	70.3	35.8	8864	267

a) Calculated density (gcm^{-3}) [ref. 19]. b) Calculated volumes (Å). c) Cation heat of formation (kJ/mol). d) Anion heat of formation (kJ/mol). e) Heat of formation (kJ/mol). f) Detonation pressure (GPa). g) Detonation velocity (ms^{-1}). h) Specific impulse (s) [calculated at an isobaric pressure of 70 bar and initial temperature of 3,300 K].

The specific impulse values of salts 10 and 11 are increased with the suggested counter anions with values that exceed TNT, FOX-7 and RDX (excluding 10b and 10c). By varying the counter anion, it can be seen that the properties of salts based on the FOX-7 and HFOX cations can be modified.

4.5.6 References

(1) a) Lawton, M.; Williams, D. B. *J. Org. Chem.* **2010**, 8351 – 8354. b) Anniyappan, M.; Talawar, M. B.; Gore, G. M.; Venugopalan, S.; Gandhe, B. R. *J. Hazard. Mater.* **2006**, *137*, 812–819. c) Gao, H.; Joo, Y.-H.; Parrish, D. A.; Vo, T.; Shreeve, J. M. *Chem. Eur. J.* **2011**, *17*, 4613–4618 [Note: For the synthesis of the potassium HFOX, 1.86 g (10 mmol) of the potassium FOX-7 salt suspended in 60 mL of absolute ethanol was used instead of 1.86g of FOX-7 with KOH in absolute ethanol. The remainder of the procedures were followed as reported. For the synthesis of

HFOX, the same procedure was followed as reported. However, after washing the product with water, it was also washed with either 1 mL of anhydrous acetonitrile (for salt **4a**) or anhydrous methanol (for salt **5**). HFOX was then allowed to air dry for < ~30 minutes prior to use.].

(2) Bellamy, A. J.; Contini, A. E.; Latypov, N. V. *Propellants Explos. Pyrotech.* **2008**, *33*, 87-88 [Note: The spontaneous combustion for one of the reaction batches of HFOX was observed to occur within 3 hours, while some other preparations were stable for several days.]

(3) COSMO V1.61, *Software for the CCD Detector Systems for Determining Data Collection Parameters.* Bruker Analytical X-ray Systems, Madison, WI (2009).

(4) Bruker (**2010**). Apex2 v2010.3-0. Bruker AXS Inc., Madison, Wisconsin, USA.

(5) Bruker (**2009**). SAINT v7.68A. Bruker AXS Inc., Madison, Wisconsin, USA.

(6) Bruker (**2008**). XPREP v2008/2. Bruker AXS Inc., Madison, Wisconsin, USA.

(7) Bruker (**2009**). SADABS v2008/1. Bruker AXS Inc., Madison, Wisconsin, USA.

(8) Bruker (**2009**). SHELXTL v2008/4. Bruker AXS Inc., Madison, Wisconsin, USA.

(9) APEX2 V2010.11-3. Software *for the CCD Detector System*; Bruker Analytical X-ray Systems, Madison, WI (2010).

(10) SAINT V 7.68A Software *for the Integration of CCD Detector System* Bruker Analytical X-ray Systems, Madison, WI (2010).

(11) SADABS V2008/2 Program for absorption corrections using Bruker-AXS CCD based on the method of Robert Blessing; Blessing, R.H. Acta Cryst. A51, 1995, 33-38.

(12) a)Sheldrick, G.M. "A short history of SHELX". *Acta Cryst*. **A64**, 2008, 112-122. b) O. V. Dolomanov, L. J. Bourhis, R. J. Gildea, J. A. K. Howard and H. Puschmann, OLEX2: a complete structure solution, refinement and analysis program. J. Appl. Cryst. (2009). 42, 339-341

(13) M. J. Frisch, G. W. Trucks, H. B. Schlegel, G. E. Scuseria, M. A. Robb, J. R. Cheeseman, J. A. Montgomery, T. V. Jr., K. N. Kudin, J. C. Burant, J. M. Millam, S. S. Iyengar, J. Tomasi, V. Barone, B. Mennucci, M. Cossi, G. Scalmani, N. Rega, G. A. Petersson, H. Nakatsuji, M. Hada, M. Ehara, K. Toyota, R. Fukuda, J. Hasegawa, M. Ishida, T. Nakajima, Y. Honda, O. Kitao, H. Nakai, M. Klene, X. Li, J. E. Knox, H. P. Hratchian, J. B. Cross, V. Bakken, C. Adamo, J. Jaramillo, R. Gomperts, R. E. Stratmann, O. Yazyev, A. J. Austin, R. Cammi, C. Pomelli, J. W. Ochterski, P. Y. Ayala, K. Morokuma, G. A. Voth, P. Salvador, J. J. Dannenberg, V. G. Zakrzewski, S. Dapprich, A. D. Daniels, M. C. Strain, O. Farkas, D. K. Malick, A. D. Rabuck, K. Raghavachari, J. B. Foresman, J. V. Ortiz, Q. Cui, A. G. Baboul, S. Clifford, J. Cioslowski, B. B. Stefanov, A. L. G. Liu, P. Piskorz, I. Komaromi, R. L. Martin, D. J. Fox, T. Keith, M. A. Al-Laham, C. Peng, A. Nanayakkara, M. Challacombe, P. M. W. Gill, B. Johnson, W. Chen, M. Wong, C. Gonzalez, J. A. Pople, *Gaussian 03, Revision D. 01*, Gaussian, Inc., Wallingford, CT, **2004**.

(14) R. G. Parr, W. Wang, Density Functional Therory of Atoms and Molecules, Oxford University Press, New York **1989**.
(15) Suleimenov, O. M.; Ha, T. K. *Chem. Phys. Lett.* **1998**, *290*,451–457.
(16) H. D. B. Jenkins, D. Tudeal, L. Glasser, *Inorg. Chem.* **2002**, *41*, 2364 – 2367.
(17) M. W. Schmidt, M. S. Gordon, J. A. Boatz, *J. Phys. Chem. A* **2005**, *109*, 7285-7295.
(18) W. J. Middleton, E. L. Little, D. D. Coffman, V. A. Engelhardt, *J.Am. Chem. Soc.* **1958**, *80*, 2795 – 2806.
(19) a) Ye, C.; Shreeve, J. M. *J. Phys. Chem. A.* **2007**, *111*, 1456–1461. b) Gao. H.; Ye, C.; Piekarski, C. M.; Shreeve, J. M. *J. Phys. Chem. C*, **2007**, *111*, 10718 – 10731.
(20) Xue, H.; Gao, H. Twamley, B.; Shreeve, J. M. *Chem. Mater.* **2007**, 1731 – 1739.

Chapter 5

Tetranitroacetimidic acid (TNAA) − A High Oxygen Oxidizer and Potential Replacement for Ammonium Perchlorate

by

Thao T. Vo, Damon A. Parrish, and Jean'ne M. Shreeve

Has been submitted for publication to

Journal of American Chemical Society

Abstract:

Considerable work has been focused on developing replacements for ammonium perchlorate, a primary choice for solid rocket and missile propellants, due to environmental concerns resulting from the release of perchlorate into ground water systems, which have been linked to thyroid cancer. Additionally, the generation of hydrochloric acid contributes to high concentrations of acid rain and to ozone layer depletion. En route to synthesizing salts which contain cationic FOX-7, a novel, high oxygen-containing oxidizer, tetranitroacetimidic acid (TNAA), has been synthesized and fully characterized. The properties of TNAA were found to be exceptional with a calculated specific impulse exceeding that of ammonium perchlorate (AP), leading to its high potential as a replacement for AP. TNAA can be synthesized easily in a one step process from the nitration of FOX-7 in high yield (> 93%). The synthesis, properties, and chemical reactivity of TNAA have been examined.

5.1 Introduction

Ammonium perchlorate (AP) has long been the primary choice as an oxidizer in propellants for rockets and missiles.[1,2] However, significant global efforts to replace AP stems from environmental concerns due to the release of perchlorate into ground water systems and the generation of hydrogen chloride during burning – enhancing acid rain and depletion of the ozone layer.[3] The contamination in soil and water has driven major health concerns as perchlorates can affect normal thyroid functions by competing with the binding sites of iodine and is linked to thyroid cancer.[4] In addition, a major disadvantage of AP is that the chlorine content causes a smoke that can be easily detected by radar or when the humidity is high, a white smoke can be seen easily.[5] Therefore, considerable effort have been made to replace AP

in propellant formulations. Among the chlorine-free oxidizers developed, ammonium dinitroamide (ADN) and hydrazinium nitroformate (HNF) have risen as potential replacements for AP since their properties are comparable and the reduced introduction of harmful contaminants into the environment make them appealing.[4,6,7] However, both suffer from drawbacks due to their sensitivity towards impact and friction and ADN's high hygroscopic nature.[5,8] Therefore, further research is required to develop oxidizers that are stable, environmentally friendly and readily synthesized (in good yields) to become suitable for replacing AP.

For some time our group has been interested in expanding the chemistry of 1,1-diamino-2,2-dinitroethene (FOX-7),[9] an insensitive energetic material which has attracted considerable attention as a potential replacement for some commonly used explosives which suffer from sensitivity towards external stimuli and are deemed toxic to the environment.[10-15] We recently examined the reactivity of FOX-7 and its hydrazine derivative, 1-amino-1-hydrazino-2,2-dinitroethene (HFOX), with a variety of strong acids which led to the first isolated salts that contain FOX-7 and HFOX cations.[16] This work demonstrates the amphoteric properties of FOX-7 and HFOX and gives rise to new potential building blocks for energetic salts. Among the acids examined, the reaction of FOX-7 with fuming nitric acid led to the formation of the title compound, tetranitroacetimidic acid (TNAA), rather than the anticipated nitrate salt. Very few examples of the conversion of gem-dinitro substrates to trinitromethyl complexes have been reported which makes the chemical formation of TNAA of interest.[17] Following characterization of TNAA, this exciting new molecule was found to have applications as an efficient oxidizer with properties exceeding those of AP and comparable to ADN and HNF. Now we describe our contributions to the new chemistry of FOX-7 and to the development of a likely new oxidizer through the synthesis and full characterization of TNAA concomitantly with its potential application as a suitable replacement for AP.

5.2 Results and Discussion

Tetranitroacetimidic acid, TNAA (**2**), was synthesized by the reaction of FOX-7 (**1**) with an excess of fuming nitric acid to leave colorless crystals when the excess acid was

removed in vacuo (Scheme 5.1). Unlike the cationic salts of FOX-7 obtained with other strong acids,[16] compound **2** is stable at room temperature for long periods and is non-hygroscopic. The colorless crystals may yellow slightly over time. TNAA is only slightly

Scheme 5.1. Synthesis of 2.

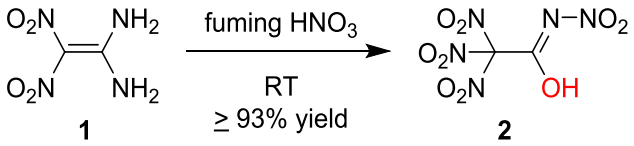

soluble in most organic solvents, but can be partially dissolved in ethyl acetate and dichloromethane. It is unstable in acetonitrile as became evident when dissolved in deuterated acetonitrile for NMR studies. The compound began to decompose, generating heat, and bubbles of a brown gas (nitrogen dioxide). Decomposition also occurs in DMSO.

The structure of **2** was determined by single crystal X-ray analysis (Figure 5.1). It crystallizes in the monoclinic space group $P2_1/c$ system with four molecules per unit cell. The C-C bond distance (1.53 Å) agrees with the average bond distance for a single C-C bond (1.54 Å). Upon closer examination of the C2-N3 and C2-O16 bond distances, the C-N bond distance of **2** (1.31 Å) is slightly shorter than the average bond distance for a single C-N bond (1.47 Å) and slightly longer than C=N (1.22 Å). Also, the C-O bond distance of 1.29 Å is slightly longer than that of C=O (1.23 Å), suggesting that TNAA may exist as an equilibrium between the two forms as shown in Figure 5.2.

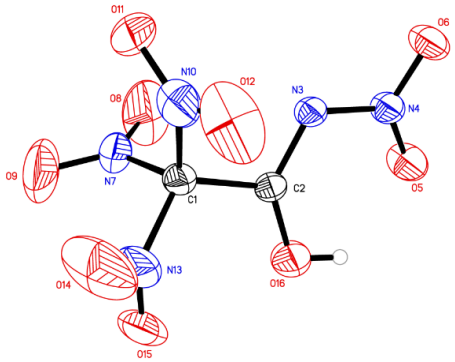

Figure 5.1. Thermal ellipsoids plot (50%) - single crystal X-ray structure of **2.**

Mass spectroscopy (EI) was also used to verify the structure of TNAA. The parent peak assigned to 239 amu, a signal at 240 amu assigned to M^+-1 and a strong signal assigned to 150 amu assigned to the trinitromethyl group [-$C(NO_2)_3$] were observed.

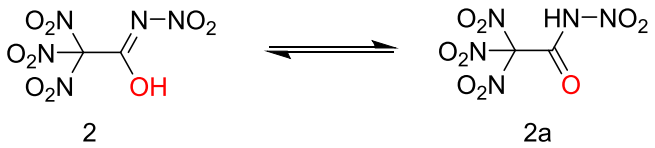

2 2a

Figure 5.2. Possible equilibrium between two forms of TNAA based on bond lengths.

The amino derivative of **2,** compound **3,** was synthesized earlier by nitrating FOX-7 with a mixture of nitric acid, trifluoroacetic anhydride, and trifluoroacetic acid (Scheme 5.2).[18] However, **3** was isolated as an oil and found to be very unstable at room temperature. Direct characterization of **3** has not been reported. Indirect structural deduction of **3** was accomplished by reacting it with ammonia in acetonitrile to obtain the stable products ammonium trinitromethanide and mononitroguanidine.[18]

Scheme 5.2. Reaction of FOX-7 with a mixture of nitric acid, trifluoroacetic anhydride (TFAA), and trifluoroacetic acid (TFA) to form compound 3.

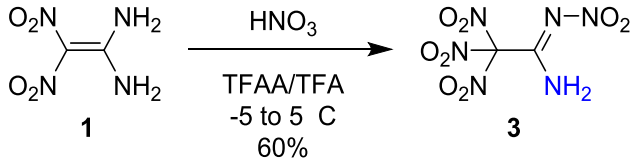

1 3

The nitration of 1,1,-diamino-2,2,-dinitroethylene derivatives examined by Baum and co-workers suggested that formation of the trinitromethyl moiety could result from two potential routes: 1) an attack on a nitronium ion by the nitrovinyl carbon with concomitant loss of a proton from the amino nitrogen or 2) nitration of the amine nitrogen; however, the reaction order is unknown (Scheme 5.3).[17]

Scheme 5.3. Nitration pathways of 1,1,-diamino-2,2,-dinitroethylenes

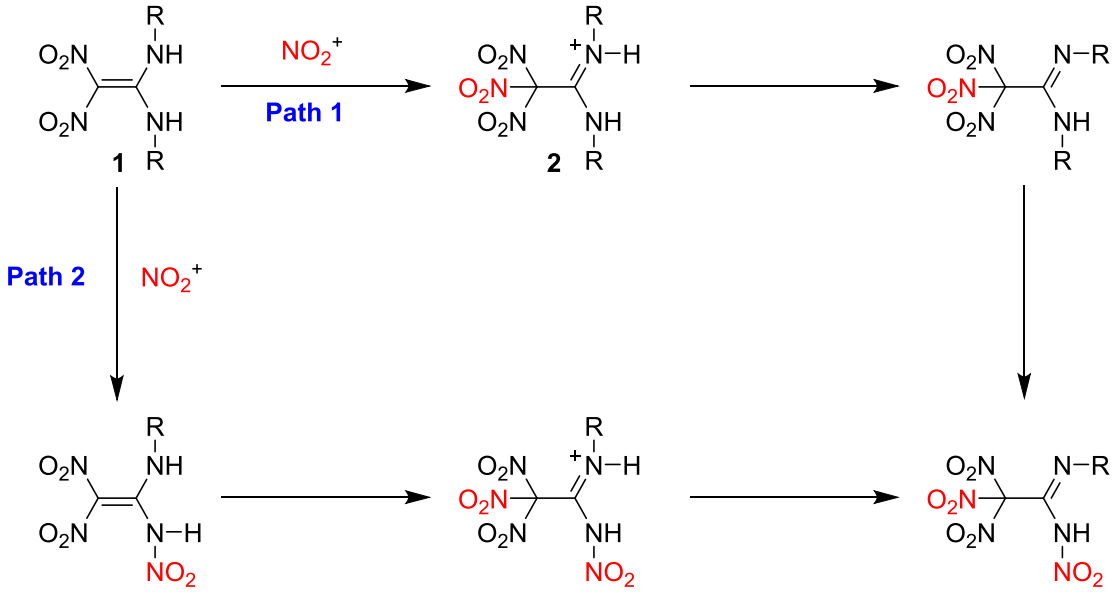

In our current work, **3** may have formed, but due to the lack of a scavenging agent to take up the water formed, the latter may react further with the amine intermediate, leading to **2** (Scheme 5.4). It should be noted that in the preparation of **2**, it is important to use freshly

Scheme 5.4. Reaction of FOX-7 in the absence of a scavenging agent to form 2.

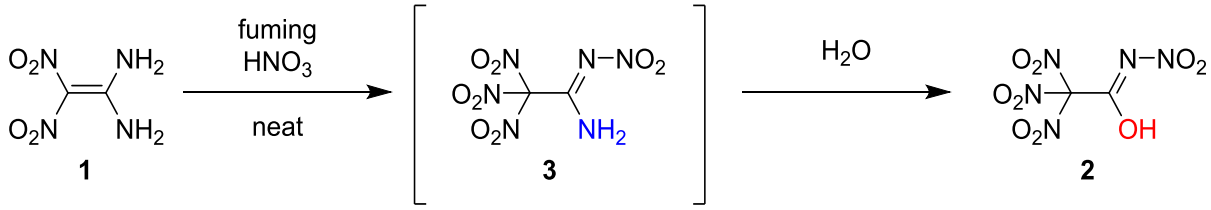

distilled fuming nitric acid and to remove all the excess acid prior to exposing the sample to air. If residual amounts of the acid remain, **2** slowly transforms to nitrourea (**4**) as was confirmed by single crystal X-ray analysis. Surprisingly, no crystal data for nitrourea were found in the records of the Cambridge Crystallographic Data Center. Its single crystal structure data are given in the Supporting Information.

The formation of TNAA is also dependent on the concentration of the nitric acid. When FOX-7 was treated with commercially available 65% nitric acid (~16 M) and allowed to stir overnight, brown gas (nitrogen dioxide) was found over the solution inside the reaction

flask. The reaction was quenched with ice and the product was extracted with dichloromethane to yield amidinoformic acid (**5**). The formation of **5** was previously reported (unexpectedly) by reacting FOX-7 with a variety of organic peroxides such as 30% hydrogen peroxide (H_2O_2), Caro's acid (H_2SO_5) or peroxytrifluoroacetic acid (CF_3CO_3H) (Scheme 5.5).[19a]

Scheme 5.5. Synthesis of 5 from 1 with organic peroxides.

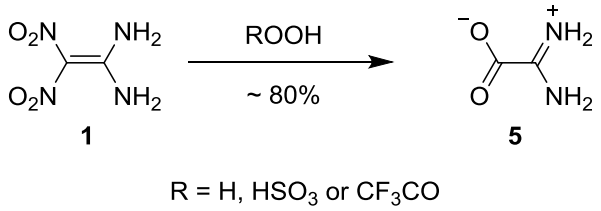

Based on the literature precedence for the formation of **5**, it is likely that the same proposed mechanism is suitable when FOX-7 is reacted with 65% HNO_3 rather than with the peroxide (Scheme 5.6). The loss of HNO_2 leads to intermediate **7** which can undergo a nitro–

Scheme 5.6. Proposed mechanism for formation of 5 from 1 with 65% HNO_3.

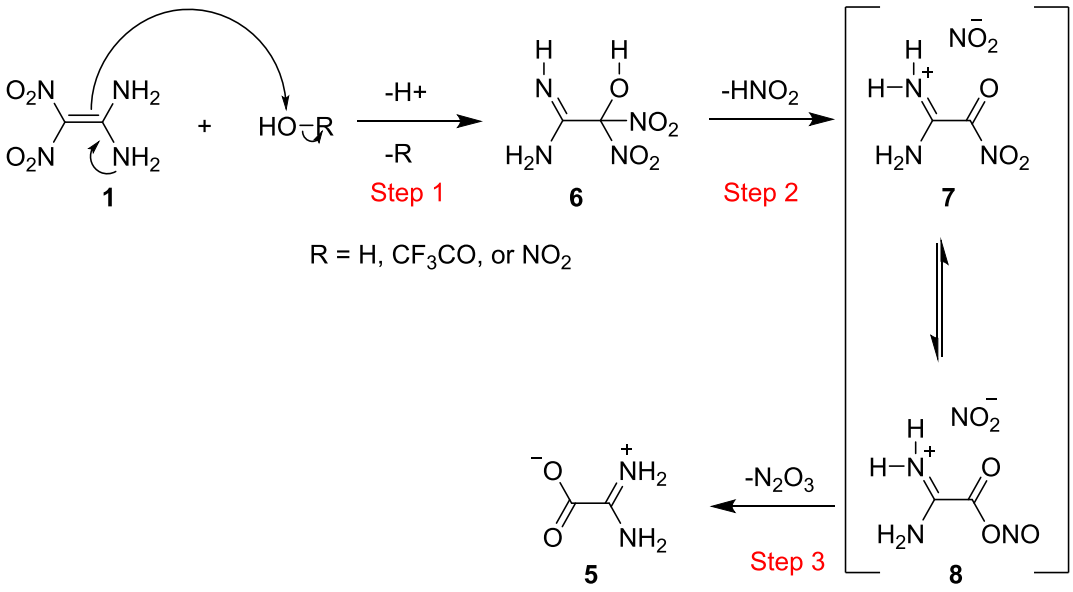

nitrito rearrangement[19b] to form **8** in step 2 of Scheme 5.6. Nucleophilic attack of the nitrite ion with intermediate **8** followed by the displacement of dinitrogen trioxide leads to the formation of product **5** (step 3). The lack of formation of **2** with 65% HNO_3 may be a result of the quenching step with water. When the reaction was attempted without quenching, the excess acid was removed under vacuum to give an unknown white solid. Therefore, the water content present in 65% HNO_3 compared to fuming HNO_3 may play a significant role in the formation of compound **5** versus **2**.

Attempts to extend this acid chemistry to HFOX with fuming nitric acid under neat conditions resulted in combustion of HFOX after the addition of the second drop of nitric acid. Subsequently HFOX was suspended in acetonitrile and cooled in an ice bath before addition of nitric acid. When the excess acid and solvent was removed, white needles were obtained. Upon repeating this reaction several times, the final product exploded at reduced pressure. Because of safety concerns, this chemistry was no longer pursued. Any attempts to study this chemistry should be accomplished with extreme caution keeping in mind that HFOX itself can spontaneously detonate.

Compound **2** is a very attractive and promising stable oxidizer (MP 91°C and $T_{d\ (onset)}$ 137 °C) with a majority of its properties (calculated via Explo5 v6.01) exceeding that of AP

Table 5.1. Physical properties of AP, ADN and TNAA

	AP	**ADN**[a]	**HNF**[b]	**2**
Formula	NH_4ClO_4	$NH_4N(NO_2)_2$	$N_2H_5C(NO_2)_3$	$C_2HN_5O_8$
Tm[c] (°C)	---	93	129	91
Tdec[d] (°C)	> 200	159	131	137
IS[e] (J)	15[f]	3–5	4	19
FS[g] (N)	> 360[h]	64–72	28	20
N[i]%	11	52	38	29
O[j]%	54	45	52	60
OB[k] %	26	26	13	30
d[l] (gcm^{-3})	1.95	1.81	1.86	1.87[m] (1.84)[n]
Isp[o] (s)	156	202[p]	265[q]	209

a) [Ref. 3] b) [Ref. 8]. c) Melting temperature. d) Decomposition temperature [onset]. e) Impact sensitivity. f) [Ref. 1]. g) Friction sensitivity. h) Measured FS. i) Nitrogen content. j) Oxygen content. k) Oxygen balance. l) density. m) Measured density. n) Crystal density. o) Specific impulse [values were obtained from Explo5 v6.01 and calculated at an isobaric pressure of 70 bar and initial temperature of 3,300 K]. p) Calculated via Explo 5 v6.01. q) [Ref. 5].

(Table 5.1). It was also found to have properties that were comparable to ADN and HNF. In comparison with AP, **2** has a significantly enhanced nitrogen and oxygen content and higher positive oxygen balance due to the trinitromethyl group. The oxygen balance is a measure of the amount of oxygen available for combustion of energetic materials. Positive OBs indicate there is more than enough oxygen to convert all carbon to carbon monoxide and all hydrogen to water whereas negative values indicate that the oxygen content is insufficient for complete oxidation. The specific impulse (Isp) is a measure of a propellant's efficiency. Compared to AP, **2** has a higher specific impulse (209 s) and is slightly more stable towards impact (19 J) with a comparable density. In comparison to ADN, **2** is significantly more stable towards impact, has a higher oxygen balance, higher oxygen content, and slightly better density and specific impulse values. However, the thermal stability and friction sensitivity of **2** ($T_{dec\ (onset)}$ =137 °C; FS = 20 N) are not competitive with AP (T_{dec} > 200 °C; FS >360) and is slightly less than that of ADN (T_{dec} = 150 °C; FS = 64-72 N). Enhancing these two properties may make **2** even more appealing and a better substitute for AP. Therefore we were prompted to study the chemical reactivity of **2** to understand and enhance the molecular structure to obtain the desired properties.

The unique structure of **2** and the likely existence of the two forms (Figure 2) may explain its challenging reaction chemistry. Our initial studies began with examining the reactivity of the hydroxyl group in **2**. Attempts to dimerize compound **2** with P_4O_{10} were unsuccessful (Scheme 5.7, structure **9**). In an effort to replace the hydroxyl group by fluorine with

Scheme 5.7. Reaction of 2 with P_2O_5 and Olah's reagent.

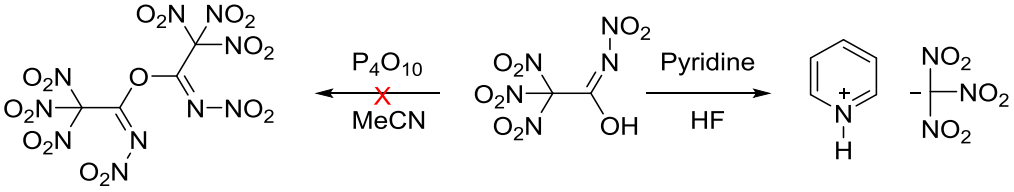

Olah's reagent (pyridine/HF), no fluorinated product was observed and rather the long known pyridinium trinitromethanide (**10**), first reported in 1920, was isolated.[20] Interestingly,

the crystal structure of **10** was not recorded at the Cambridge Crystallographic Data Centre. Suitable crystals of **10** were isolated and single crystal X-ray analysis was obtained to complete the structural identification.

The reactivity of **2** with simple bases was then examined. When sodium hydroxide or sodium bicarbonate was added to a suspension of **2** in water, sodium salts **11** and **12** were isolated (Scheme 5.8). Similar results were observed when ammonia or guanidinium

Scheme 5.8. Reaction of 2 with NaOH.

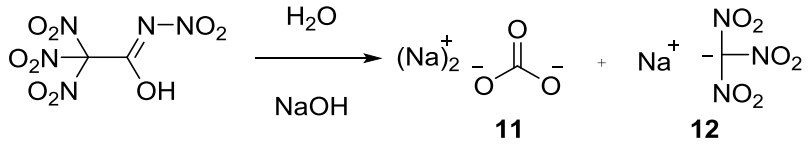

carbonate was reacted with **2** where the corresponding trinitromethanide salt was isolated and verified by elemental and crystal structure analysis. These results indicated the highly reactive nature of the amide moiety with bases. Compound **2** with acids was also examined. By studying a variety of weak and strong acids [i.e., trifluoroacetic acid (pKa = 0.5), hydrochloric acid (pKa = -7), and perchloric acid (pKa = -10)], it was found that **2** only reacted with triflic acid (CF_3SO_3H; pKa = -15). When **2** was stirred with an excess of triflic acid under neat conditions for 30 minutes at 25 $^{\circ}$C, colorless crystals were obtained after the removal of the majority of the acid over an extended period in vacuo. These hygroscopic crystals were identified as the cocrystal salt **13** containing a 1:1 ratio of 1-amino-2,2,2-trinitroethaniminium triflate and triflate hydrate via single crystal X-ray analysis (Scheme 5.9; Figure 5.33) and can be stored at room temperature under vacuum for several weeks without decomposition.

Scheme 5.9. Reaction of 2 with CF_3SO_3H.

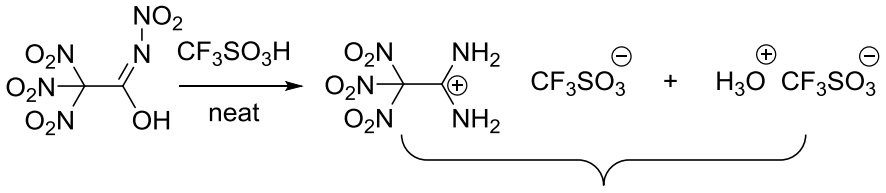

13

In addition to X-ray crystal structure, the structure of **13** was also supported by ^{13}C and ^{19}F NMR, elemental analysis. The cocrystal salt (**13**) crystallizes in a triclinic space group P-1

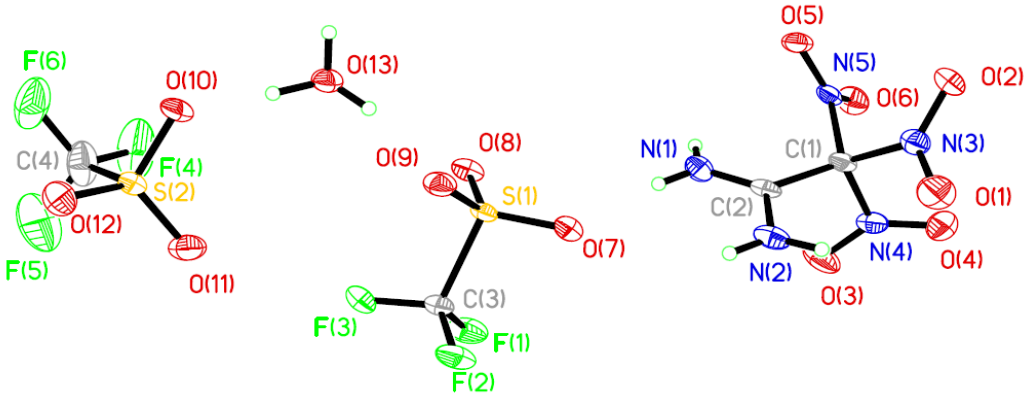

Figure 5.3. Single crystal X-ray structure of salt **13** - thermal ellipsoids plot (50%).

with two molecules per unit cell and has a crystal density of 1.48 gcm^{-3}. The C-C bond distance (C1-C2, 1.53 Å) agrees with the average bond distance for a single C-C (1.54 Å) bond. Examining the bond distance of C2-N1 (1.29) and C2-N2 (1.30), the C-N bond distance is shorter than the average bond distance for a single C-N single bond (1.47 Å) and longer than the average C=N double bond(1.22 Å) indicating the positive charge is delocalized over the atoms N1-C2-N2.[16]

The unexpected reduction of the N-NO_2 group of **2** in the formation of the trinitroethaniminium cation in **13** is supported by the literature for the unique ability of triflic acid to reduce the nitro group in nitrobenzyl alcohol (Scheme 5.10).[22] However, further investigation is necessary to understand the mechanistic transformation of the 1-amino-2,2,2-trinitroethaniminium cation.

Scheme 5.10. Reduction of the nitro group via triflic acid.

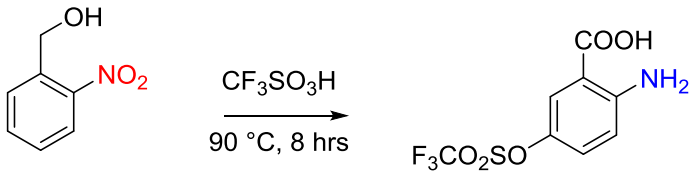

14 **15**

The existence of the 1-amino-2,2,2-trinitroethaniminium cation in **13** is interesting due to its appeal as a precursor for energetic salts. Typical cations used for energetic salts have high nitrogen and low oxygen content; however, the **13** cation has both high nitrogen and oxygen content, making it an ideal building block for energetic salts. The density of trinitroethaniminium triflate of cocrystal salt **13** was calculated (by literature method)[21a] to be 2.09 gcm^{-3} with a detonation pressure (D) and velocity (V), calcluated via Explo 5 v6.01, of 25 Gpa and 7208 ms^{-1}. The low energetic performance is expected as the counter ion is non-energetic. When the 1-amino-2,2,2-trinitroethaniminium cation is parlayed with dinitroamide [$N(NO_2)_2^-$] (**14**), the density (cacluated)[21a] was found to be 2.06 gcm^{-3} and the detonation performances were found to be high (D = 9053 ms^{-1}; P = 36 Gpa) for the dinitroamide salt, exceeding the values of FOX-7 (D = 8771 ms^{-1}, P = 35 GPa) and RDX (cyclo-1,3,5-trimethylene-2,4,6-trinitramine; D = 8864 ms^{-1}, P = 36 GPa) (see Supporting Information). The density of trinitroethaniminium triflate of cocrystal salt **13** was calculated be 2.09 gcm^{-3} with a detonation pressure and velocity of 25 Gpa and 7208 ms^{-1} respectively and a specific impulse of 247.[21a] Further investigation is required to enhance the stability of **13** with anions that are suitable to stabilize the 1-amino-2,2,2-trinitroethaniminium cation which may give rise to interesting and powerful energetic salts.

5.3 Conclusion

In summary, the chemical reactivity of FOX-7 has been expanded via the synthesis and characterization of a new oxidizer, TNAA (**2**), which results from a simple single step process from FOX-7 in high yield ($\geq$ 93%). This novel molecule has a high potential for replacing ammonium perchlorate as an oxidizer for applications in solid rocket propellants and missiles. TNAA (**2**) was fully characterized via single crystal X-ray analysis and the

calculated specific impulse further supports the potential of **2** as an efficient oxidizer with enhanced properties compared to AP and some properties which are comparable to ADN. Compound **2** is more stable towards impact relative to AP and ADN. The reaction chemistry of **2** leads to some interesting insights in its synthesis and reactivity such as the formation of **13**. The 1-amino-2,2,2-trinitroethaniminium cation of **13** represents a very promising energetic precursor for energetic salts due to its high nitrogen and oxygen content. Compound **2** exhibits an interesting molecular structure that is thermally and chemically stable. The formation of such a structure adds to the examples of transformation of the gem-dinitro system to trinitromethyl-containing materials. As is the case for FOX-7, the chemical reactivity of **2** needs further investigation in order to fully explore its reaction chemistry.

ASSOCIATED CONTENT

Supporting Information

Experimental procedures, characterization data (single crystal X-ray), and heat of formation calculations. This material is available free of charge via the Internet at http://pubs.acs.org.

AUTHOR INFORMATION

Corresponding Author

jshreeve@uidaho.edu

Notes

The authors declare no competing financial interest.

ACKNOWLEDGMENTS

The authors gratefully acknowledge the support of ONR (N00014-12-1-0536 and N00014-11-AF-0-0002), Dr. Clifford Bedford, and the Defense Threat Reduction Agency (HDTRA 1-11-1-0034). We are indebted for Mr. Scott Economu and Dr. Brendan Twamley for considerable assistance with crystal structuring.

5.4 References

(1) Klapötke, T. M. *Chemistry of High-Energy Materials*; Walter de Gruyter GmbH & Co. KG:Berlin/New York, **2011**; pp 179–184.

(2) Klapötke, T. M.; Gökçinar, E. *Turk. J. Chem.* **2010**, *34*, 953–967.

(3) Nagamachi, M. Y.; Oliveira, J. I. S.; Kawamoto, A. M.; Dutram, R. C. L. *J. Aerosp. Technol. Manag.*, **2009**, *1*, 153–160.

(4) Mandal, A. K.; Kunjir, G. M.; Singh, J.; Adhav, S. S.; Singh, S. K.; Pandey, R. K.; Bhattacharya, B.; Kantam, M. L. *Cent. Eur. J. Energetic Mater.,* **2014**, *11*, 83–97.

(5) Silva, G. D.; Rufino, S. C.; Iha, K. *J. Aerosp. Technol. Manag.* **2013**, *5*, 139–144.

(6) Jadhav, H. S.; Talawar, M. B.; Dhavale, D. D.; Asthana, S. N.; Krishnamurthy, V. N. *Indian J. Chem. Tech.* **2005**, *12*, 187–192.

(7) Dendage, P.S.; Sarwade, D. B.; Asthana, S. N.; Singh, H. *J. Energ.Mater.***2001**, *19*, 41–78.

(8) Joo, Y.-H.; Min, B. S. *New J. Chem.* **2014**, *38*, 50–54.

(9) (a) Garg, S.; Gao, H.; Joo, Y.-H.; Parrish, D. A.; Shreeve, J. M. *J. Am. Chem. Soc.* **2010**, *132*, 8888–8890 and references cited therein. (b) Garg, S.; Gao, H.; Parrish, D. A.; Shreeve, J. M. *Inorg. Chem.* **2011**, *50*, 390–395 and references cited therein. (c) Vo, T. T.; Shreeve, J. M. FOX-7 as a Coordinating Ligand or Anion in Metal Salts. Abstracts from the 66th Northwest Regional Meeting of the American Chemical Society, Portland, OR, June 26–29, **2011**; NORM 188. (d) Gao, H.; Shreeve, J. M. *Chem. Rev.* **2011**, *111*, 7377–7436. (e) Gao, H.; Joo, Y.-H.; Parrish, D. A.; Vo, T.; Shreeve, J. M. *Chem. Eur. J.* **2011**, *17*, 4613–4618. (f) Vo, T. T.; Parrish, D. A.; Shreeve, J. M. *Inorg. Chem.* **2012**, 51, 1963–1968 and references cited therein. (g) Vo, T. T.; Zhang, J.; Parrish, D. A.; Twamley, B.; Shreeve, J. M. *J. Am. Chem. Soc.* **2013**, *135*, 11787–11790.

(10) (a) Latypov, N. V.; Bergman, J.; Langlet, A.; Wellmar, U.; Bemm, U. *Tetrahedron* **1998**, *54*, 11525–1153. (b) Hervé, G.; Jacob, G.; Latypov, N. *Tetrahedron* **2005**, *61*, 6743–6748. (c) Bellamy, A. J. FOX-7 (1,1-Diamino-2,2-dinitroethene). In *High Energy Density Materials*; Klapötke, T. M., Ed.; Structure and Bonding 125; Springer-Verlag: Berlin/Heidelberg, **2007**; pp 1–33 and references cited therein.

(11) Agrawal, J. P.; Hodgson, R. D. *Organic Chemistry of Explosives*; John Wiley & Sons, Ltd.: Chichester, **2007**; p 243.

(12) Krause, H. H. In *Energetic Materials*; Teipel, U., Ed.; VCH: Weinheim, **2005**; pp 1–25.

(13) Hervé, G. *Propellants Explos. Pyrotech.* **2009**, *34*, 444–451.

(14) Anniyappan, M.; Talawar, M. B.; Gore, G. M.; Venugopalan, S.; Gandhe, B. R. *J. Hazard. Mater.* **2006**, *137*, 812–819.

(15) Sandberg, C.; Latypov, N. V.; Goede, P.; Tryman, R.; Bellamy, A. J. New Trends Res. Energ. Mater., Proc. Semin. 5th, **2002**, 292–299.

(16) Vo, T. T.; Parrish, D. A.; Shreeve, J. M. *J. Am. Chem. Soc. pending.*

(17) (a) Baum, K.; Nguyen, N. V.; Gilardi, R.; Flippen-Anderson, J. L.; George, C. *J. Org. Chem.* **1992**, *57*, 3026–3030. (b) Baum, K. U.S. Army Research Office *Chemistry of Polynitroethane Derivatives Final Report (Contract DAAL03-88-C-0013)*; **1992**, 1-6.

(18) Hervé, G.; Jacob, G.; Latypov, N. *Tetrahedron*, **2005**, *61*, 6743–6748.

(19) (a) Hervé, G.; Jacob, G. *Tetrahedron*, **2007**, *63*, 953–959. (b) Amin, M. R.; Dekker, L.; Hibbert, D. B.; Ridd, J. H.; Sandall, J. P. B. *J. Chem. Soc., Chem. Commun.* **1986**, 658 – 659.
(20) Schmidt, E.; Fischer, H. *Ber. Dtsch. Chem. Ges.*, 1920, **53**, 1529 – 1537.
(21) (a) Ye, C.; Shreeve, J. M. *J. Phys. Chem. A.* **2007**, *111*, 1456–1461. b) Gao. H.; Ye, C.; Piekarski, C. M.; Shreeve, J. M. *J. Phys. Chem. C*, **2007**, *111*, 10718–10731.
(22) Austin, R. P.; Ridd, J. H. *J. Chem. Soc., Perkin Trans.2*, **1994**, 1411–1414.

5.5 Supporting Information

Tetranitroacetimidic acid (TNAA) − A High Oxygen Oxidizer and Potential Replacement for Ammonium Perchlorate

Thao T. Vo [§], Damon A. Parrish[‡], and Jean'ne M. Shreeve[*,§],

[§] Department of Chemistry, University of Idaho, Moscow, Idaho 83833-2343

[‡] Naval Research Laboratory, 4555 Overlook Avenue, Washington, D. C. 20375

E-mail: jshreeve@uidaho.edu

Table of Contents

(Compounds are numbered as in the paper)

5.5.1 Experimental

1. General experimental methods: : ^{1}H, ^{13}C, and ^{19}F spectra were recorded on a 300 MHz (Bruker AVANCE 300) nuclear magnetic resonance spectrometer operating at 300.1 MHz, 75.47 MHz, and 282.40 MHz respectively. Analysis of ^{13}C, ^{19}F, and ^{14}N were also recorded on a 500 MHz (Bruker AVANCE 500) nuclear magnetic resonance spectrometer operating at 125.76 MHz, 470.59 MHz, and 36.14 MHz, respectively. CD_3CN was used as a locking solvent unless otherwise stated. Chemical shifts in ^{1}H and ^{13}C spectra were reported relative to Me_4Si. The melting and decomposition points were recorded with a differential scanning calorimeter (DSC, TA Instruments Q10) at a scan rate of 5 ºC min^{-1} in closed aluminum containers. IR spectra were recorded using KBr pellets for solids on a BIORAD model 3000 FTS spectrometer. Elemental analyses were obtained on a CE-440 elemental analyzer (EAI Exeter Analytical).

Safety Precautions: While we have experienced no difficulties in syntheses and characterization of these materials, proper protective measures should be used. Manipulations must be carried out in a hood behind a safety shield. Eye protection and leather gloves must be worn. Caution should be exercised at all times during the synthesis, characterization, and handling of any of these materials, and mechanical actions involving scratching or scraping must be avoided.

Note: Acetonitrile was dried over molecular sieves (3Å) prior to use.[1] FOX-7 was synthesized according to literature procedures.[2]

2. Tetranitroacetimidic acid (TNAA, 2):

To a round bottomed flask charged with 0.5 g (3.4 mmol) of FOX-7, 4 mL of freshly distilled fuming nitric acid was added drop wise at room temperature. The reaction was capped and allowed to stir for an additional 10 minutes. The excess acid was then removed under vacuum to give colorless crystals (> 93% yield). [Note: it is important to use freshly distilled nitric acid and to remove all the acid under vacuum.]. Compound 2 can be recrystallized with dichloromethane. Structural identification was completed by single crystal X-ray analysis. ^{13}C

NMR: δ = 150.74 ppm (C-OH),122.92 ppm (C-NO_2). IR (KBr): $\tilde{\nu}$ = 3425, 3333, 3301, 1638, 1610, 1522, 1474, 1395, 1352, 1248, 1171, 1030, 858, 791, 751, 642, 622, 577, 521cm^{-1}. Elemental analysis ($C_2HN_5O_9$, 239.06): Calcd. C, 10.05%; H, 0.42%; N, 29.30%. Found C, 9.99%; H,0.76_; N,33.64%. Tm = 91°C; Tdec(onset) = 137 °C.

3. Synthesis of Amidinoformic acid (5)

To a round bottom charged with 0.25 g (1.7 mmol) FOX-7, 2.3 mL of commercially available 65% HNO3 was added dropwise. The reaction was capped and allowed to stir overnight. The reaction was then quenched with water and the final product was extracted with dichloromethane (67% yield). Structural verification was obtained via crystal structure. IR (KBr): $\tilde{\nu}$ = 3354, 3323, 3171, 3020, 1715, 1645, 1489, 1358, 1303, 1130, 1105, 885, 851, 826, 763, 671 cm^{-1}. Tm = 274 °C. Elemental analysis ($C_2H_4N_2O_2$, 88.07): Calcd. C, 27.28%; H, 4.58%; N, 31.81%. Found C, 27.28; H, 4.52; N, 31.52%

4. Synthesis of cocrystal 1-amino-2,2,2-trinitroethaniminium triflate – triflate hydrate (13):

To a round bottom charged with (0.34g) 1.3 mmol of TNAA, 0.8 mL triflic acid (CF_3SO_3H) was added dropwise at room temperature. The reaction vessel was capped and the mixture was stirred vigorously for approximately 45 minutes (until all the starting material dissolved). The majority of the excess acid was removed under high vacuum for ~ 3 days. Colorless hygroscopic crystals of the new product formed within 2 days that were suitable for single crystal X-ray analysis (79% yield). ^{13}C NMR: δ = 151.84 ppm (C-OH), [125.16, 122.63, 120.1, 117.56 (CF_3SO_3), 119.78 ppm (C-NO_2). ^{19}F NMR: δ = -79.87 ppm. ^{14}N NMR: δ = -34.53 ppm (N-NO2), -41.90 ppm ([C-NO2]3), -262.34ppm (N-NO2). IR (KBr): $\tilde{\nu}$ = 3416, 3277, 3269, 3089, 1716, 1637, 1614, 1491, 1458, 1248, 1175, 1096, 1040, 850, 798, 735, 642 cm^{-1}. [Note: extended NMR studies showed the product reacting with the solvent, potentially reacting with water which is absorbed over time.]. Tdec(onset) = 135 °C. Elemental analysis ($C_4H_7N_5O_{12}F_6S_2$, 671.35): Calcd. C, 9.40%; H, 1.38%; N, 13.70%. Found C, 9.12%; H, 1.71%; N, 13.82%

5.5.2 X-ray crystallography:

A colorless prism of dimensions 0.51 x 0.26 x 0.03 mm^3 (**2**), a colorless prism of 0.16 x 0.15 x 0.04 mm^3 (**4**), a yellow plate crystal of dimensions 0.071 x 0.170 x 0.175 mm^3 (**10**), and a colorless plate of 0.884 × 0.238 × 0.192 mm^3 (**13**) were mounted with a MiteGen MicroMesh and a small amount of Cargille Immersion Oil (**2**, **4**, and **10**) or a Nylon loop with paratone oil (**13**). Data were collected on a Bruker three-circle platform diffractometer equipped with a SMART APEX II CCD detector. The crystals were irradiated using graphite monochromated MoK_α radiation (λ = 0.71073). An Oxford Cobra low temperature device was used to keep the crystals at a constant 124(2) K [**3a** and **3b**], and 150(2) K [**4a**] during data collection. For compound **9**, data were collected using a Bruker CCD (charge coupled device) based diffractometer equipped with an Oxford Cryostream low-temperature apparatus operating at 293 K (**2**), 100 (K) (**4**), 150 (**10**) and 173K (**13**), . Data were measured using omega and phi scans of 1.0° per frame for 30 s. The total number of images was based on results from the program COSMO[3] where redundancy was expected to be 4.0 and completeness to 0.83 Å to 100%.

For all the salts, data collection was performed, and the unit cell was initially refined using APEX2 [v2009.3-0].[4] Data reduction was performed using SAINT [v7.60A][5]and XPREP [v2008/2].[6] Corrections were applied for Lorentz, polarization, and absorption effects using SADABS [v2008/1].[7] The structure was solved and refined with the aid of the programs in the SHELXTL-plus [v2008/4] system of programs (**3a**, **3b**, and **4a**).[8] The full-matrix least-squares refinement on F^2 included atomic coordinates and anisotropic thermal parameters for all non-H atoms. The H atoms were included using a riding model. Details of the data collection and refinement are given in Table S1.

For cocrystal salt **13**, cell parameters were retrieved using APEX II software[9] and refined using SAINT on all observed reflections. Data reduction was performed using the SAINT software[10] which corrects for Lp. Scaling and absorption corrections were applied using SADABS[11] multi-scan technique, supplied by George Sheldrick. The structures are solved by the direct method using the SHELXS-97 program and refined by least squares method on F^2, SHELXL-97,[12] which are incorporated in OLEX2[13]. The structure was solved in the space group $P\bar{1}$ (# 2). All non-hydrogen atoms are refined anisotropically. Hydrogens were calculated by geometrical methods and refined as a riding model.

5.5.3 Crystal data and structural refinement:

Table 5.S1. Crystallographic data for salts **3a**, **3b**, **4a**, and compound **9**

	2	**4**	**10**	**13**
Formula	C2HN5O9	$CH_3N_3O_3$	$C_6H_4N_4O_6$	$C_4H_7N_5O_{12}F_6S_2$
MW	239.06	105.06	228.13	671.35
CCDC	1008515	1008514	1008745	1008513
T [K]	293(2)	100(2)	150(2)	173(2)
Wavelength (Å)	0.71073	0.71073	0.71073	0.71073
Crystal system	Monoclinic	Tetragonal	monoclinic	Triclinic
Space group	$P2_{1/c}$	$P4_32_12$	P121/c	P-1
a (Å)	11.866(4)	4.8710(8)	8.416(4)	5.8369(3)
b (Å)	6.713(2)	4.8710(8)	8.646(4)	10.0255(6)
c (Å)	10.848(4)	32.266(6)	12.186(5)	14.6488(10)
α (°)	90	90	90	99.062(3)
β (°)	93.929(4)	90	90.944(7)	90.651(3)
γ (°)	90	90	90	97.731(3)
Volume ($Å^3$)	862.0(5)	765.6(2)	886.6(6)	838.36(9)
Z	4	8	4	2
Density (calculated; g cm^{-3})	1.842	1.823	1.709	1.480
Absorption coefficient	0.192	0.177	0.156	0.271
F(000)	480	432	464	377.0
Crystal size (mm^3)	0.51 x 0.26 x 0.03	0.16 x 0.15 x 0.04	0.071 x 0.170 x 0.175	0.884 × 0.238 × 0.192
Theta range for data collection (°)	1.72 to 26.56	2.52 to 26.77	1.67 to 29.10	4.63 to 54.278
Index ranges	-14<=h<=14, -8<=k<=7, -13<=l<=13	-6<=h<=6, -5<=k<=6, -40<=l<=40	-11<=h<=11, -11<=k<=11, -16<=l<=16	-7 ≤ h ≤ 7, -12 ≤ k ≤ 12, -18 ≤ l ≤ 18
Reflections collected	7352	6993	13102	8126
Independent reflections	1771 [R_{int} = 0.0214]	807 [R_{int} = 0.0242]	2360 [R(int) = 0.1700]	3655 [R_{int} = 0.0322, R_{sigma} = 0.0458]

Table 5.S1 (continued). Crystallographic data for salts **2**, **4**, **10**, and compound **13**

	2	**4**	**10**	**13**
Absorption correction	Semi-empirical from equivalents	Semi-empirical from equivalents	Multi-scan	Multi-scan
Max. and Min. Transmission	0.9943 and 0.9084	0.9929 and 0.9722	0.4825 to 0.7452	0.884 to 0.238
Refinement method	Full-matrix least-squares on F^2	Full-matrix least-squares on F^2	Full-matrix least-squares on F^2	Full-matrix least-squares on F^2
Data/restraints/parameters	1771 / 12 / 174	807 / 0 / 64	2360 / 0 / 146	3655/0/299
Goodness-of-fit on F2	1.071	1.139	1/151	1.052
Final R indices [I>2sigma(I)]	R_1 = 0.0775, wR_2 = 0.2329	R_1 = 0.0239, wR_2 = 0.0656	R1 = 0.0987, wR2 = 0.2784	R_1 = 0.0488, wR_2 = 0.1127
R indices (all data)	R_1 = 0.0962, wR_2 = 0.2577	R_1 = 0.0261, wR_2 = 0.0672	R1 = 0.1349, wR2 = 0.3233	R_1 = 0.0683, wR_2 = 0.1220
Largest diff. peak and hole (e $Å^{-3}$)	0.627 and -0.408	0.146 and -0.189	0.677 and -0.611	0.66 and -0.50

5.5.4 Selected bond lengths and bond angles:

Compound 2

Table5.S2. Bond lengths [Å] and angles [°] for **2**.

C(1)-N(13)	1.520(5)	C(1)-N(10)	1.525(5)
C(1)-C(2)	1.534(4)	C(1)-N(7)	1.557(5)
C(1)-N(13')	1.57(2)	C(1)-N(10')	1.60(2)
C(1)-N(7')	1.64(2)	C(2)-O(16)	1.294(4)
C(2)-N(3)	1.314(4)	N(3)-N(4)	1.392(3)
N(4)-O(6)	1.214(4)	N(4)-O(5)	1.219(3)
N(7)-O(9)	1.199(6)	N(7)-O(8)	1.211(6)
N(7')-O(9')	1.204(10)	N(7')-O(8')	1.238(10)
N(10)-O(11)	1.211(5)	N(10)-O(12)	1.226(7)
N(10')-O(12')	1.213(10)	N(10')-O(11')	1.214(10)
N(13)-O(14)	1.186(6)	N(13)-O(15)	1.221(6)
N(13')-O(14')	1.214(10)	N(13')-O(15')	1.222(10)
O(16)-H(16)	0.8400		
N(13)-C(1)-N(10)	108.8(3)	N(13)-C(1)-C(2)	116.2(3)
N(10)-C(1)-C(2)	110.0(3)	N(13)-C(1)-N(7)	103.1(3)
N(10)-C(1)-N(7)	108.6(3)	C(2)-C(1)-N(7)	109.6(3)
N(13)-C(1)-N(13')	47.4(7)	N(10)-C(1)-N(13')	134.7(9)
C(2)-C(1)-N(13')	115.2(8)	N(7)-C(1)-N(13')	58.3(7)
N(13)-C(1)-N(10')	67.8(7)	N(10)-C(1)-N(10')	46.8(7)
C(2)-C(1)-N(10')	109.7(7)	N(7)-C(1)-N(10')	139.4(7)
N(13')-C(1)-N(10')	111.9(10)	N(13)-C(1)-N(7')	134.0(9)
N(10)-C(1)-N(7')	73.0(6)	C(2)-C(1)-N(7')	104.9(8)
N(7)-C(1)-N(7')	40.7(7)	N(13')-C(1)-N(7')	97.4(9)
N(10')-C(1)-N(7')	117.4(9)	O(16)-C(2)-N(3)	133.1(3)
O(16)-C(2)-C(1)	118.3(3)	N(3)-C(2)-C(1)	108.7(2)
C(2)-N(3)-N(4)	116.7(2)	O(6)-N(4)-O(5)	123.5(3)
O(6)-N(4)-N(3)	114.1(2)	O(5)-N(4)-N(3)	122.3(3)
O(9)-N(7)-O(8)	130.0(6)	O(9)-N(7)-C(1)	114.2(5)
O(8)-N(7)-C(1)	115.3(4)	O(9')-N(7')-O(8')	165(3)
O(9')-N(7')-C(1)	107.2(18)	O(8')-N(7')-C(1)	87.9(19)
O(11)-N(10)-O(12)	132.0(5)	O(11)-N(10)-C(1)	116.4(4)
O(12)-N(10)-C(1)	111.5(5)	O(12')-N(10')-O(11')	123(3)
O(12')-N(10')-C(1)	110.6(16)	O(11')-N(10')-C(1)	118(2)
O(14)-N(13)-O(15)	127.9(6)	O(14)-N(13)-C(1)	117.0(5)
O(15)-N(13)-C(1)	115.1(5)	O(14')-N(13')-O(15')	142(3)
O(14')-N(13')-C(1)	106.2(18)	O(15')-N(13')-C(1)	111(2)
C(2)-O(16)-H(16)	109.5		

Compound 4

Table 5.S3. Bond lengths [Å] and angles [°] for **4**.

N(1)-C(2)	1.3183(18)
N(1)-H(1A)	0.8800
N(1)-H(1B)	0.8800
C(2)-O(7)	1.2410(17)
C(2)-N(3)	1.4012(19)
N(3)-N(4)	1.3730(16)
N(3)-H(3)	0.8800
N(4)-O(5)	1.2229(16)
N(4)-O(6)	1.2265(15)
C(2)-N(1)-H(1A)	120.0
C(2)-N(1)-H(1B)	120.0
H(1A)-N(1)-H(1B)	120.0
O(7)-C(2)-N(1)	124.73(13)
O(7)-C(2)-N(3)	114.00(12)
N(1)-C(2)-N(3)	121.26(12)
N(4)-N(3)-C(2)	127.84(12)
N(4)-N(3)-H(3)	116.1
C(2)-N(3)-H(3)	116.1
O(5)-N(4)-O(6)	126.03(12)
O(5)-N(4)-N(3)	114.92(11)
O(6)-N(4)-N(3)	119.04(11)

Compound 10

Table S4. Bond lengths [Å] and angles [°] for **10**.

O(1)-N(3)	1.247(5)	O2-N4	1.251(5)
O(3)-N(3)	1.234(5)	O4-N4	1.264(5)
O(5)-N(7)	1.224(6)	O6-N7	1.220(5)
C(1)-N(2)	1.332(6)	C1-C3	1.380(7)
N(2)-H(2)	0.88	N2-C4	1.333(6)
N(3)-C(6)	1.371(6)	N4-C6	1.352(6)
C(2)-H(2A)	0.95	C2-C3	1.366(7)
C(2)-C(5)	1.377(8)	C3-H3	0.95
C(4)-H(4)	0.95	C4-C5	1.373(8)
C(6)-N(7)	1.450(5)		
N(2)-C(1)-C(3)	118.6(4)	C(1)-N(2)-H(2)	118.4
C(1)-N(2)-C(4)	123.2(4)	C(4)-N(2)-H(2)	118.4
O(1)-N(3)-C(6)	115.8(3)	O(3)-N(3)-O(1)	122.4(4)
O(3)-N(3)-C(6)	121.8(4)	O(2)-N(4)-O(4)	121.4(4)
O(2)-N(4)-C(6)	121.6(4)	O(4)-N(4)-C(6)	117.0(4)
C3-C(2)-H(2A)	120.0	C(3)-C(2)-C(5)	120.0(5)
C(5)-C(2)-H(2A)	120.0	C(1)-C(3)-H(3)	120.1
C(2)-C(3)-C(1)	119.8(5)	C(2)-C(3)-H(3)	120.1
N(2)-C(4)-H(4)	120.2	N(2)-C(4)-C(5)	119.5(5)
C(5)-C(4)-H(4)	120.2	C(4)-C(5)-C(2)	118.9(5)
N(3)-C(6)-N(7)	116.4(4)	N(4)-C(6)-N(3)	127.7(4)
N(4)-C(6)-N(7)	115.8(4)	O(5)-N(7)-C(6)	118.3(4)
O(6)-N(7)-O(5)	124.7(4)	O(6)-N(7)-C(6)	117.0(4)

Compound 13

Table 5.S5. Bond lengths [Å] and angles [°] for **13**.

O(1)-N(3)	1.220(3)	S(2)-O(11)	1.428(2)
O(2)-N(3)	1.207(3)	S(2)-O(12)	1.437(2)
O(3)-N(4)	1.212(4)	S(2)-C(4)	1.816(4)
O(4)-N(4)	1.204(4)	F(4)-C(4)	1.319(4)
O(5)-N(5)	1.215(3)	F(5)-C(4)	1.321(5)
O(6)-N(5)	1.210(3)	F(6)-C(4)	1.331(5)
N(1)-C(2)	1.285(4)	S(1)-O(7)	1.437(2)
N(2)-C(2)	1.305(4)	S(1)-O(8)	1.436(2)
N(3)-C(1)	1.525(4)	S(1)-O(9)	1.450(2)
N(4)-C(1)	1.538(4)	S(1)-C(3)	1.835(3)
N(5)-C(1)	1.530(4)	F(1)-C(3)	1.331(4)
C(1)-C(2)	1.534(4)	F(2)-C(3)	1.322(3)
S(2)-O(10)	1.448(2)	F(3)-C(3)	1.315(3)

O(1)-N(3)-C(1)	115.4(2)	O(11)-S(2)-C(4)	104.67(18)
O(2)-N(3)-O(1)	126.8(3)	O(12)-S(2)-O(10)	113.35(15)
O(2)-N(3)-C(1)	117.7(2)	O(12)-S(2)-C(4)	103.25(16)
O(3)-N(4)-C(1)	114.3(2)	F(4)-C(4)-S(2)	111.5(3)
O(4)-N(4)-O(3)	128.8(3)	F(4)-C(4)-F(5)	108.4(4)
O(4)-N(4)-C(1)	116.8(3)	F(4)-C(4)-F(6)	108.7(3)
O(5)-N(5)-C(1)	114.8(2)	F(5)-C(4)-S(2)	110.2(3)
O(6)-N(5)-O(5)	129.0(2)	F(5)-C(4)-F(6)	108.4(3)
O(6)-N(5)-C(1)	116.3(2)	F(6)-C(4)-S(2)	109.6(3)
N(3)-C(1)-N(4)	105.8(2)	O(7)-S(1)-O(9)	113.92(14)
N(3)-C(1)-N(5)	105.8(2)	O(7)-S(1)-C(3)	104.07(13)
N(3)-C(1)-C(2)	115.6(2)	O(8)-S(1)-O(7)	115.24(13)
N(5)-C(1)-N(4)	106.4(2)	O(8)-S(1)-O(9)	113.81(13)
N(5)-C(1)-C(2)	112.8(2)	O(8)-S(1)-C(3)	104.84(13)
C(2)-C(1)-N(4)	109.9(2)	O(9)-S(1)-C(3)	103.14(13)
N(1)-C(2)-N(2)	123.8(3)	F(1)-C(3)-S(1)	109.9(2)
N(1)-C(2)-C(1)	118.6(3)	F(2)-C(3)-S(1)	110.8(2)
N(2)-C(2)-C(1)	117.3(3)	F(2)-C(3)-F(1)	108.1(2)
O(10)-S(2)-C(4)	102.99(18)	F(3)-C(3)-S(1)	110.72(19)
O(11)-S(2)-O(10)	113.06(14)	F(3)-C(3)-F(1)	108.2(2)
O(11)-S(2)-O(12)	117.41(14)	F(3)-C(3)-F(2)	109.0(2)

5.5.5 Theoretical studies:

Energetic performances were calculated using Explo5 v6.01. The heats of formation for all the compounds were calculated using Gaussian 03 (Revision D. 01).[14]The geometric optimization of the structures was based on single-crystal structures, and frequency analyses were carried out using the B3LYP functional with 6-31+G** basis set. Single-point energies were calculated at the MP2/6-311++G** level.[15] Atomization energies for compound were calculated using the G2 ab initio method.[16a] All of the optimized structures were characterized to be true local energy minima on the potential energy surface without imaginary frequencies. Isodesmic reactions were used to calculated the heat of formation for compound (**2**) and the 1-amino-2,2,2-trinitroethaniminium triflate of salt **13** was determined using an isodesmic reaction (Scheme 5.S1).

Scheme 5.S1. Isodesmic reactions used to calculate the heats of formation for 2 and 1-amino-2,2,2-trinitroethaniminium triflate of salt 13.

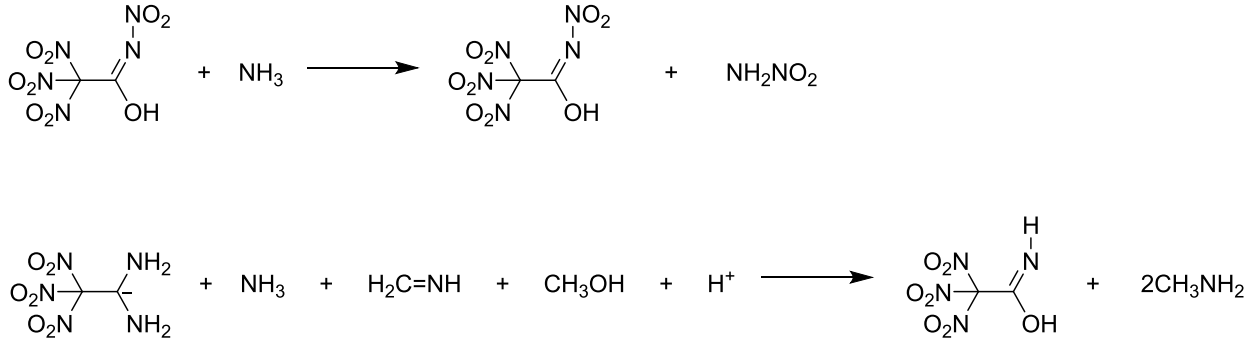

The standard heats of formation of the salts were calculated based on the Born-Haber energy cycle (Scheme5.S2) and Equation (1).[16b]

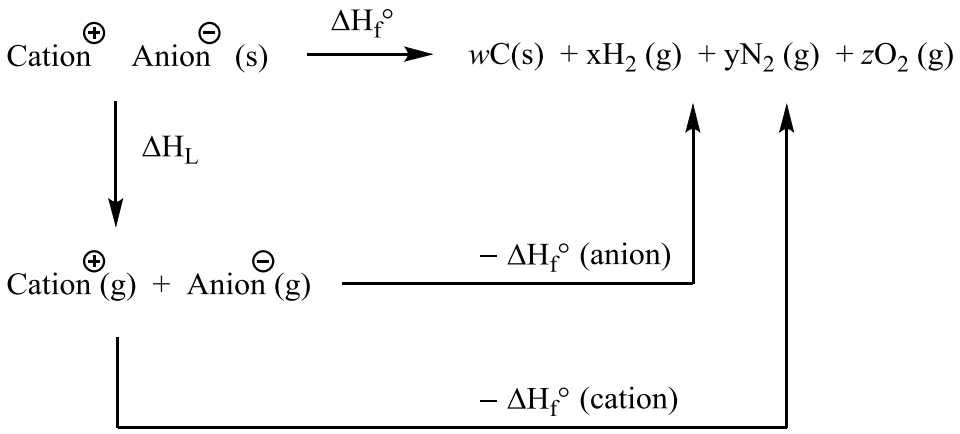

(*"*w, x, y, z" represent the number of moles of each product)*

Figure 5.S2. Born-Haber cycle for formation of energetic salts.

$$\Delta H_f^\circ \text{ (salt, 298K)} = \Delta H_f^\circ \text{ (cation, 298K)} + \Delta H_f^\circ \text{ (anion, 298K)} - \Delta H_L \qquad (1)$$

The lattice energy (ΔH_L) of the salts C_pD_q are calculated using Equation (2) suggested by Jenkins, et al.[17]:

$$\Delta H_L = U_{POT} + [p(n_C/2\text{-}2) + q(n_D/2\text{-}2)]RT \qquad (2)$$

where n_M and n_x are dependent on the ions of C^{p+} and D^{q-} (q and p represent the charges on the cation and anion) and assigned values 3 for monoatomic ions, 5 for linear polyatomic ions, and 6 for nonlinear polyatomic ions. The lattice potential energy, U_{POT}, (reported as kJ mol^{-1}) can be calculated from Equation (3):

$$U_{POT} = \gamma[\rho_m(M_m)^{1/3} + \delta \qquad (3)$$

where ρ_m is the density (gcm^{-3}), M_m is the chemical formula mass of the ionic material (g), and the coefficients γ (kJ mol^{-1}cm) and δ (kJ mol^{-1}) values are obtained from the literature.[18,19]

The heats of formation for compounds **2**, 1-amino-2,2,2-trinitroethaniminium triflate of salt **13** and it's the corresponding dinitroamide salt (**14**) along with their energetic properties are shown in Table 5.S7 below.

Table 5.S7. Energetic Properties of 2 and 1-amino-2,2,2-trinitroethaniminium triflate of salt 13 and the 1-amino-2,2,2-trinitroethaniminium dinitroamide

	2	**13**	**14**
ρ^{a} (gcm^{-3})	1.84	2.09	2.06
$\Delta H_f{}^{b}{}_{(cation)}$ (kJ/mol)	-	676.1	676.1
$\Delta H_f{}^{c}{}_{(anion)}$ (kJ/mol)	-	-337.3	-156.2
ΔH^{d} (kJ/mol) / kJ / g)	-134.6 / -0.563	-131.7 / -0.323	34.4 / 0.114
P^{e} (GPa)	23	25	36
D^{f} (ms^{-1})	7503	7208	9053
Isp^{g} (s)	209	247	238

a) calculated density [Ref. 19]. b) Cation heat of formation. c) Anion heat of formation. d) Heat of formation. e) Detonation pressure. f) Detonation velocity. g) Specific impulse [calculated at an isobaric pressure of 70 bar and initial temperature of 3,300 K].

5.5.6 References

(1) Lawton, M.; Williams, D. B. *J. Org. Chem.* **2010**, 8351–8354.

(2) Anniyappan, M.; Talawar, M. B.; Gore, G. M.; Venugopalan, S.; Gandhe, B. R. *J. Hazard. Mater.* **2006**, *137*, 812–819.

(3) COSMO V1.61, *Software for the CCD Detector Systems for Determining Data Collection Parameters*. Bruker Analytical X-ray Systems, Madison, WI (2009).

(4) Bruker (**2010**). Apex2 v2010.3-0. Bruker AXS Inc., Madison, Wisconsin, USA.

(5) Bruker (**2009**). SAINT v7.68A. Bruker AXS Inc., Madison, Wisconsin, USA.

(6) Bruker (**2008**). XPREP v2008/2. Bruker AXS Inc., Madison, Wisconsin, USA.

(7) Bruker (**2009**). SADABS v2008/1. Bruker AXS Inc., Madison, Wisconsin, USA.

(8) Bruker (**2009**). SHELXTL v2008/4. Bruker AXS Inc., Madison, Wisconsin, USA.

(9) APEX2 V2010.11-3. Software *for the CCD Detector System*; Bruker Analytical X-ray Systems, Madison, WI (2010).

(10) SAINT V 7.68A Software *for the Integration of CCD Detector System* Bruker Analytical X-ray Systems, Madison, WI (2010).

(11) SADABS V2008/2 Program for absorption corrections using Bruker-AXS CCD based on the method of Robert Blessing; Blessing, R.H. Acta Cryst. A51, 1995, 33–38.

(12) Sheldrick, G.M. "A short history of SHELX". *Acta Cryst*. **A64**, 2008, 112–122.

(13) O. V. Dolomanov, L. J. Bourhis, R. J. Gildea, J. A. K. Howard and H. Puschmann, OLEX2: a complete structure solution, refinement and analysis program. J. Appl. Cryst. (2009). 42, 339–341

(14) M. J. Frisch, G. W. Trucks, H. B. Schlegel, G. E. Scuseria, M. A. Robb, J. R. Cheeseman, J. A. Montgomery, T. V. Jr., K. N. Kudin, J. C. Burant, J. M. Millam, S. S. Iyengar, J. Tomasi, V. Barone, B. Mennucci, M. Cossi, G. Scalmani, N. Rega, G. A. Petersson, H. Nakatsuji, M. Hada, M. Ehara, K. Toyota, R. Fukuda, J. Hasegawa, M. Ishida, T. Nakajima, Y. Honda, O. Kitao, H. Nakai, M. Klene, X. Li, J. E. Knox, H. P. Hratchian, J. B. Cross, V. Bakken, C. Adamo, J. Jaramillo, R. Gomperts, R. E. Stratmann, O. Yazyev, A. J. Austin, R. Cammi, C. Pomelli, J. W. Ochterski, P. Y. Ayala, K. Morokuma, G. A. Voth, P. Salvador, J. J. Dannenberg, V. G. Zakrzewski, S. Dapprich, A. D. Daniels, M. C. Strain, O. Farkas, D. K. Malick, A. D. Rabuck, K. Raghavachari, J. B. Foresman, J. V. Ortiz, Q. Cui, A. G. Baboul, S. Clifford, J. Cioslowski, B. B. Stefanov, A. L. G. Liu, P. Piskorz, I. Komaromi, R. L. Martin, D. J. Fox, T. Keith, M. A. Al-Laham, C. Peng, A. Nanayakkara, M. Challacombe, P. M. W. Gill, B. Johnson, W. Chen, M. Wong, C. Gonzalez, J. A. Pople, *Gaussian 03, Revision D. 01*, Gaussian, Inc., Wallingford, CT, **2004**.

(15) a) R. G. Parr, W. Wang, Density Functional Therory of Atoms and Molecules, Oxford University Press, New York **1989**. b) Gao, H.; Joo, Y.-H.; Parrish, D. A.; Vo, T.; Shreeve, J. M. *Chem. Eur. J.* **2011**, *17*, 4613–4618.

(16) Suleimenov, O. M.; Ha, T. K. *Chem. Phys. Lett.* **1998**, *290*,451–457.

(17) H. D. B. Jenkins, D. Tudeal, L. Glasser, *Inorg. Chem.* **2002**, *41*, 2364–2367.

(18) M. W. Schmidt, M. S. Gordon, J. A. Boatz, *J. Phys. Chem. A* **2005**, *109*, 7285-7295.

(19) a) Ye, C.; Shreeve, J. M. *J. Phys. Chem. A.* **2007**, *111*, 1456–1461. b) Gao. H.; Ye, C.; Piekarski, C. M.; Shreeve, J. M. *J. Phys. Chem. C*, **2007**, *111*, 10718 – 10731.